ELECTRONIC SPECTRA OF ORDERED AND DISORDERED SYSTEMS

Thesis

submitted for the award of the degree of

DOCTOR OF PHILOSOPHY

in

PHYSICS

By

MADAN MOHAN PANT

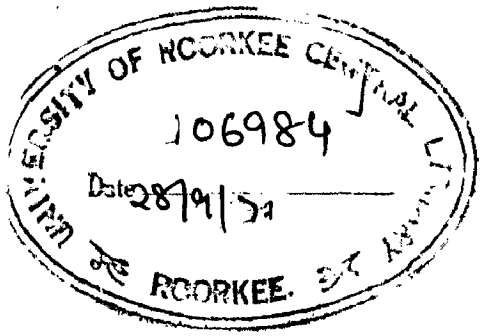

DEPARTMENT OF PHYSICS
UNIVERSITY OF ROORKEE
ROORKEE, U.P.
(INDIA)

October, 1970

C E R T I F I C A T E

Certified that the thesis entitled 'ELECTRONIC SPECTRA OF ORDERED AND DISORDERED SYSTEMS' which is being submitted by Sri Madan Mohan Pant in fulfilment for the award of the Degree of Doctor of Philosophy in Physics of University of Roorkee is a record of his own work carried out by him under my supervision and guidance. The matter embodied in this thesis has not been sumbitted for the award of any other Degree.

This is further to certify that he has worked for a period equivalent to 24 months full time research for preparing his thesis for Ph.D. Degree at the University.

October 22/70.
Dated:

S. K. Joshi

(S.K. Joshi)
Prof. and Head of Physics Dept.
University of Roorkee
Roorkee, U.P. (India)

A C K N O W L E D G M E N T S

I wish to express my most sincere gratitude and thanks to Professor S.K. Joshi, Head of the Physics Department, University of Roorkee, India, for his patience, kindness, constant encouragement and valuable guidance throughout the period of this investigation.

I also take this opportunity to thank all the members of the Physics Department for their cooperation and useful discussions.

I am grateful to the authorities of the Structural Engineering Research Centre, Roorkee, and The Tata Institute of Fundamental Research, Bombay for the use of their computer facilities.

Finally, the financial support from the C.S.I.R., the U.G.C., and the Department of Atomic Energy, Government of India is very gratefully acknowledged.

Madan Mohan Pant

Madan Mohan Pant

R E S U M E

The work reported in this thesis is the result of the author's attempts to investigate the nature of electron states in disordered alloys. In particular, the interest was in alloys of the noble metals. It was clear that two aspects of the problem must be explored.

1) The choice of the one-electron potential and
2) The scheme for determining eigenvalues. Both these choices must be such that for the corresponding pure host, they give an adequate description of the band structure.

The first part of the thesis is therefore concerned with an energy-band calculation of silver and its change with different choices of the crystal potential. The 2nd chapter is devoted to an exposition of one of the methods of energy band calculation of metals, namely the Green's function method of Korringa, Kohn and Rostoker (also called the KKR method), and its comparison with other methods. The reasons for the choice of the KKR method for this investigation are also indicated. The 3rd chapter gives details of methods of constructing the crystal potentials and some other details relevant to the calculation. The IVth chapter deals with the application of the method to calculate the energy bands in silver and presents the conclusions regarding the choice of a crystal potential.

The remaining chapters deal with an extension of these ideas to the disordered alloy problem. In the Vth chapter we discuss what we call 'Virtual Crystal Models', and though these differ slightly in the actual approximations, they are all characterised by assuming an infinite life time for the eigenstates. There is thus a unique energy-wavevector $E(\underline{k})$ relationship and the effect of alloying is assumed simply to alter this from that of the host. However, one knows that in a disordered alloy, we cannot speak of an $E(\underline{k})$ relationship. Rather, we must formulate in terms of densities such as $\rho(E,\underline{k})$ and this does not have a δ-function peak but is broadened. Such a treatment, based on a multiple scattering description is carried out in the subsequent chapters. An attempt is made to evaluate the T matrix for the assembly of scatterers and to find the spectral function $\rho(E,\underline{k})$ from it. The T matrix of the system is expressed as an infinite series in the t-matrices of the individual atoms and the problem is to sum it and average it over all configurations. For the case of a perfect lattice the series is geometric and it is found that $\rho(E,\underline{k})$ is non zero only when E and $\underline{k}$ satisfy a certain relationship, which is exactly the equation for the KKR method, discussed in Chapter II. In chapter VI we sum the series for the disordered case, under the geometric approximation, and present the results for disordered β-brass. An alternative multiple scattering description is the coherent potential model, which postulates an effective potential at each site, a

LIST OF PUBLICATIONS

1. Crystal Potentials in Energy Band Calculations of Noble Metals, Phys. Rev. 184, 639 (1969).
2. Electronic Structure of α-Brass, Phys. Rev. 184, 635 (1969).
3. Green's Function method for Energy Bands in Disordered Alloys, Phys. Rev. 186, 675 (1969).
4. Green's Function Method for Energy Bands in Disordered Alloys II. Band Structure of disordered Cu_3Au, Phys. Rev. B1, 506 (1970).
5. Spectral Density of States in Disordered β-Brass, Phys. Rev. B1, 2532 (1970).
6. Coherent potential approach to electron states in α-Brass, Phys. Rev. B1 (Sept.1970).
7. Band Structure of dilute Ag-In alloys, Phys. Letters 28A 556 (1969).
8. Electronic Structure of Cu-Al from a Coherent potential approach,Phys. Letters 31A, 238(1970).
9. T matrix theory of density of states in disordered alloys—application to β-brass, National Bureau of Standards, Washington Nov.3-6 (1969).
10. Coherent Potential and pseudoatoms in a model alloy, Solid State Communications (to be published).
11. Density Matrix Approach to Knight Shift in simple metals use of a model pseudopotential, J. Phys. C(to be published

12. Density of States in Liquid Be, J. Phys. C(to be published)

13. Surface-State resonances in LEED from copper, Surf. Sci(to be published).

C O N T E N T S

INTRODUCTION

A knowledge of the electronic spectra is fundamental to an understanding of the physical properties of materials. For the case of perfectly periodic solids, the nature of the electronic spectra is well understood. The basic mathematical formalisms had been known for a long time and one has an adequate general prescription for determining the energy bands, and wave functions in perfect lattices. With the availability of high speed and large memory electronic computers and standardized programs, such calculations have become a routine procedure in some laboratories.[1] Energy band calculations became more sophisticated with the development of experimental techniques such as the de Haas van Alphen effect, (dHvA) which give direct information about the topology of the Fermi surface.[2]

Disordered systems have attracted much attention in the last decade - alloys, liquid metals, crystals with impurities and even long molecular chains may be regarded as such systems. Our understanding of disordered systems is still far from complete. There are experimental as well as theoretical difficulties. In disordered systems, the short mean free path renders the observation of such (dHvA) oscillations difficult. Attempts have been made, however, to apply dHvA to dilute alloys, by using high magnetic fields and sensitive measurement techniques to overcome the

amplitude reduction caused by impurity scattering. The effect requires that $\omega_c \tau > 1$, where $\omega_c = eH/m^*c$ is the cyclotron frequency and τ is the lifetime of an electron in an orbit, between scattering events. It is clear therefore that with increasing impurity concentration, higher magnetic fields will be required and the method becomes inappropriate for non-dilute alloys. Recourse has therefore to be taken to measurements of other properties, not so directly related to the Fermi surface, and hence, the interpretation of the results is not always unambiguous. In recent years more and more experimental data related to electronic states in disordered systems is becoming available and this has stimulated a great deal of theoretical work, and the interest in the field is rapidly increasing. Before proceeding further with the theories, we mention here some of the different types of measurements made to study electron states in disordered alloys, and refer to the original papers or review articles for details.

A phenomenon whose observation is not restricted by the requirement of long electron relaxation times is that of magnetoresistance. Berlincourt et al.[3] have made pulsed magnetic field studies of the magnetoresistivities of Ti - Mn and Cu - Mn alloys. There has been considerable investigation of the optical properties of alloys, both in the visible and soft X-ray region. There are two conference reports[4,5] which deal with these electromagnetic probes. The interpretation of the data is not straightforward. It is not possible to attribute the absorptivity peaks only to

'direct' transitions, for even in the case of pure metals, it has been argued that indirect transitions are important. In the case of X-ray spectra many body effects play an important role. Extensive observations of the optical absorption in noble metals alloys have been reported by Rayne and his collaborators[6] and these are used frequently to compare the results of theoretical calculations. They have also carried out measurements for specific heat (which is related to the density of states at the Fermi energy) for a number of alloy systems. Another optical method, which has been applied to the study of noble metal alloys by Stern, McGroddy et al. is the polar reflection Faraday effect.[7] The experiment consists in measuring the rotation of surface polarized light on the metal (or alloy) with a magnetic field applied perpendicular to the surface. This method has been applied to Ag - Au alloys to observe their absorption spectrum in the visible and ultraviolet region.

When positrons annihilate in a solid, the gamma-rays emitted are not exactly anticolinear and their angle is determined by the motion of the electrons in the solid where the annihilation takes place. Since for most of the metals, detailed investigations of the Fermi surface are available, this is not of much interest. Because the techniques of measuring electron momentum by positron annihilation do not require specimens of high purity or long mean free paths, they are more useful for examining

the Fermi surface and electron structure of disordered alloys. Several alloy systems have been investigated by this method, some examples, being Cu_3Au, Ni_3Mn, LiMg and Cu-Al.[8,9]

The existence of Kohn anomalies in phonon dispersion curves measured by X-ray and neutron scattering is well known and can yield information about the Fermi surface. Moss[10] has shown in a recent work, that similar anomalies occur in the local order diffuse scattering of X-rays and neutrons. The detectability of the anomaly depends upon the curvature of the Fermi surface and its diffuseness at the particular temperature. If the mean free path becomes too small, the singularity will be smeared out. These ideas were applied to existing data on Cu_3Au and β-CuZn alloys to make qualitative conjectures about the Fermi surface. Though Moss's interpretation of the existing data is interesting, the method is not of general applicability, and the interpretation of the data not entirely unambiguous.

A novel method for deriving information about the Fermi surface topology and the electronic density of states was proposed by Higgins and Kaehn.[11] It consists in the precise measurement of the superconductivity transition temperature Tc and its pressure derivative $\frac{dTc}{dp}$. The results of the measurements are interpreted within the BCS framework[12] and it is seen that dTc/dp is essentially proportional to the energy-derivative of the electronic density of states, and therefore reflects strong structure

at values of E_F near the van Hove singularities in the density of states.

Thus, being equipped with a good understanding of the perfect lattice and with the large amount of data available from experiments, it was natural to enquire, what happens to the electron states, when the periodicity of the lattice is destroyed by introducing substitutionally a large number of atoms of a different kind. This is the subject matter of this thesis. One faces enormous difficulties in building up a rigorous theory of such systems and approximations have to be made. The great simplification resulting from the Bloch theorem in the case of the perfect lattice problem is not there in a disordered system. Apart from the intrinsic theoretical interest, the presence of disorder leads sometimes to interesting physical effects which may be of technological importance. A well known example is the Ovshinsky effect[13] in amorphous materials. Another example, which is more directly related to the work reported in this thesis concerns alkali-noble metal alloys. Li, Cs, Ag and Au are all metals, but when one makes the alloys LiAg and CsAu, one finds that LiAg still retains a metallic character, while CsAu behaves like an extrinsic semiconductor.[14]

The work reported in this thesis is the result of the author's attempts to investigate the nature of electron states in disordered alloys. Our interest was in alloys of the noble metals, It was clear that two aspects of

the problem must be explored:

1) The choice of the one-electron potential and 2) The scheme for determining eigenvalues. Both these choices must be such that for the pure host, it gives an adequate description of the band structure. For this reason and because the theories of alloys, discussed here are based on a multiple scattering framework, we discuss in the beginning of the thesis a theory for energy bands in periodic lattices and apply it to see the dependence of the energy bands on the choice of crystal potentials for silver.

The 2nd chapter is devoted to an exposition of the Green's function method of Korringa, Kohn and Rostoker (also called the KKR method),[15] for energy band calculations of metals, and its comparison with other methods. The chief feature of the KKR method which renders it more suitable for this investigation is the separation of the structural and potential parts of the problem. Other advantages of the KKR method are also mentioned. The 3rd chapter discusses some prevalent methods for constructing crystal potentials and presents some relevant details. The 4th chapter deals with the application of the method to calculate the energy bands in silver and presents conclusions regarding choice of crystal potential.

The remaining chapters deal with the study of electronic states in disordered alloys. In the 5th chapter we discuss, what we call 'virtual crystal models', and

though the models we discuss differ slightly in details they are all characterized by assuming an infinite lifetime for the eigenstates. There is thus a unique energy wave-vector $E(\underline{k})$ relationship, and the effect of alloying is assumed to only alter this from that of the host, However, one knows that $\underline{k}$ is no longer a good quantum number in a disordered system and it is no longer appropriate to speak in terms of an $E(\underline{k})$ relationship. Rather we must formulate in terms of spectral functions $\rho(E,\underline{k})$

$$\rho(E,\underline{k}) = \sum_n \delta(E-E_n) \; | \psi_n(\underline{k}) |^2$$

where $\psi_n(\underline{k})$ is the k^{th} Fourier component of the eigenfunction ψ_n, and E_n is the corresponding eigenvalue. This function is no longer the δ-function characteristic for the periodic lattice, but is broadened. Multiple scattering theory[16] is used to evaluate the T matrix for the assembly of scatterers and to find the spectral function $\rho(E,\underline{k})$ from it. The T matrix is expressed as an infinite series in the t-matrices of the individual atoms and the problem is to sum it and average it over all configurations. For the case of a perfect lattice the series is geometric and it is found that $\rho(E,\underline{k})$ is non-zero only when E and $\underline{k}$ satisfy a certain relationship, which is exactly the equation for the KKR method. In Chapter 6, we sum the series for the disordered alloy case, under the geometric approximation, with explicit

introduction of short range order. The method is applied to disordered β-brass. The above mentioned geometric approximation, in the absence of short-range order reduces to the averaged t matrix approximation, which consists in placing at each site of the alloy lattice, an effective potential, such that its t-matrix is equal to the average of the t matrices of the constituents. Later investigations by Soven showed that the use of the averaged t-matrix approximation leads to a spurious band gap both for model one-dimensional and 3-dimensional alloys. The coherent-potential model, which seems to be best of the single site approximations overcomes this difficulty. Soven and Velicky et al. have developed the coherent potential approximation (CPA) and applied it to several models. They view a given scatterer as embedded in an effective medium whose choice is made self consistently. The physical condition corresponding to this choice is simply that the scatterer embedded inthis effective medium should produce no further scattering on the average. The final self-consistent equations can be solved exactly to give the effective potential, only for very special cases. Applications to real systems therefore involve some further approximations. These are discussed in Chapter 7, and results of actual computations are presented for Cu-Zn and Cu-Al.

The applications to real systems are usually to alloys of noble metals, the copper-zinc alloy (brass), being one of them. A brief description of the phase diagram and the definitions and nomenclatures of the different phases is therefore given here.

Primary and Secondary Alloys:

When a small amount of a metal B dissolves in a metal A, the resulting alloy has the same crystal structure as A, and is formed by B atoms replacing A atoms in the lattice. Such a substitutional alloy is called a primary alloy. Interstitial alloys are also possible when one atom is very much smaller than the other. The smaller atom, usually hydrogen, boron, carbon or nitrogen does not displace a metal atom from its lattice, but fits into the spaces which exist in the original structure. For some pairs of metals, which have the same crystal structure, the primary alloy may exist for all concentrations, examples being AuAg, CuPt and NiMn.

When the metals have different crystal structures, it is impossible for a primary solid solution to extend over the whole of the concentration range. For some concentrations, either the alloy must consist of a mixture of two primary solid solutions, or else an alloy must be formed whose crystal structure differs from those of the parent metals. Such alloys are called secondary or intermediate solid solutions.

As example, we show in Fig.1.1 the phase diagram for the copper-zinc alloy system and introduce some nomenclature, which is prevalent in the literature and used in this thesis. When zinc is added to copper, the first or α-phase is face-centred cubic and is a primary solution of zinc in copper; it persists upto 35% of zinc. Between the limits of 35% and 46% of zinc, a two-phase region, corresponding to the α-β brasses occurs, while for concentrations between 46% and 49% the alloys are body centred cubic and are known as the β-brasses. The β-phase undergoes an order-disorder transition at a temperature of about 540^{o}C below which we have an ordered β'-phase of CsCl structure. At higher zinc concentrations we have a cubic γ-phase, an hexagonal ϵ-phase with an axial ratio in the neighborhood of 1.56 and a hexagonal η-phase with an axial ratio near 1.8. The η-phase, like the α-phase is a primary solid solution, but of copper in zinc, while the β- γ and ϵ-phases are secondary solutions.

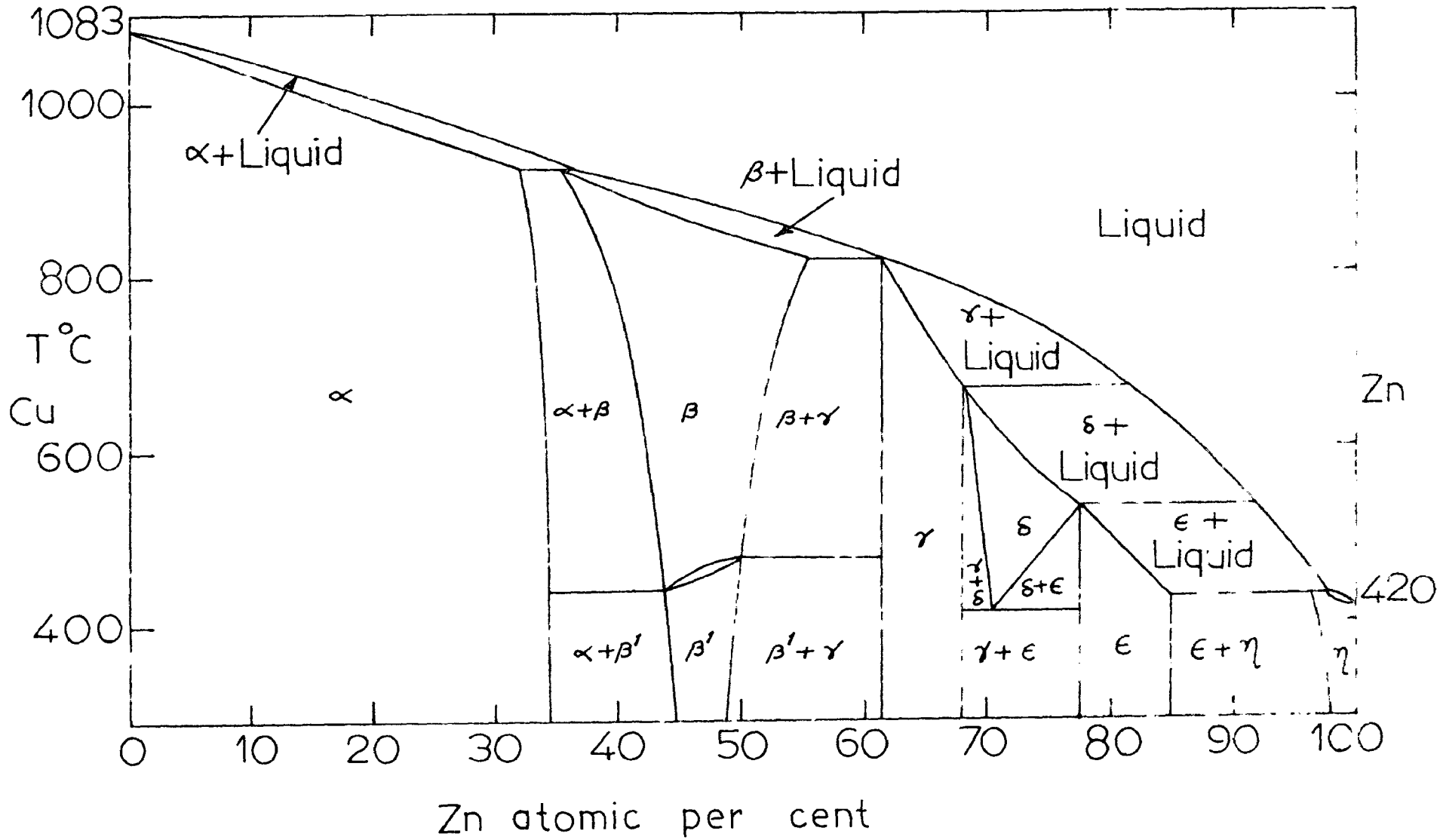

FIG. 1.1:—THE PHASE DIAGRAM OF THE COPPER-ZINC ALLOYS

CHAPTER II

The Green's Function Method for Energy Bands in Periodic Lattices:

To determine the energy band structure of a perfect crystal, one has to solve a one-electron Schrödinger equation, with a suitably determined periodic potential $V(\underline{r})$. The equation to be solved is

$$[-\nabla^2 + V(\underline{r}) - E]\,\psi(\underline{r}) = 0 \qquad (2.1)$$

where $$V(\underline{r}) = V(\underline{r} + \underline{l}). \qquad (2.2)$$

We look for propagating solutions (Bloch functions) of the form

$$\psi(\underline{r} + \underline{l}) = \exp(i\underline{k}.\underline{l})\,\psi(\underline{r}), \qquad (2.3)$$

where $\underline{k}$ is the crystal momentum vector, and $\underline{l}$ is any translation vector of the lattice. We introduce a Green's function defined by

$$(\nabla^2 + E)\,G(\underline{r}, \underline{r}') = \delta(\underline{r} - \underline{r}'). \qquad (2.4)$$

With the help of Eq.(2.4), the Schrodinger equation (2.1) may be rewritten as an integral equation

$$\psi(\underline{r}) = \int G(\underline{r}, \underline{r}')\,V(\underline{r}')\,\psi(\underline{r}')\,d\underline{r}' \qquad (2.5)$$

where the integral is over the unit cell of volume $\mathcal{T}$.

From this stage, one can proceed in two ways, using either a variational principle or otherwise. Both these approaches were discussed by Kohn and Rostoker in their original paper.[15] The variational method starts with constructing a functional Λ such that Eq.(2.5) is obtained from the condition

$$\delta \Lambda = 0 \ . \qquad (2.6)$$

It is seen that the following functional satisfies this condition

$$\Lambda = \int_{\mathcal{J}} d\underline{r}\ \psi^*(\underline{r})\ V(\underline{r}) \left[\psi(\underline{r}) - \int G(\underline{r},\underline{r}') V(\underline{r}')\ \psi(\underline{r}')\, d\underline{r}' \right]. \qquad (2.7)$$

Thus, if $\psi(\underline{r})$ is the exact solution of (2.1) or (2.5), then

$$\Lambda(\psi(\underline{r}),\ \underline{k},\ E) = 0. \qquad (2.8)$$

On the other hand, if we have a trial function of the form

$$\psi_t(\underline{r}) = \psi(\underline{r}) + \epsilon \chi(\underline{r}) \ ,$$

where ϵ is a small parameter, then

$$\begin{aligned}
\Lambda(\psi_t(\underline{r}),\ \underline{k},\ E_t) &= \int_{\mathcal{J}} d\underline{r}\ (\psi(\underline{r}) + \epsilon\chi(\underline{r}))^*\ V(\underline{r})(\psi(\underline{r}) + \epsilon\chi(\underline{r})) \\
&- \int_{\mathcal{J}} \int_{\mathcal{J}'} d\underline{r}\ d\underline{r}'\ (\psi(\underline{r}) + \epsilon\chi(\underline{r}))^*\ V(\underline{r})\ G(\underline{r},\underline{r}')\ V(\underline{r}')(\psi(\underline{r}') + \epsilon\chi(\underline{r}')) \\
&= \int_{\mathcal{J}} d\underline{r}\ \psi^*(\underline{r})\ V(\underline{r}) \left[\psi(\underline{r}) - \int_{\mathcal{J}'} G(\underline{r},\underline{r}')\ V(\underline{r}')\ \psi(\underline{r}')\ d\underline{r}' \right] \\
&+ \epsilon \int_{\mathcal{J}} d\underline{r}\, \chi^*(\underline{r})\ V(\underline{r}) \left[\psi(\underline{r}) - \int_{\mathcal{J}'} G(\underline{r},\underline{r}')\ V(\underline{r}')\ \psi(\underline{r}')\ d\underline{r}' \right] \\
&+ \epsilon \int_{\mathcal{J}'} d\underline{r}'\, V(\underline{r}')\chi(\underline{r}') \left[\psi^*(\underline{r}) - \int_{\mathcal{J}} G^*(\underline{r}',\underline{r})\ V(\underline{r})\ \psi(\underline{r})\ d\underline{r} \right] \\
&+ \epsilon^2 \left[\int_{\mathcal{J}} \chi^*(\underline{r})\ V(\underline{r})\chi(\underline{r})\ d\underline{r} - \int_{\mathcal{J}} \int_{\mathcal{J}'} \chi^*(\underline{r})\ V(\underline{r})\ G(\underline{r},\underline{r}')\ V(\underline{r}')\chi(\underline{r}')\, d\underline{r} \right.
\end{aligned}$$

Since the correct $\psi(\underline{r})$ satisfies (2.5), we are left with

$$\Lambda(\psi_t, \underline{k}, E_t) = 0\ (\epsilon^2)$$

and hence

$$E_t - E = 0(\epsilon^2). \qquad (2.9)$$

This is an important result showing that the error in the energy is of the second order of the error in the wavefunction. This is one of the advantages of the KKR method, that one can get fairly good energy values with a small number of trial wave functions. Having set up the variational principle we use the Rayleigh Ritz technique, and choose a trial wave function of the form

$$\psi_t(r) = \sum_{o}^{n} c_i \phi_i(\underline{r})$$

in Eq.(2.7) for Λ.

If we define Λ_{ij} as

$$\Lambda_{ij} = \int_{\tau} \phi_i^*(\underline{r})\ V(\underline{r})\ \phi_j(\underline{r})\ d\underline{r} - \int_{\sigma}\int_{\tau'} \phi_i^*(\underline{r})\ V(\underline{r})\ G(\underline{r},\underline{r}')\ V(\underline{r}')\phi_j(\underline{r}')d\underline{r}'\ d\underline{r} \qquad (2.10)$$

then

$$\Lambda = \sum_{i,j=o}^{n} c_i^*\ \Lambda_{ij}\ c_j\ . \qquad (2.11)$$

The conditions

$$\partial\Lambda/\partial c_i = 0 \text{ for } i = o,1,.....n$$

then give the linear equations

$$\sum_{j=o}^{n} \Lambda_{ij}\ c_j = 0 \qquad i = o,1.....n$$

and a solution exists only if

$$\text{Det } ||\Lambda_{ij}|| = 0. \tag{2.12}$$

These equations represent a formal solution to the problem, but the practicability depends upon whether the elements Λ_{ij} can be evaluated with a reasonable effort. In general, this is a formidable task requiring first the calculation of the Green's function for various $\underline{k}$ and E and then the evaluation of the 6-dimensional integrals, which have to be performed over the complicated atomic polyhedron. A great simplification can be achieved if one confines oneself to 'muffin-tin' potentials $V(\underline{r})$ with the following form

$$\begin{aligned} V(\underline{r}) &= V(r) && r < r_{mt} \\ &= V_o \ . && r > r_{mt} \end{aligned} \tag{2.13}$$

That is $V(\underline{r})$ is spherically symmetric within a'muffin-tin' sphere of radius r_{mt} and constant outside. We then shift the zero of energy to V_o so that $V(\underline{r}) = 0$ for $r > r_{mt}$.

Because of the spherical symmetry of the potential within the muffin-tin sphere, the trial function can be chosen to be of the form

$$\psi(r) = \sum_{l=o}^{l_{max}} \sum_{m} i^{l} C_{lm} R_l(r) Y_{lm}(\hat{\underline{r}}) \tag{2.14}$$

within the spheres. Here $R_l(r)$ is a radial wave function satisfying the radial differential equation

$$\left[(-1/r^2)\ d/dr(r^2 d/dr) + l(l+1)/r^2 + V(r) - E\right] R_l(r) = 0, \tag{2.15}$$

for the same value of E used in constructing $G(\underline{r},\underline{r}')$. The functions $\gamma_{\ell m}(\hat{\underline{r}})$ are linear combinations of spherical harmonics chosen to transform according to the irreducible representations of the symmetry group of the wave vector $\underline{k}$ and they are normalized real, and mutually orthogonal.

$$\int_0^{2\pi} d\phi \int_0^{\pi} \sin\theta \, d\theta \, \gamma_{\ell m}(\hat{\underline{r}}) \, \gamma_{\ell' m'}(\hat{\underline{r}}) = \delta_{ll'} \, \delta_{mm'}. \qquad (2.16)$$

To deal properly with the singularities of G, we must use a limiting procedure in evaluating Λ. The integration over r′ is done within a sphere of radius $r_{mt} - \epsilon$ and the r integration over a sphere of radius $r_{mt} - 2\epsilon$. Here ϵ is a small number which tends to zero. Thus

$$\Lambda = \lim_{\epsilon \to 0} \Lambda_\epsilon$$

where

$$\Lambda_\epsilon = \int_{r<r_{mt}-2\epsilon} d\underline{r} \, \psi^*(r) \, V(\underline{r}) \left[\psi(\underline{r}) - \int_{r'<r_{mt}-\epsilon} d\underline{r}' \, G(\underline{r},\underline{r}') \, V(\underline{r}') \, \psi(\underline{r}') \right]. \qquad (2.17)$$

Using Eq.(2.1) satisfied by $\psi(\underline{r})$ and (2.4) by $G(\underline{r},\underline{r}')$ and then transforming the volume integrals into surface integrals, we have

$$\psi(\underline{r}) - \int_{r'<r_{mt}-\epsilon} d\underline{r}' \, G(\underline{r},\underline{r}') \, V(\underline{r}') \, \psi(\underline{r}')$$

$$= \psi(\underline{r}) - \int_{r'<r_{mt}-\epsilon} d\underline{r}' \, G(\underline{r},\underline{r}') \, (\nabla'^2 + E) \, \psi(\underline{r}')$$

$$= - \int_{r'=r_{mt}-\epsilon} dS' \left[G(r,r') \frac{\partial}{\partial r'} \psi(r') - \psi(r') \frac{\partial}{\partial r'} G(r,r') \right].$$

Substituting into Eq.(2.17) and noting that

$$\int_{r<r_{mt}-2\epsilon} d\underline{r}\, \psi^*(\underline{r})\, V(\underline{r})\, G(\underline{r},\underline{r}') = \int_{r<r_{mt}-2\epsilon} d\underline{r}\, (\nabla^2+E)\, \psi^*(\underline{r})\, G(\underline{r},\underline{r}')$$

$$= \int_{r=r_{mt}-2\epsilon} dS \left[\frac{\partial \psi(r)}{\partial r}\, G(r,r') - \psi(r)\frac{\partial}{\partial r}\, G(\underline{r},\underline{r}')\right].$$

We then find that

$$\epsilon = \int_{r=r_{mt}-2\epsilon} dS \int_{r'=r_{mt}-\epsilon} dS' \left[\frac{\partial \psi^*(r)}{\partial r} - \psi^*(r)\frac{\partial}{\partial r}\right]\left[\psi(r')\frac{\partial}{\partial r'}, G(r,r') - G(r,r')\frac{\partial}{\partial r'}, \psi(r')\right] \tag{2.18}$$

The Green's function $G(\underline{r},\underline{r}')$ can be expanded for $r<r'<r_{mt}$ as

$$G(\underline{r},\underline{r}') = \sum_{lm}\sum_{l'm'} \left[i^{l-l'} B_{lml'm'}\, j_l(\kappa r)\, j_{l'}(\kappa r') + \kappa\delta_{ll'}\,\delta_{mm'} j_l(\kappa r) n_l(\kappa r')\right] \times Y_{lm}(\hat{\underline{r}})\, Y_{l'm'}(\hat{\underline{r}}') \tag{2.19}$$

where j_l and n_l are the spherical Bessel and Neumann functions.

Substituting for $G(\underline{r},\underline{r}')$ and $\psi(\underline{r})$ from (2.19) and (2.14) into (2.18) we arrive at

$$\Lambda = \sum_{lm}\sum_{l'm'} C^*_{lm}\, \Lambda_{lm\, l'm'}\, C_{l'm'}$$

where

$$\Lambda_{lm\, l'm'} = [R_l(r),\, j_l(\kappa r)]\, B_{lm\, l'm'}\, [R_l(r),\, j_l(\kappa r)] + \kappa\,\delta_{ll'}\,\delta_{mm'}\,[R_l(r),\, n_l(\kappa r)] \; . \tag{2.20}$$

The brackets $[F,G]$ denote expressions of the form

$$[F(r),G(r)] = \left[F(r)\frac{dG(r)}{dr} - G(r)\frac{dF(r)}{dr}\right]_{r=r_{mt}},$$

and

$$\chi = E^{1/2} \quad \text{if } E > 0$$

$$= i(-E)^{1/2} \quad \text{if } E<0.$$

The solution of the problem is therefore

$$\text{Det } ||\Lambda_{lm\ l'm'}|| = 0$$

which may be rewritten as

$$|B_{lm\ l'm'} + \chi\, \delta_{ll'}\, \delta_{mm'} \frac{n_l' - n_l L_l}{j_l' - j_l L_l}| = 0 \qquad (2.21)$$

Or in terms of the phase shifts η_l of the potential V(r) as

$$| B_{lm\ l'm'} + \chi \cot\eta_l \delta_{ll'}\, \delta_{mm'}| = 0 \qquad (2.22)$$

The phase shifts η_l are defined by

$$\cot\eta_l = \frac{n_l' - n_l L_l}{j_l' - j_l L_l}$$

and completely determine thescattering from the potential V(r). The potential makes its influence felt only through these phase snifts.

Non-Variational Derivation of the Secular Equation:

We start with Eq.(2.5)

$$\psi(\underline{r}) = \int G(\underline{r},\underline{r}') \, V(\underline{r}') \, \psi(\underline{r}') \, d\underline{r}'$$

$$= \int G(\underline{r},\underline{r}') \, (\nabla'^2 + E) \, \psi(\underline{r}') \, d\underline{r}'$$

$$= \int [G(\underline{r},\underline{r}') \, \nabla'^2 \psi(\underline{r}') - \psi(\underline{r}') \, \nabla'^2 G(\underline{r},\underline{r}')] \, d\underline{r}'$$

$$+ \int \psi(\underline{r}') \, \delta(\underline{r},-\underline{r}') \, d\underline{r}'$$

or using Green's theorem as a surface integral

$$\int \left\{ G(\underline{r},\underline{r}') \frac{\partial}{\partial r'} \psi(r') - \psi(r') \frac{\partial}{\partial r'} G(r,r') \right\} dS' = 0$$

Substituting as above from Eqs. (2.19) and (2.14) for $G(\underline{r},\underline{r}')$ and $\psi(\underline{r})$ we arrive at the same equations (2.21) and (2.22).

Yet another derivation of this secular equation was given by Beeby[16] and elaborated by Ziman[17] but that will be discussed later (Chapter,6). Eq.(2.22) is the fundamental secular equation of the KKR method and is an implicit equation for the $E(\underline{k})$ relationship.

This is a convenient point to evaluate the KKRmethod for its usefulness and consider its relationships with the other well-known methods for energy-band calculations, e.g. the tight binding method, the orthogonalised plane wave (OPW) and pseudopotential methods, the cellular method, and the augmented plane wave (APW) method. These methods have been discussed in several texts.[18-21]

The tight-binding method is suitable for core states or localized electrons, such as say, the d-bands in the transition metals. The pseudopotential is most suitable for the other extreme - the nearly free electron energy bands such as in the alkali metals. The APW and the KKR methods, resulted as developments of the cellular method. In these methods, the difficulty of satisfying the periodic boundary conditions on the boundary of the unit cell is removed as the boundary conditions are built into the formulation. Before going further into the relationships between the APW and the KKR methods, we say a few words about the OPW method.

The OPW method requires the electrons in the crystal to be separated into two categories - core electrons and itinerant electrons, and such a categorisation is not easy in the case of transition and noble - metals. The electrons in partially filled d-shells do not fall naturally into either category. However, for those systems, where this is possible the OPW method has an advantage over the APW and the KKR method because there is no implicit dependence of the matrix elements on the energy. It is therefore much faster (in computer time), than the APW and the KKR methods, because in these methods, it is necessary to examine the secular determinant as a function of the energy to find its zero, hence the eigenvalues. The APW and the KKR methods do not require

this separation of the electrons into core and itinerant electrons. The other disadvantage of the OPW method is that it is more difficult to apply to crystals containing heavy elements with more core states, because the plane wave has to be orthogonalised to more core states. Besides, the core states in the OPW method are to be taken as the eigenfunctions of the crystal potential and these are not the same as atomic states.

Both the APW and the KKR methods are based on the muffin-tin model for the crystal potential. The unit cell is divided into two regions by non-overlapping spheres, centred on each lattice site. Inside the spheres, the potential is spherically symmetric, and outside it is a constant. This is a fair approximation in most cases, but may be a poor representation in case of group IV diamond-lattice semiconductors, where there is a directional bonding.

By intercomparison of the results of APW and the KKR methods for copper with the same potential, it has been established that they give identical results.[22,23] There have been attempts to prove a formal equivalence between the two methods. The efforts of Ziman,[17] Slater,[24] Lloyd[25] and Johnson[26] have resulted in an understanding of the differences between them and to put them into a common basis within the framework of the pseudopotential method. Slater tried to transform the Ziman form of the

KKR method, to a form very similar to the APW form, but it could not be transformed exactly into the APW formulation.

Both the APW and the KKR methods involve a summation over atomic orbitals (lm) inside the spherical region and a summation over reciprocal lattice vectors. In the APW method, the coefficients in the atomic orbital expansion are specified, and those in the reciprocal lattice vector expansion are determined variationally. The size of the secular determinant is equal to the number of reciprocal lattice vectors included, and this is 20-40 in most cases. The number of terms in the atomic expansion is usually about 12. On the other hand, in the KKR method, the reciprocal lattice expansion is carried out formally, and the atomic orbital coefficients are determined variationally. The size of the secular determinant is now $(l_{max} + 1)^2$, where l_{max} is the maximum value of l included in the summation in Eq.(2.14). In practice it is found that l = 2,3 is adequate. A plausible explanation for the fact that l = 2,3 is adequate will be given in Chapter 6, in connection with another derivation of the KKR method. The size of the secular determinant in the KKR method is thus smaller than that in the APW method and it therefore requires less computer time to evaluate. Another advantage of the KKR method stems from the structure of the secular equation (2.22). The coefficients $B_{lm\,l'm'}$

which occur there, are dependent on the energy, the crystal structure and the wave vector of the electron state, but not the muffin-tin potential. The calculation of these is elaborated in an Appendix A1. The potential makes its influence felt only through the phase shifts η_l. If the structure dependence is tabulated once and for all via the coefficients $B_{lm\,l'm'}$, then the KKR method is very convenient for studying the effect of changes in the crystal potential upon the band structure. Such a program has been carried out by the author, with a view to find a suitable crystal potential for noble metals, and this work is reported in the following Chapters 3 and 4.

We may add here that the OPW, APW and KKR methods have all been generalized to the relativistic case.[27-29] It is estimated that relativistic effects become significant in metals with atomic number Z greater than 55, and for $Z > 71$, they should not be ignored.

CHAPTER III

Crystal Potentials in Energy Band Calculations:

Our problem is to find the energy eigenstates for conduction electrons moving in a perfect lattice. Obviously, the problem must be treated in some kind of a self-consistent field approximation. Somehow, we must set up a potential in which an individual electron moves, representing not only the action on this electron of the nuclei but of some sort of average of the effect of the other electrons. Having set up this potential, we must solve the Schrodinger Equation of an individual electron in such a periodic potential, by one of the methods discussed in Chapter II. When we have done this, we should determine the resulting charge distribution, assuming that the lowest states are occupied while those above certain energy (the Fermi energy) are empty. We use the resulting charge distribution to compute the potential and carry out iterations of this procedure until the resulting potential is identical with the one with which we started.

In the work reported here, a self-consistent calculation has not been performed. Rather, the aim has been to look for a potential, which with only one part of this cycle will give a reasonable description of the energy bands. Because of the variational principle in the KKR method, the energies are given to a greater accuracy

than the wave functions, the successive cycles are more expensive in computer time. Another reason for not undertaking a self-consistent calculation was the fact that this work had been motivated to lead to the choice of an appropriate starting potential for the constituents, in the alloy problem. As will be discussed later in this thesis, the prevalent theories for electron states in disordered alloys involve fairly drastic approximations, and it was therefore thought that the additional effort of performing a self-consistent calculation for the pure metal case, was not worthwhile.

One of the simplest choice for V(r) would be to take it to be the same as the atomic potential within the muffin-tin sphere and cut it off outside. For the atomic potential, Gaspar and Ivanecsko[30] have suggested phenomenologically, simple analytical forms or one could use the results of a self-consistent Hartree-Fock-Slater calculation of the type performed by Herman and Skillman.[31] We will return to these only later when discussing the results for energy bands of silver obtained with such a potential.

It is clear that the potential experienced by an itinerant electron within the lattice is not quite the same as that felt by an electron in an atom. Thus, one method of constructing the crystal potential regards it as a sum of several individual contributions of the core and conduction electrons. Such a scheme is commonly used in OPW calculations for simple metals. Heine[32] first

used it for aluminium, Falicov[33] for magnesium and more recently Gaspari and Das[34] for calculation of Knight shift in Indium. Following Heine,[32] we enumerate the various contributions to the crystal potential:

(i) potential due to ion-core
(ii) exchange among ion-core electrons
(iii) correlation among ion-core electrons
(iv) exchange between conduction and core electrons
(v) correlation between conduction and core-electrons
(vi) potential due to the conduction electrons
(vii) deviation from spherical symmetry
(viii) exchange among conduction electrons
(ix) correlation among conduction electrons.

The main contributions come from (i) and (vi). Next in importance are (ii), (iv) and (viii). It is difficult to make accurate estimates of the contribution due to correlation effects, and these are generally ignored, or taken in account in rather simplified ways. In a simple scheme, which we apply to silver, in the next chapter, we take contributions (i) and (ii) from Hartree-Fock-Slater calculations for the ion-core, add contributions (vi) and (vii), and the contributions due to exchange and correlation between core and conduction electrons are taken into account in a simple way. We now indicate in brief how these contributions are evaluated. It is convenient to express the potential in a form

$$V(r) = - 2Z(r)/r \qquad (3.1)$$

and we will now enumerate the various contributions to $Z(r)$.

$Z_1(r)$ - Contribution of the ion-core:

This is taken to be the sum of the Coulomb contribution of the nucleus with charge Z and the surrounding core electrons, and exchange between core electrons. The wave functions for the core electrons were obtained from the Herman-Skillman program, run for the bare ion. The charge density due to the core is

$$\rho_{core}(r) = \sum_i \psi_i^*(r)\, \psi_i(r) \qquad (3.2)$$

the summation being over the core states. The wave function is expressed in terms of another function

$$P_{nl}(r) = r\, R_{nl}(r)$$

where $R_{nl}(r)$ is the radial wave function. The charge density is then

$$\rho_{core}(r) = \sum_{nlm} 2 \frac{P_{nl}^2(r)}{r^2} Y_{lm}^*(\theta,\phi)\, Y_{lm}(\theta,\phi)$$

$$= \frac{1}{4\pi} \sum_{\substack{n,l \\ (core)}} 2(2l+1) P_{nl}^2(r)/r^2. \qquad (3.3)$$

The corresponding potential $V_1(r)$ may be written from the solution of Poissons' equation as

$$V_1(r) = 2\left(-\frac{Z}{r} + \int \frac{\rho(r')}{|r-r'|}\, dr'\right). \qquad (3.4)$$

Performing the integration, and substituting for $V_1(r)$ gives the final result for $Z_1(r)$ as

$$Z_1^c(r) = Z - \int_0^r \rho_r(r')dr' + r\int_0^r dr'\rho_r(r')/r' - r\int_0^\infty dr'\rho_r(r')/r' \quad (3.5)$$

where

$$\rho_r(r) = 4\pi r^2 \rho_{core}(r) = \sum_{nl} 2(2l+1)\, P_{nl}^2(r). \quad (3.6)$$

Numerical integration of the above equation gives the Coulomb contribution. To this is added the exchange contribution, obtained from Slater's local density approximation,[35]

$$V_{ex}(r) = -6\,[3\rho(r)/8\pi]^{1/3} \quad (3.7)$$

and $Z_1^{ex}(r) = -r\,V_{ex}(r)/2$.

The total contribution of $Z_1^c(r)$ and $Z_1^{ex}(r)$ is then the $Z_1(r)$ corresponding to the effect of the core.

$Z_2(r)$ - <u>Coulomb potential between conduction electrons:</u>

This is calculated by assuming a uniform distribution of the conduction electrons in the Wigner-Seitz spheres. The potential resulting from such a distribution is easily seen to be

$$Z_3(r) = \frac{N_e}{2}\,\frac{r}{r_s^3}\,(r^2 - 3r_s^2) \qquad r<r_s$$
$$= -N_e \qquad r>r_s \quad (3.8)$$

where N_e is the number of conduction electrons per unit cell. This uniform distribution should be corrected for the oscillations due to orthogonalisation to core states. However, a more important correction is due to the fact that a sum of Wigner-Seitz spheres does not completely map the crystal. This correction is essentially a geometrical problem and has been given by Heine[32] and Falicov.[33] Once the correction is estimated for a given lattice structure, it can be used for any metal with the same structure, by scaling with respect to the lattice parameter and the number of conduction electrons.

$Z_3(r)$ - Exchange and Correlation among core and conduction electrons:

The Hartree-Fock theory takes into account the correlations between electrons of parallel spin but neglects Coulomb correlation. This results in an exchange potential that is too large. What Robinson et al.[36] have tried to do is to obtain an expression which has the simplicity of the Slater formula (i.e. a local density, k independent approximation) but takes into account some correlation effects as well. Effectively, they replace the Coulomb interaction e^2/r_{12} in Slater's derivation by $\frac{e^2}{r_{12}} \exp(-k_s r_{12})$, where k_s is the Thomas-Fermi screening factor. The resulting screened Slater exchange potential is

$$V_{sc.ex} = - 6 \left[3\rho(r)/8\pi\right]^{1/3} F(\alpha) \qquad (3.9)$$

where $F(\alpha)$ depends on the charge density in the following way

$$F(\alpha) = 1 - \frac{4}{3}\alpha \tan^{-1}(2/\alpha) + \frac{\alpha^2}{2}\log(1+4/\alpha^2) - \frac{\alpha^2}{6}\left(1-\frac{\alpha^2}{4}\log(1+4/\alpha^2)\right) \tag{3.10}$$

where $\alpha = 0.646/[\rho(r)]^{1/6}$.

The correction factor $F(\alpha)$ has the effect of reducing the unscreened exchange potential at all distances but this reduction becomes most severe in the low density region. It has been shown[37] that the Slater formula overexaggerates exchange effects in the low density region, resulting in a potential with a rather long tail. The screened Slater exchange used here does oversimplify correlation effects, but it has the advantage of correcting the unscreened Slater potential in a region where it is known to be inaccurate while retaining a form which is convenient for calculation.

There can be several variants within the above framework of constructing the crystal potential, depending upon the treatment of exchange and correlation effects. Kohn and Sham[38] had shown that 2/3 of the Slater formula is a better approximation. Snow[39] had concluded that a coefficient between 2/3 and 1 would be best, according to his results of self-consistent APW band calculations for copper and silver and found that the coefficient 5/6 gave good agreement with experimental results. Recent theoretical work by Lundqvist[40] seems to lend support to this conclusion.

An alternative method for constructing the crystal potential starts from the total atomic charge densities and overlaps them. The atomic charge densities are obtained usually from the Hartree-Fock-Slater calculations of Herman and Skillman,[31] but for heavier elements it is preferable to use the results of Liberman's calculations[41] based on the relativistic Dirac equation. Such an approach was first used by Mattheiss[42] in connection with his APW calculations. The motivation is that in the central portion, the crystal potential also has an atomic character and in the outer portion, there is overlap from neighboring atoms. To evaluate the magnitude of this overlap, two approximations are made,

(1) The atomic potentials which are overlapped are spherically symmetric, and

(2) Only the spherically symmetric contributions from neighbors are retained.

The superposition is done using Lowdin's α-function expansion technique, and this is outlined briefly.[43]

In Fig.(3.1) we have the point P, whose coordinates are $(r_1,\hat{r}_1)$ and $(r_2,\hat{r}_2)$ about the origins 1 and 2. We want to expand a function

$$\psi_{lm}(\underline{r}_1) = f_l(r_1)\, Y_{lm}(\hat{\underline{r}}_1) \qquad (3.11)$$

centred at the origin 1 in terms of spherical harmonics

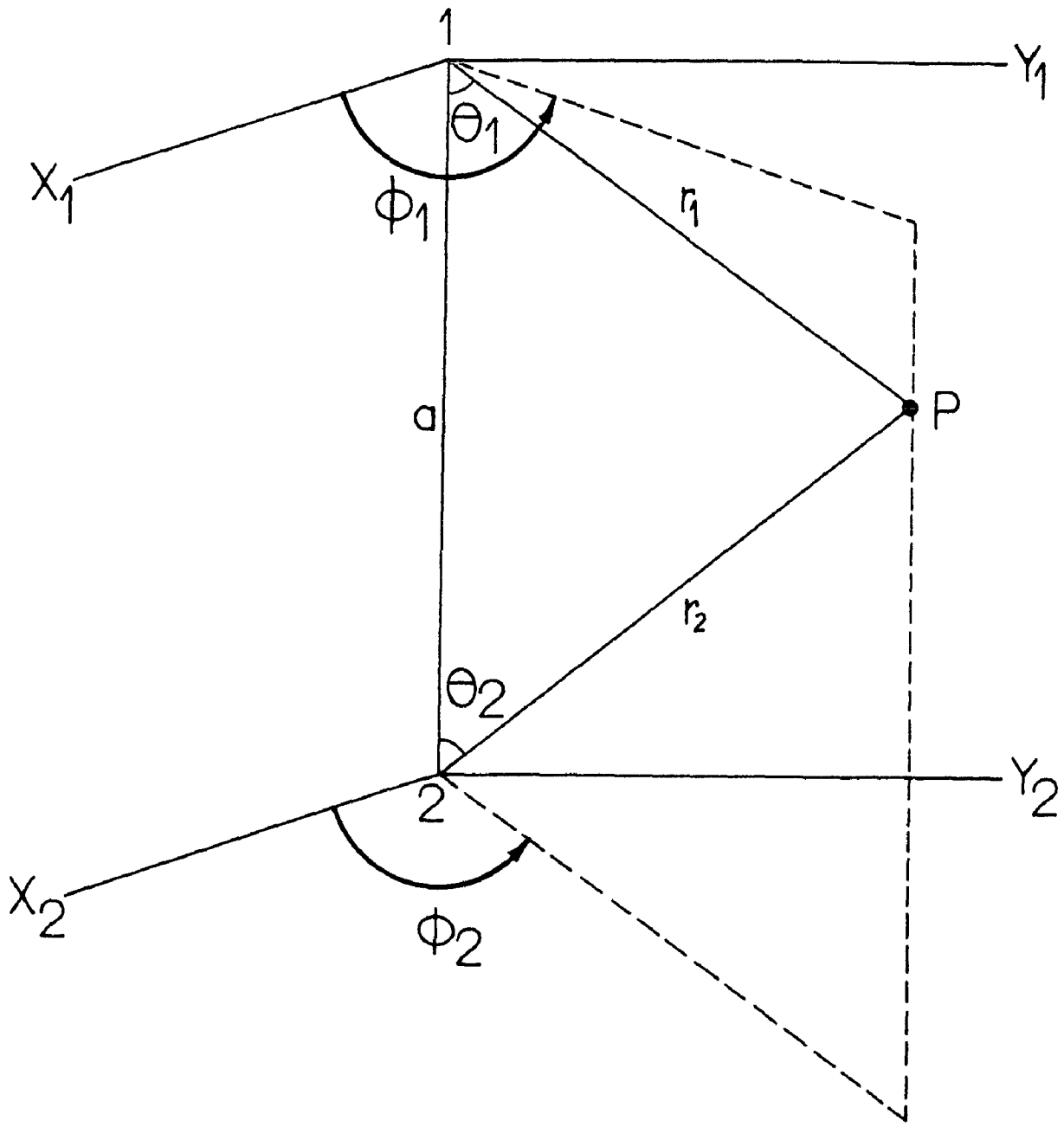

FIG. 3.1 Geometry for α-function expansions for crystal potentials

centred at 2. Thus

$$\psi_{lm}(\underline{r}_1) = \sum_{l'=0}^{\infty} \sum_{m=-l'}^{l'} \alpha(l'm'|lm)\, Y_{l'm'}(\hat{r}_2), \qquad (3.12)$$

where the coefficients $\alpha(l'm'|lm)$ are to be determined. Multiplying both sides by $Y^*_{l'm'}(r_2)$ and integrating over the angular variables gives

$$\alpha(l'm'|lm) = \int Y^*_{l'm'}(\hat{\underline{r}}_2)\, \psi_{lm}(r_1)\, d\hat{\underline{r}}_2 \quad . \qquad (3.13)$$

In view of the two assumptions mentioned above only the $l = o$, $m = o$ and $l' = o$, $m' = o$ contributions are required

$$\psi_{oo}(r_1) = f(r_1)/\sqrt{4\pi}$$

and $$\alpha(00|00) = \tfrac{1}{4}\pi \int f(r_1)\, d\hat{r}_2 = f(a|r_2).$$

Now, from the geometry of the problem

$$\begin{aligned} \phi_1 &= \phi_2 \\ r_1 \cos\theta_1 + r_2 \cos\theta_2 &= a \\ r_1 \sin\theta_1 &= r_2 \sin\theta_2 \\ r_1^2 &= a^2 + r_2^2 - 2ar_2 \cos\theta_2 \end{aligned} \qquad (3.14)$$

Performing the angular integration and using the relation $\sin\theta_2\, d\theta_2 = r_1 dr_1/(ar_2)$, from the above expressions, we have

$$f(a|r_2) = \frac{1}{2ar_2} \int_{|a-r_2|}^{a+r_2} f(r_1) r_1 dr_1 \quad . \qquad (3.15)$$

This gives the contribution at r_2, measured from the origin 2, due to the function $f(r_1)$ centred at the origin 1, the two origins being separated by the distance a.

In the Mattheiss prescription, the exchange and Coulombic contributions to the muffin-tin potential are treated separately. The Coulomb part is obtained by integrating the Poisson's equation in a way similar to that discussed before. If $V_o(r)$ is the Coulomb contribution to the atomic potential, then the Coulomb part of the crystal potential is

$$V_c(r) = V_o(r) + \sum_i V_o\ (a_i|r) \qquad (3.16)$$

where a_i are lattice vectors. To calculate the exchange, the charge densities are overlapped to give the crystal charge density as

$$\rho_c\ (r) = \rho_o(r) + \sum_i \rho_o\ (a_i|r) \qquad (3.17)$$

and the exchange calculated by using Slater's formula, with another factor (2/3 or 5/6) with this density $\rho_c(r)$.

$$V_{ex}(r) = -\ 6\ (3\rho_c(r)/8\pi)^{1/3}\ . \qquad (3.18)$$

The total crystal potential is then simply

$$V_T(r) = V_c(r) + V_{ex}(r). \qquad (3.19)$$

The Mattheiss prescription has the advantages of

simplicity and generality. It does not demand a distinct categorisation into core and conduction electrons, and is therefore equally applicable to noble and transition metals. The only information required is the total atomic charge density, and this choice is sometimes critical. We will discuss this point in the next chapter, in connection with results for energy bands in silver.

The restriction to spherically symmetric muffin-tin potentials is a feature of all the work that is discussed in this thesis. Attempts to include effects of the non-muffin tin contributions in self-consistent APW calculations by Rudge[44] show that the muffin-tin model is reasonable for metals. However, in the case where directional bonding is important, say the diamond lattice semiconductors, the muffin-tin approximation may be poor.

CHAPTER IV

Energy Band Structure of Silver:

In this chapter we discuss the energy bands for silver resulting from a KKR calculation and employing some of the crystal potentials of Chapter III. Copper has been the subject of several first principle energy band calculation using different potentials as well, and the shape of the Fermi surface is rather well established.[45-50] The main part of the surface, referred to as the 'belly' is nearly spherical like the free electron Fermi sphere, but in the eight (111) directions, there are 'necks' which contact the hexagonal zone faces. Experiments indicate that silver too, has a Fermi surface which is quite similar to that for copper. Joseph and Thorsen[51] have studied the deHaas van Alphen (dHvA) effect in silver and Jan and Templeton[52] made precision measurements for the <111> neck dHvA frequencies. Bohm and Easterling[53] have performed magnetoacoustic measurements, and optical properties have been studied by Cooper et al.[54] Berglund and Spicer[55] have carried out photoemission studies for silver to determine the density of states and certain energy level separations.

The purpose of the work reported here was to examine the various prescriptions for constructing crystal potentials discussed in Chapter III. A comparison of the results for copper (from available calculations) and silver (this calculation) would allow some general conclusions to be drawn

with respect to the suitability of a given potential for noble metals. The KKR method was used in preference to the APW method for reasons discussed in Chapter II. Calculations were performed for the various irreducible representations at the symmetry points Γ, X, and L and along the Δ, Λ and Σ axes. This limited calculation does not allow an accurate determination of the density of states, nor does it give detailed information about the Fermi surface. It is, however, sufficient to depict the salient features, such as the widths of the sp and d bands, their relative locations and the Fermi level, which can be compared with optical data. Contact of the Fermi surface at the zone face is investigated, and under certain approximations[22] (which do not involve errors of more than 3-5%) the neck and belly radii can be estimated and compared with experimental results.

The steps of the calculation are briefly as follows:

1) Construction of the crystal potential by one of the methods discussed in Chapter III.

2) Solution of the radial Schrodinger equation for this potential to get the phase shifts. This is done by using the Numerov method,[56-58] discussed in Appendix 2. The other part of the calculation is independent of the choice of potential and involves only the structure of the lattice.

3) Calculation of the structure constants using the formulae of Appendix 1. Full use is made of symmetry considerations to reduce the size of the secular determinant

and the number of structure constants required.

4) For a chosen $\underline{k}$ value and a given symmetry representation, the secular determinant is evaluated as a function of energy. The zero of the determinant is then interpolated by using the method of regula and falsi.[59]

5) Once the energy values, in a given direction are obtained, the points are joined together to form a continuous curve, taking into consideration the compatibility relations between the different representations.[19]

6) To estimate the neck and belly radii, we follow a method used by Segall[22] in his calculations for copper, and this involves two assumptions.

(i) The volume of the belly (the total volume less the volume of the necks) is approximately equal to the volume of a sphere with a radius $\overline{k}$ which is an average of the $|k|$'s in the (100) and (110) directions.

(ii) The energy in the vicinity of the point L is given by

$$E(\underline{k}) = \frac{h^2 k_\perp{}^2}{2m^*} + E(\underline{k}_{//}) \qquad (4.1)$$

with $\underline{k} = k_\perp + k_{//}$ where $k_{//}$ and $k_\perp$ are the components of the wave vector along and perpendicular to the (111) axis, and m* is the 'neck' effective mass. $E(\underline{k}_{//})$ is obtained from the band structure along the Γ-L axis. On the circle at which the neck joins the belly, the relation $\overline{k}^2 = k_\perp^2 + k_{//}^2$ is satisfied. From this and Eq.(4.1), the limits of $\underline{k}_{//}$ for the neck region are found for a given energy. The

neck volume is then found by straightforward integration. By adding the volume of the eight necks to that of the sphere and making a small correction for the eight spherical caps, the total volume within the constant energy surface is evaluated. The Fermi energy is than determined by the requirement that the volume equal one-half the volume of the Brillouin Zone, so that the correct number of states are occupied.

We now discuss the results of the calculations done with different crystal potentials, and also compare these with experiments.

A. Gaspar potential:

Gaspar and Ivanecsko[30] have suggested a phenomenological potential of the form

$$V(r) = -\frac{2Z}{r}\,\frac{\exp(-\lambda_o r)}{1+A_o r} - \frac{C\exp(-\alpha r)}{1+Ar}\, f_{ex}$$

where the first term simulates the Coulomb contribution and the second the exchange. f_{ex} is a parameter which was varied through a range of values 0.60 to 1.70, and the values of the other parameters used in the calculation were

$\lambda_o = 0.74883$ $\qquad$ $\alpha = 0.16305$

$A_o = 4.28017$ $\qquad$ $A = 36.68715$

$C = 39.75900$ $\qquad$ $Z = 47$.

Best results were obtained with f_{ex} equal to 1.50 and are shown in Table 4.1 together with results of other calculations, but even here the agreement with experiments

is not good.

B. Atomic Potential

Next we have evaluated the $E(\underline{k})$ for a self-consistent atomic potential of silver derived from a Hartree-Fock-Slater scheme. For silver, such a potential, derived from the Herman-Skillman program[31] gives results which are surprisingly close to experimental results. The Fermi surface touches the zone face at L and $E_F - L_{2'}$ has a value of 0.016 Ry, which is close to the experimental value of 0.022 Ry. The $L_{2'} - L_1$ gap is 0.267 Ry compared with the experimental value of 0.31 Ry. The state $\Gamma_{25'}$ is pulled below Γ_1 ; the $\Gamma_{25'} - \Gamma_1$ gap being -0.01 Ry, which is equal to the value obtained by Snow from a self consistent APW calculation with a potential constructed according to the Mattheiss prescription and using the full Slater exchange. But the d-bands are pushed below the Fermi level considerably more than predicted by experiments. It would appear that an atomic potential should be a poor approximation to the crystal potential. However, the following considerations indicate that the crystal potential in some situations, may not be very much different from the atomic potential.

In Chapter III, we saw that the crystal potential may be built up by superposition of atomic Coulomb potentials, and charge densities. The exchange is propertional to the cube root of charge density. The Slater exchange is thought to exaggerate the actual exchange and various

schemes have been suggested to approximate the exchange in a better way. It is just possible that the crystal Coulomb potential plus a reduced Slater exchange derived from the crystal charge density may more or less equal the atomic Coulomb potential plus the full Slater exchange for the atomic charge density. Further, a comparison of the Herman-Skillman atomic potential for silver with self consistent crystal potentials obtained by Snow[49] shows that the atomic potential is close to the self-consistent potential using the full Slater exchange.

C. Heine Potential

This has been outlined in Chapter III. A problem which one faces in trying to build up a crystal potential along these lines is how to distinguish the core from the conduction states, and for the noble metals this is not a trivial matter.

We regarded the core as Ag^+ and assumed one conduction electron to be uniformly distributed over the Wigner Seitz cell to calculate the three main contributions mentioned in Chapter III.

The results of the calculations indicate that such a potential is not suitable. The d bands are too high and at the point X, the X_5 state is found to be higher than X_4'. There is a pronounced discrepancy for the widths of the d bands as measured by the energy difference $X_5 - X_1$ which is twice the experimental value. The width of the sp bands

as measured by $X_4' - \Gamma_1$ is 0.69 Ry which is of the same order as obtained from other calculations.

D. Superposed Atomic Potentials

Reference has been made in Chapter III to the Mattheiss prescription for constructing crystal potentials from a superposition of atomic potentials. The critical point here is the choice of the electronic configuration for obtaining the atomic charge densities. Mattheiss and Snow et al. have carried out such investigations. More recently, Davis et al.[50] have studied the effects of changing the atomic wave functions on the band structure of copper. They conclude in the light of the abundant experimental data for copper, that the potential generated for a $3d^{10}4s^1$ configuration by using atomic wave functions for a $3d^9 4s^2$ configuration gave the best results. This may be understood because the effective occupation number changes on going from a free atom to a crystalline environment, because of the overlap of d and s bands. For silver, we have accordingly chosen to calculate the charge density for a $4d^{10}5s^1$ configuration from atomic wave functions obtained from the Hermann-Skillman program for an assumed $4d^9 5s^2$ configuration. The superposition of the atomic potentials and charge densities is done through sixth neighbors. For charge densities obtained from this configuration, best results were obtained, with the potential constructed using full Slater exchange.

TABLE 4.1: Important energy-level separations from various calculations on Ag (in Rydbergs).

	$\Gamma_{25'} - \Gamma_1$	$X_5 - \Gamma_1$	$X_5 - X_1$	$X_4' - \Gamma_1$	$E_f - X_5$	$E_f - L_3$	$E_f - L_{2'}$	$L_{2'} - L_1$
Experimental:								
Berglund and Spicer			0.26		0.28	0.28	0.022	0.31
Previous Calc:								
Segall:								
Hartree	0.26	0.40	0.27	0.66	0.14	0.16	0.03	0.40
Hartree-Fock	0.07	0.19	0.24	0.73	0.23	0.29	-0.09	0.20
Snow:								
Slater = 1	-0.011	0.105	0.198	0.665	0.387	0.400	-0.013	not
Slater = 5/6	0.090	0.221	0.235	0.667	0.290	0.304	0.007	quoted
Present calculations:								
Herman Skillman pot.	-0.010	0.044	0.185	0.662	0.43	0.41	0.016	0.267
Gaspar potential	0.395	0.567	0.386	0.710	0.035	0.207	0.074	0.446
$f_{ex} = 1.50$								
Overlap of charge densities from a $4d^9 5s^2$ configuration	0.316	0.434	0.275	0.700	0.131	0.149	0.074	0.42

TABLE 4.2: Schematic Comparison of results for energy bands of copperand silver using similar potentials.

Potential	Copper	Silver
Gaspar -Empirical	Successful with $f_{ex} = 0.4$	Not successful
Herman-Skillman atomic potential	d-bands too narrow Fermi surface does not touch Brillouin zone	remarkably good close to self-consistent
Heine type	not tried except in our calculations on α-brass (Ref.67) $L_2' - L_1$ gap too large.	d-bands too high d-bands too wide
Superposed potentials	Best results obtained for $3d^{10}4s^1$ charge densities using $3d^94s^2$ wave functions	Best results obtained for $4d^{10}5s^1$ charge densities using $4d^95s^2$ configuration wave functions.

FIGURE CAPTIONS

Fig.4.1 'Charge' $Z(r) = -rV(r)/2$ for the potentials employed in the calculations for silver and for Snow's self-consistent potentials.

Fig.4.2 Energy bands of silver for a potential constructed from overlap of atomic potentials obtained for $4d^{10}5s^{1}$ configuration from wave functions for a $4d^{9}5s^{2}$ configuration.

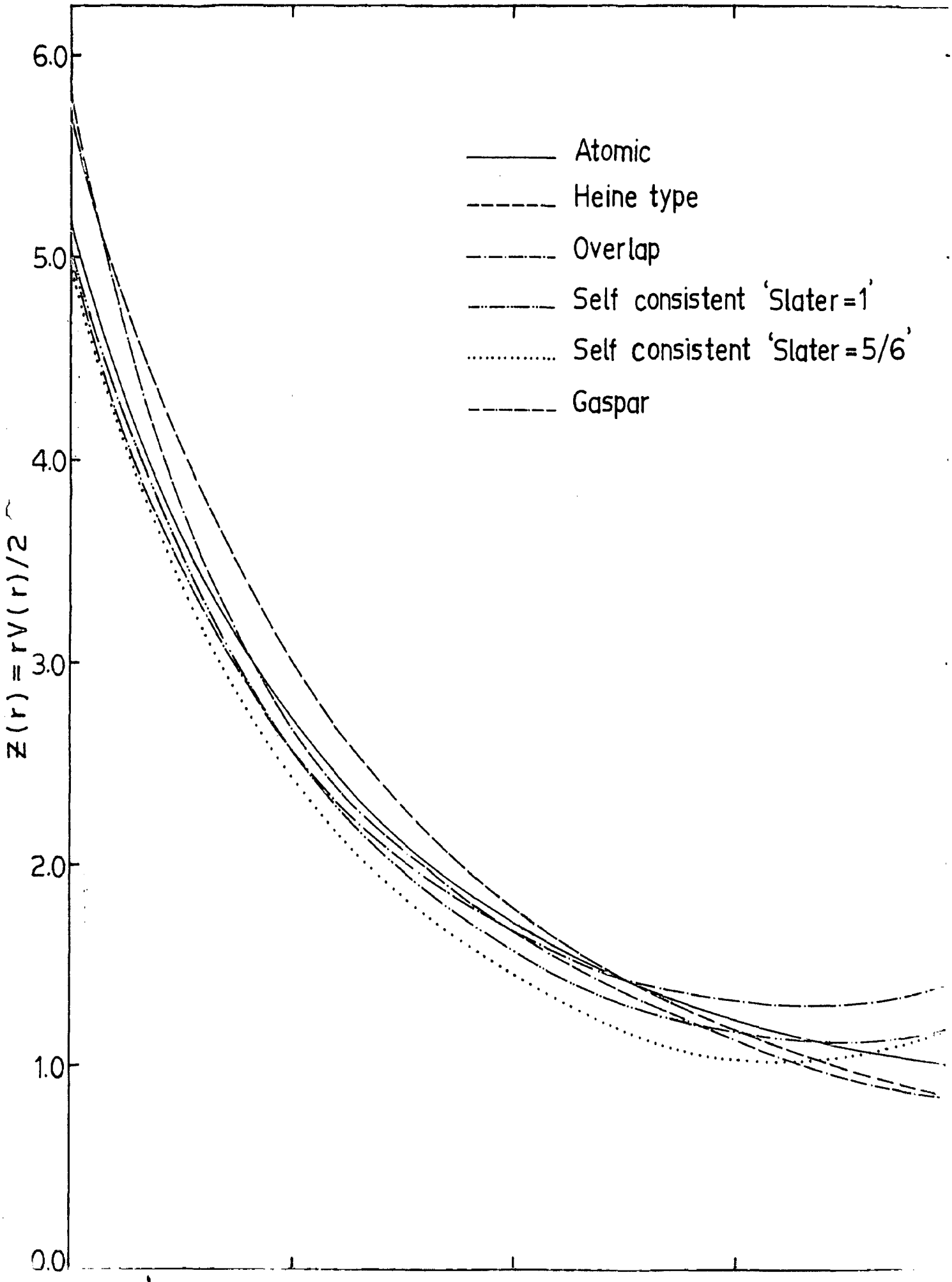
Atomic
Heine type
Overlap
Self consistent 'Slater=1'
Self consistent 'Slater=5/6'
Gaspar
6.0
5.0
4.0
3.0
2.0
1.0
0.0
Z(r) = rV(r)/2
1.0
1.5
2.0
2.5
RADIUS (BOHR UNITS)

FIG.4.1

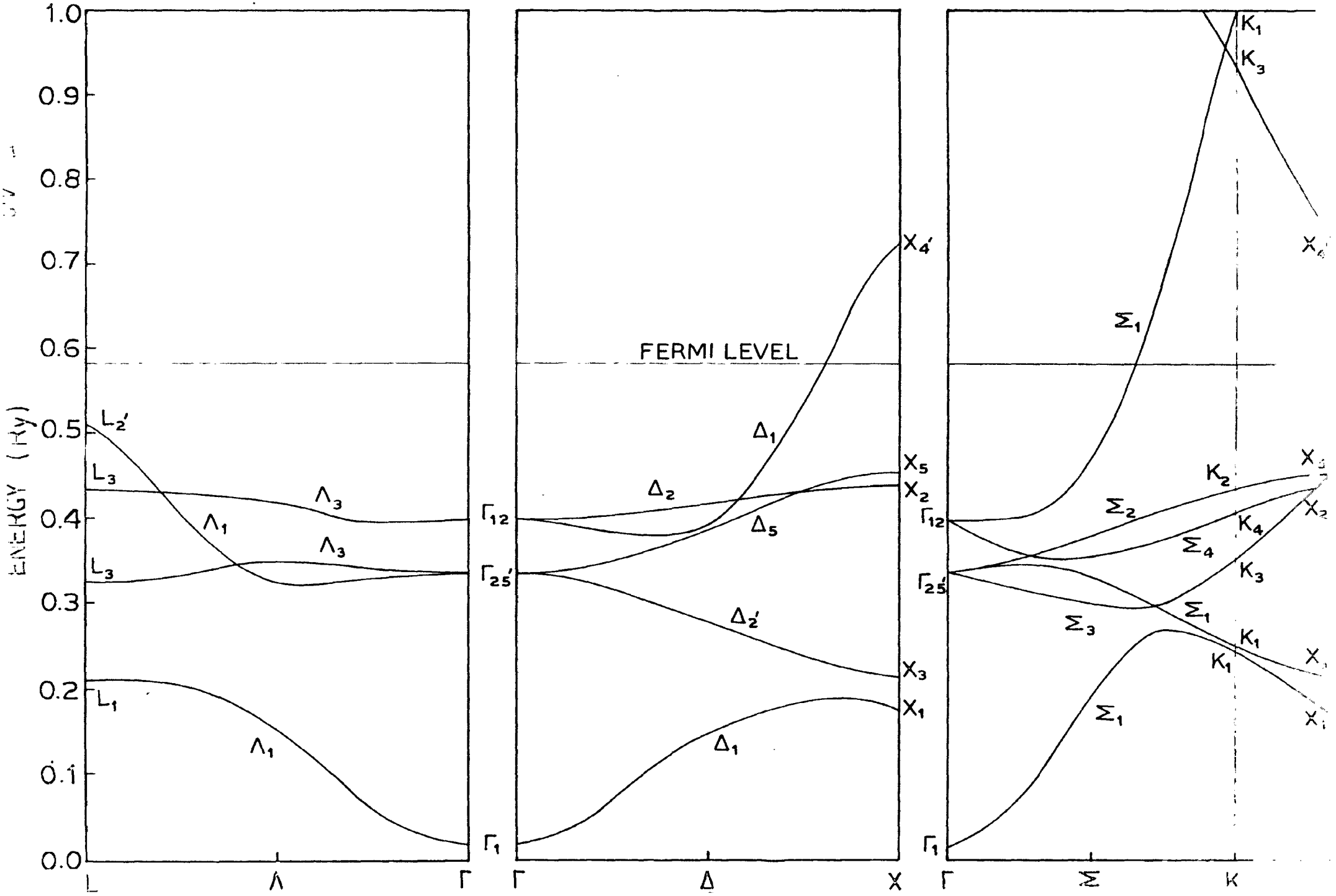
ENERGY (Ry)
1.0
0.9
0.8
0.7
0.6
0.5
0.4
0.3
0.2
0.1
0.0
FERMI LEVEL
L
Λ
Γ
Δ
X
Σ
K
L2'
L3
L3
L1
Λ1
Λ3
Λ3
Λ1
Γ12
Γ25'
Γ1
Δ1
Δ2
Δ5
Δ2'
Δ1
X4'
X5
X2
X3
X1
Σ1
Σ2
Σ4
Σ3
Σ1
Σ1
K1
K3
K2
K4
K3
K1
K1
X4
X5
X2
X3
X1

CHAPTER V

Virtual Crystal Models for electron states in Disordered Alloys:

The energy-band structure of pure metals and ordered alloys may be calculated by any of the standard techniques, such as the APW or the KKR method. Both techniques have been shown to give identical energy bands when the same potential is employed in the calculation. We can now claim to have a good understanding of the problem and with the availability of high speed computers, the calculations can also be carried out to a high degree of accuracy. The theories of disordered alloys, on the other hand, are still in a primitive stage, all the more so, at the level of application to real systems of interest.

We discuss in this chapter, some simple theories for disordered alloys, in which a kind of band structure is assumed to persist and an $E(\underline{k})$ relationship is derived. The effect of alloying is assumed only to alter this from that for the pure host. The results are compared usually with optical data with the assumption that direct transitions alone are important.

The simplest treatment of the disordered alloy problem invokes the virtual crystal approximation (VCA).[61,62] The VCA consists in replacing the disordered alloy by an equivalent ordered lattice where each site carries a

potential, which is the mean value over all possible configurations. Amar et al.[63-65] in their calculations for α-brass as well as β-brass use the KKR method and assume that the effective potential is given by

$$V(r) = m_A U_A^{(a)}(r) + m_B U_B^{(a)}(r). \qquad (5.1)$$

Here $U_A^{(a)}(r)$ and $U_B^{(a)}(r)$ are the atomic potentials and m_A, m_B are the atomic concentration of the constituents. It is clear that the virtual crystal approximation is an oversimplification . of the problem.[66]

An attempt to use better starting potential within the virtual crystal approximation, led to the conclusion that this itself is not enough.[67] In the virtual crystal approximation no account is taken of any short range ordering effects that may be present. The theory to be developed in the following is a generalization of the KKR theory of chapter II, to a disordered alloy, also taking into account any short-range order that may be present. The study was motivated by a suggestion of Phariseau and Ziman[68] that the KKR method can be generalized to the case of disordered systems. In treating a one component disordered system, Ziman[69] used Foldy's[70] Coherent wave approximation to define a configurationally averaged wave function. This wave function obeys a Bloch-type condition and can be used to determine the electronic spectra of liquid metals. Our problem differs

from that treated by Ziman in that, whereas in the case of liquid metals the disorder arises because the distance between the scattering centres is not fixed, in the present case it is because the spheres located at the lattice sites are not identical.

We consider only disordered substitutional binary alloys, and assume that the state of the alloy is completely specified by the short-range order parameters. In this formulation, the sense of the 'configuration averaging' is generalized beyond Ziman's considerations to derive Bloch-type conditions. The order parameters enter through the Green's function as well as through the averaged potentials. The secular determinant becomes a function of the state of order, besides the crystal structure and constituents of the alloy. The order parameters can be obtained from X-ray, electron or neutron diffraction measurements.[71-74]

We regard the alloy as consisting of two types of closed-shell positive ion cores, A and B, embedded in a medium of electrons. The potential at any point is built up as a superposition of screened potentials.

$$V(\underline{r}) = \sum_j U_j(\underline{r}-\underline{x}_j) \qquad (5.2)$$

where $\underline{x}_j$ is the position vector of the j^{th} ion carrying a potential $U_j(\underline{r})$. The potential $U_j(\underline{r})$ is approximated by a muffin-tin form. For the present application, this is

a fairly good approximation, and to a certain extent unavoidable.

Leaving aside the practical difficulties associated with the construction of the potential function, our problem is to solve the Schrodinger equation

$$[-\nabla^2 + V(\underline{r})]\,\psi(\underline{r}) = \kappa^2\,\psi(\underline{r}) \qquad (5.3)$$

where κ^2 is the energy of the electron state under consideration. The Schrodinger equation (4.3) is equivalent to the integral equation

$$\psi(\underline{r}) = \int G_o(\underline{r}-\underline{r}')\; V(\underline{r}')\,\psi(\underline{r}')\; d\underline{r}' \qquad (5.4)$$

where

$$G_o(\underline{r}-\underline{r}') = \frac{1}{4\pi}\;\frac{\exp(i\kappa|\underline{r}-\underline{r}'|)}{|\underline{r}-\underline{r}'|} \qquad (5.5)$$

is the free electron propagator. With the help of (5.2) we can write (5.4) as

$$\psi(r) = \sum_j \int G_o(\underline{r}-\underline{r}')\; U_j(\underline{r}'-\underline{x}_j)\;\psi(\underline{r}')\,d\underline{r}' \qquad (5.6)$$

$U_j(\underline{r}'-\underline{x}_j)$ is zero in the interstitial regions and therefore the integral equation relates the wave function to itself only in and on the spheres. We now introduce a variable $\underline{\rho}$ defined by

$$\underline{r} = \underline{x}_j + \underline{\rho}$$

when $\underline{r}$ is within or on the boundary of the j^{th} sphere, and write $\psi_j(\underline{\rho})$ for $\psi(\underline{x}_j+\underline{\rho})$. With this notation, we can

write Eq.(5.6) as

$$\psi_j(\underline{\rho}) = \sum_{j'} \int G_o(\underline{\rho}-\underline{\rho}'+\underline{x}_j-\underline{x}_{j'}) \, U_{j'}(\underline{\rho}') \, \psi_{j'}(\underline{\rho}') \, d\underline{\rho}' \, . \qquad (5.7)$$

In order to proceed ahead, we need another relation between $\psi_j(\underline{\rho})$ and $\psi_{j'}(\underline{\rho})$. In the case of a perfect crystal, the potential at all lattice sites is the same, and we can use the Bloch theorem

$$\psi_j(\underline{\rho}) = e^{i\underline{k}.(\underline{x}_j - \underline{x}_{j'})} \psi_{j'}(\underline{\rho}) \qquad (5.8)$$

to obtain the relation

$$\psi(\underline{\rho}) = \int G_{k\mathbf{x}}(\underline{\rho},\underline{\rho}') \, U(\underline{\rho}') \, \psi(\underline{\rho}') \, d\underline{\rho}' \qquad (5.9)$$

Here $G_{k\mathbf{x}}(\underline{\rho},\underline{\rho}')$ is the complete Green's function of the system given by

$$G_{k\mathbf{x}}(\underline{\rho},\underline{\rho}') = \sum_{j'} G_o(\underline{\rho}-\underline{\rho}'+\underline{x}_j-\underline{x}_{j'}) \, e^{i\underline{k}(\underline{x}_{j'}-\underline{x}_j)} \qquad (5.10)$$

This forms the starting point of the KR method.

For the case of a liquid metal, Ziman has shown that a Bloch type condition holds for the configurationally averaged wave function. We again arrive at Eq.(5.9), but the Green's function now becomes

$$G_{k\mathbf{x}}(\underline{\rho},\underline{\rho}') = G_o(\underline{\rho}-\underline{\rho}') + \int G_o(\underline{\rho}-\underline{\rho}'-\underline{x}) \, e^{i\underline{k}\underline{x}} \, n(\underline{x}) \, d\underline{x} \, .$$

The first term on the right hand side arises due to i = j in Eq.(5.10), while for the remaining terms, the summation has been replaced by an integration containing

$n(\underline{x})$, the probability of finding another sphere at a distance $\underline{x}$ from the one considered first.

We consider two types of configuration averages for a binary alloy, $\langle\psi_j(\underline{\rho})\rangle_A$ the average over all permissible configurations in which an A atom is in the sphere at $\underline{x}_j$ and $\langle\psi_j(\underline{\rho})\rangle_B$ the average over all configurations with B at $\underline{x}_j$. It is made plausible in the Appendix 3 that Ziman's conditions may be generalized to

$$\langle\psi_j(\underline{\rho})\rangle_A = e^{i\underline{k}(\underline{x}_j'-\underline{x}_j)}\langle\psi_{j'}(\underline{\rho})\rangle_A$$

and

$$\langle\psi_j(\underline{\rho})\rangle_B = e^{i\underline{k}(\underline{x}_j'-\underline{x}_j)}\langle\psi_{j'}(\underline{\rho})\rangle_B \qquad (5.11)$$

The summation in Eq.(5.7) is now divided in two parts Σ' over A atoms only and Σ'' over B atoms only:

$$\psi_j(\underline{\rho}) = \sum_{j'}' \int G_o(\underline{\rho}-\underline{\rho}'+\underline{x}_j-\underline{x}_{j'})\, U_A(\underline{\rho}')\,\psi_{j'}(\underline{\rho}')\, d\underline{\rho}'$$
$$+ \sum_{j'}'' \int G_o(\underline{\rho}-\underline{\rho}'+\underline{x}_j-\underline{x}_{j'})\, U_B(\underline{\rho}')\,\psi_{j'}(\underline{\rho}')\, d\underline{\rho}' . \qquad (5.12)$$

Introducing the configuration averages of Eq.(5.11) into (5.12), we arrive at the relations

$$\langle\psi_j(\underline{\rho})\rangle_A = \sum_{j'}' \int G_o^{AA}(\underline{\rho}-\underline{\rho}'+\underline{x}_j-\underline{x}_{j'})U_A(\underline{\rho}')\langle\psi_{j'}(\underline{\rho}')\rangle_A d\underline{\rho}'$$
$$+ \sum_{j'}'' \int G_o^{AB}(\underline{\rho}-\underline{\rho}'+\underline{x}_j-\underline{x}_{j'})U_B(\underline{\rho}')\langle\psi_{j'}(\underline{\rho}')\rangle_B d\underline{\rho}'$$

and

$$\langle\psi_j(\underline{\rho})\rangle_B = \sum_{j'}' \int G_o^{BA}(\underline{\rho}-\underline{\rho}'+\underline{x}_j-\underline{x}_{j'})\, U_A(\underline{\rho}')\langle\psi_{j'}(\underline{\rho}')\rangle_A d\underline{\rho}'$$
$$+ \sum_{j'}'' \int G_o^{BB}(\underline{\rho}-\underline{\rho}'+\underline{x}_j-\underline{x}_{j'})U_B(\underline{\rho}')\langle\psi_{j'}(\underline{\rho}')\rangle_B d\underline{\rho}'$$

Here, the first and the second superscripts on the free electron propagator denote the kind of atom located at the j^{th} and j'^{th} site, respectively. We now make use of the Bloch type conditions of Eq.(5.11) to obtain the following two equations

$$\langle\psi_j(\underline{\rho})\rangle_A = \sum_{j'}{}' \int G_o^{AA}(\underline{\rho}-\underline{\rho}'+\underline{x}_j-\underline{x}_{j'})\, U_A(\underline{\rho}')\, e^{i\underline{k}(\underline{x}_{j'}-\underline{x}_j)} \langle\psi_{j'}(\underline{\rho}')\rangle_A d\underline{\rho}'$$

$$+ \sum_{j}{}'' \int G_o^{AB}(\underline{\rho}-\underline{\rho}'+\underline{x}_j-\underline{x}_{j'}) U_B(\underline{\rho}')\, e^{i\underline{k}\cdot(\underline{x}_{j'}-\underline{x}_j)} \langle\psi_{j'}(\underline{\rho}')\rangle_B d\underline{\rho}'$$

and

$$\langle\psi_j(\underline{\rho})\rangle_B = \sum_{j'}{}' \int G_o^{BA}(\underline{\rho}-\underline{\rho}'+\underline{x}_j-\underline{x}_{j'})\, U_A(\underline{\rho}')\, e^{i\underline{k}(\underline{x}_{j'}-\underline{x}_j)} \langle\psi_{j'}(\underline{\rho}')\rangle_A d\underline{\rho}'$$

$$+ \sum_{j} \int G_o^{BB}(\underline{\rho}-\underline{\rho}'+\underline{x}_j-\underline{x}_{j'})\, U_B(\underline{\rho}')\, e^{i\underline{k}(\underline{x}_{j'}-\underline{x}_j)} \langle\psi_{j'}(\underline{\rho}')\rangle_B d\underline{\rho}' .$$

These expressions may be rewritten in terms of a set of in complete Green's function as

$$\langle\psi(\underline{\rho})\rangle_A = \int G_{k\chi}^{AA}(\underline{\rho},\underline{\rho}') U_A(\underline{\rho}')\langle\psi(\underline{\rho}')\rangle_A d\underline{\rho}' + \int G_{k\chi}^{AB}(\underline{\rho},\underline{\rho}') U_B(\underline{\rho}')\langle\psi(\underline{\rho}')\rangle_B d\underline{\rho}' \qquad (5.13a)$$

and

$$\langle\psi(\underline{\rho})\rangle_B = \int G_{k\chi}^{BA}(\underline{\rho},\underline{\rho}') U_A(\underline{\rho}')\langle\psi(\underline{\rho}')\rangle_A d\underline{\rho}' + \int G_{k\chi}^{BB}(\underline{\rho},\underline{\rho}') U_B(\underline{\rho}')\langle\psi(\underline{\rho}')\rangle_B d\underline{\rho}' . \qquad (5.13b)$$

The incomplete Green's functions occuring in the above expressions are defined by

$$G^{ss'}_{k\kappa}(\underline{\rho},\underline{\rho}') = G_0(\underline{\rho}-\underline{\rho}')\ \delta_{ss'} + \Sigma' G_0(\underline{\rho}-\underline{\rho}'-\underline{x})\, e^{i\underline{k}\underline{x}}\, P^{ss'}(\underline{x}). \quad (5.14)$$

Here $P^{ss'}(\underline{x})$ is the probability that a site at a distance $\underline{x}$ from an atom of the s^{th} type is of the s'^{th} type, and the prime on the summation sign denotes that the $x = 0$ term is excluded. Within the sphere of variables $\underline{\rho},\underline{\rho}'$ the Green's functions satisfy the following equation

$$(\nabla^2 + \kappa^2)\ G^{ss'}_{k\kappa}(\underline{\rho},\underline{\rho}') = \delta_{ss'}\delta(\underline{\rho}-\underline{\rho}').$$

The Green's functions depend upon k and κ, but these subscripts will be dropped henceforth.

In Eq.(5.13), we replace the potential $U_s(\underline{\rho})$ by its configurational average and treat $\langle\psi(\underline{\rho})\rangle_s$ as a solution of the Schrodinger equation for this averaged potential. A typical term of Eqs.(5.13a) and (5.13b) then simplifies as follows:

$$\begin{aligned}
&\int G^{AA}(\underline{\rho},\underline{\rho}')\, U_A(\underline{\rho}')\, \langle\psi(\underline{\rho}')\rangle_A\, d\underline{\rho}' \\
&= \int G^{AA}(\underline{\rho},\underline{\rho}')\, [\nabla^2\langle\psi(\underline{\rho}')\rangle_A + \kappa^2\langle\psi(\underline{\rho}')\rangle_A]\, d\underline{\rho}' \\
&= \int [G^{AA}(\underline{\rho},\underline{\rho}')\, \nabla'^2\langle\psi(\underline{\rho}')\rangle_A - \langle\psi(\underline{\rho}')\rangle_A \nabla'^2 G^{AA}(\underline{\rho},\underline{\rho}')]\, d\underline{\rho}' \\
&\qquad + \int \delta(\underline{\rho}-\underline{\rho}')\, \langle\psi(\underline{\rho}')\rangle_A\, d\underline{\rho}' .
\end{aligned}$$

We use Green's theorem to convert the volume integral into a surface integral over the muffin-tin sphere, and obtain

$$\int G^{AA}(\underline{\rho},\underline{\rho}')\, U_A(\underline{\rho}')\, \langle\psi(\underline{\rho}')\rangle_A\, d\underline{\rho}'$$

$$= \int [G^{AA}(\underline{\rho},\underline{\rho}')\nabla\langle\psi(\underline{\rho}')\rangle_A - \langle\psi(\underline{\rho}')\rangle_A \nabla G^{AA}(\underline{\rho},\underline{\rho}')]\, ds'$$

$$+ \int \delta(\underline{\rho}-\underline{\rho}')\, \langle\psi(\underline{\rho}')\rangle_A\, d\underline{\rho}'.$$

Simplifying the other terms on the right hand side of (5.13a) and (5.13b) in a similar manner, we have

$$\langle\psi(\underline{\rho})\rangle_A = \int [G^{AA}(\underline{\rho},\underline{\rho}')\, \frac{\partial}{\partial\rho'}\, \langle\psi(\underline{\rho}')\rangle_A - \langle\psi(\underline{\rho}')\rangle_A\, \frac{\partial}{\partial\rho'}\, G^{AA}(\underline{\rho},\underline{\rho}')]\, ds'$$

$$+ \int \delta(\underline{\rho}-\underline{\rho}')\langle\psi(\underline{\rho}')\rangle_A\, d\underline{\rho}'$$

$$+ \int [G^{AB}(\underline{\rho},\underline{\rho}')\, \frac{\partial}{\partial\rho'}\langle\psi(\underline{\rho}')\rangle_B - \langle\psi(\underline{\rho}')\rangle_B\, \frac{\partial}{\partial\rho'}\, G^{AB}(\underline{\rho},\underline{\rho}')]\, ds'$$

and

$$\langle\psi(\underline{\rho})\rangle_B = \int [G^{BA}(\underline{\rho},\underline{\rho}')\, \frac{\partial}{\partial\rho'}\langle\psi(\underline{\rho}')\rangle_A - \langle\psi(\underline{\rho}')\rangle_A\, \frac{\partial}{\partial\rho'}\, G^{BA}(\underline{\rho},\underline{\rho}')]\, ds'$$

$$+ \int [G^{BB}(\underline{\rho},\underline{\rho}')\, \frac{\partial}{\partial\rho'}\langle\psi(\underline{\rho}')\rangle_B - \langle\psi(\underline{\rho}')\rangle_B\, \frac{\partial}{\partial\rho'}\, G^{BB}(\underline{\rho},\underline{\rho}')]\, ds'$$

$$+ \int \delta(\underline{\rho}-\underline{\rho}')\, \langle\psi(\underline{\rho}')\rangle_B\, d\underline{\rho}' \qquad (5.15)$$

The integrals involving δ-functions cancel with the terms on the left.

The steps now onwards proceed in a manner parallel to that of the non-variational derivation of the KKR method. The spherical symmetry of the potential within the muffin-tin sphere enables us to write

$$\langle\psi(\underline{\rho})\rangle_S = \sum_L i^l\, \alpha_L^{(s)} R_l^{(s)}(\rho)\, Y_L(\hat{\underline{\rho}}).$$

Here, L denotes the pair of angular momentum quantum

numbers l and m and $Y_L(\hat{\underline{\rho}})$ are real spherical harmonics as used in Chapter II, and $R_\ell^{(s)}(\rho)$ are the solutions of the radial part of the Schrodinger equation for the s^{th} potential. The Green's functions may also be expanded as

$$G^{ss'}(\underline{\rho},\underline{\rho}') = \sum_L \sum_{L'} \Big[i^{\ell-\ell'} B^{ss'}_{LL'} \, j_l(\varkappa\rho) \, j_{l'}(\varkappa\rho') + \varkappa \, \delta_{LL'} \, \delta_{ss'} \, j_l(\varkappa\rho) \, n_{l'}(\varkappa\rho') \Big] Y_L(\hat{\underline{\rho}}) Y_{L'}(\hat{\underline{\rho}}') \qquad (5.16)$$

where j_l and n_l denote, respectively, spherical Bessel and Neumann functions, and $B^{ss'}_{LL'}$ are coefficients to be determined. On substituting these expressions in Eq.(5.15) we arrive at

$$\sum_{L'} \sum_{s'} \Big[B^{ss'}_{LL'} + \varkappa \cot \eta_l^{(s)} \, \delta_{LL'} \, \delta_{ss'} \Big] \beta^{s'}_{L'} = 0. \qquad (5.17)$$

Here, we have redefined the parameters of the trial function as

$$\beta_L^{(s)} = \alpha_L^{(s)} \Big[R_l^{(s)}(r) \frac{d}{dr} [j_l(\varkappa r)] - j_l(\varkappa r) \frac{d}{dr} [R_l^{(s)}(r)] \Big]_{r=r_{mt}}$$

and $\eta_\ell^{(s)}$ is the phase shift of the l^{th} partial wave for the s^{th} atom defined by

$$\cot \eta_\ell^{(s)} = \left[\frac{R_l^{(s)}(r)(d/dr)[n_l(\varkappa r)] - n_l(\varkappa r)(d/dr)[R_l^{(s)}(r)]}{R_l^{(s)}(r)(d/dr)[j_l(\varkappa r)] - j_l(\varkappa r)(d/dr)[R_l^{(s)}(r)]} \right]_{r=1}$$

and r_{mt} is the radius of the muffin-tin sphere.

The structure constants depend on the energy and the wave vector, and the phase shifts depend on the energy. The condition (5.17), therefore, leads to the following implicit relationship between the energy and the wave vector.

$$\det \left| B_{LL'}^{ss'} + \kappa \cot \eta_{\ell}^{(s)} \delta_{LL'} \delta_{ss'} \right| = 0 \qquad (5.18)$$

The energy eigenvalues are determined by locating the values of E for which the determinant vanishes. The procedure adopted is analogous to the usual KKR method. The structure constants, logarithmic derivatives of the radial functions, the Bessel functions are tabulated at a sequence of energies. The determinant is then evaluated for these energies and interpolated to locate the zero.

Ziman[69] showed that for a one-component disordered system, a Bloch-type condition can be obtained, provided the wave function within any sphere is interpreted as the average value of the wave function for an ensemble where this sphere is fixed, while the remaining spheres take all the permitted configurations. In the pure metal case, the rearrangement of the atoms among the lattice site does not produce any new configuration. Therefore the configurationally-averaged wave function is just the same as the wave function for the potential at a site. However, in the case of a disordered binary alloy, the averaged wave function is different from the wave function for a crystal of either A or B atoms.

The average potential around any site is taken to be the actual potential at the site plus contributions from neighbouring atoms, their average arrangement being described in terms of the short-range order parameters. Let $P[B|A(i)]$ denote the probability that if a given site is occupied by a B atom, then a site which is its i^{th} neighbor is occupied by an A atom. We denote this by p_i and assume that a knowledge of $p_i (i = 1,2,\ldots)$ gives an adequate description of the state of order in the alloy crystal.

If $\underline{r}_\alpha$ denotes the position of the various lattice sites referred to the B site under consideration as origin, then the potential at a point B distant $\underline{r}$ from B, is, on the average:

$$\overline{V}_B(\underline{r}) = U_B^{(a)}(\underline{r}) + \sum_\alpha \left\{P[B|A(i)]U_A^{(a)}(\underline{r}-\underline{r}_\alpha) + P[B|B(i)]U_B^{(a)}(\underline{r}-\underline{r}_\alpha)\right\}$$

The summation is over all lattice sites, though it is only the contribution from the immediate neighborhood, that is significant, Similarly, we have for an A atom,

$$\overline{V}_A(r) = U_A^{(a)}(\underline{r}) + \sum_\alpha \left\{P[A|A(i)]U_A^{(a)}(\underline{r}-\underline{r}_\alpha) + P[A|B(i)]U_B^{(a)}(\underline{r}-\underline{r}_\alpha)\right\}$$

In fact, the P's are related to the p_i's by the following relationships[75]

$$P[B|A(i)] = p_i$$

$$P[B|B(i)] = 1 - p_i$$

$$P[A|A(i)] = 1 - p_i m_B/m_A$$

$$P[A|B(i)] = p_i m_B/m_A$$

We can now write the final expressions for $\overline{V}_A(\underline{r})$ and $\overline{V}_B(\underline{r})$ in terms of p_i alone as

$$\overline{V}_A(\underline{r}) = U_A^{(a)}(\underline{r}) + \sum_\alpha \left[(1-p_i m_B/m_A)U_A^{(a)}(\underline{r}-\underline{r}_\alpha)+(p_i m_B/m_A)U_B^{(a)}(\underline{r}-\underline{r}_\alpha)\right] \tag{5.19}$$

and

$$\overline{V}_B(\underline{r}) = U_B^{(a)}(\underline{r}) + \sum_\alpha \left[p_i U_A^{(a)}(\underline{r}-\underline{r}_\alpha) + (1-p_i)U_B^{(a)}(\underline{r}-\underline{r}_\alpha)\right] \tag{5.20}$$

We require the potentials $\overline{V}_A(\underline{r})$ and $\overline{V}_B(\underline{r})$ to be of the muffin-tin form. The overlap from neighbouring sites is therefore, evaluated using Lowdin's α-function expansion technique and retaining only the spherically symmetric term.

The potential is built up as a sum of a Coulomb and an exchange part; both being obtained from free-atom wave functions. The Coulomb potential due to a given site plus contribution from Coulomb potentials on neighboring sites gives the crystal Coulomb potential. The crystal charge density is obtained by an overlap of the atomic charge densities. The exchange potential can then be obtained by Slater's formula. The contribution due to a particular kind of atom from a given neighborhood is multiplied by its occupation probability and summed as in Eqs. (5.19) and (5.20) to give the averaged potentials.

Except for the introduction of these probability factors, the procedure is exactly similar to the well-known Mattheiss prescription[42] for constructing a muffin-tin potential. The radial functions $R_l^{(s)}(r)$ are the solution of the Schrodinger equation for these potentials.

Evaluation of Structure Constants:

The $B_{LL'}^{ss'}$ occurring in Eq.(5.18) are the coefficients in the angular momentum representations of the incomplete Green's functions of Eq.(5.14). These are given by the expression

$$G^{ss'}(\underline{R}) = -\frac{1}{4\pi} \sum_{\alpha} \frac{e^{ix|\underline{R}-\underline{r}_\alpha|}}{|\underline{R}-\underline{r}_\alpha|} e^{i\underline{k}.\underline{r}_\alpha} P^{ss'}(\underline{r}_\alpha), \quad (5.21)$$

where the summation is over all lattice sites and $P^{ss'}(\underline{r}_\alpha)$ is the probability of finding an s'^{th} type atom at a position $\underline{r}_\alpha$ with respect to an atom of the s^{th} type. For the case of a perfect lattice $P^{ss'}(r_\alpha)$ is always unity ($s \equiv s'$), and Ham and Segall[76] have used the Ewald's method to express this infinite series in direct space as a sum of two rapidly convergent series - one in direct space and the other in reciprocal space. For the case of the disordered alloy the presence of the $P^{ss'}(\underline{r}_\alpha)$ term does not allow us to follow such an approach. Therefore, we assume that the short-range order extends only upto a neighborhood σ. Then we have

$$G^{ss'}(\underline{R}) = P_R^{ss'} G(\underline{R}) - \sum_{\alpha<\sigma} \frac{\exp(i\kappa|\underline{R}-\underline{r}_\alpha|)}{|\underline{R}-\underline{r}_\alpha|} e^{i\underline{k}\cdot\underline{r}_\alpha}$$

multiplication always

$$\times [P^{ss'}(\underline{r}_\alpha) - P_R^{ss'}] \qquad (5.22)$$

we may expand these Greenians as

$$G^{ss'}(\underline{R}) = -\frac{1}{4\pi} \frac{\mathrm{Cos}(\kappa R)}{R} + \sum_L i^{\ell} D_L^{ss'} j_l(\kappa R) Y_L(\hat{\underline{R}}). \qquad (5.23)$$

$D_L^{ss'}$ are called the structure constants and are related to the $B_{LL'}^{ss'}$ of Eq.(5.18) by

$$B_{LL'}^{ss'} = \sum_{L''} D_{L''} C_{LL'L''}$$

and $C_{LL'L''}$ are related to the Clebsch-Gordon coefficients. Comparing Eqs.(5.22) and (5.23), we arrive at the following expression for the structure constants

$$D_L^{ss'} = P_R^{ss'} D_L + \kappa i^{-1} \sum_{\alpha<\sigma}' e^{i\underline{k}\cdot\underline{r}_\alpha} [n_l(\kappa r_\alpha) - i\, j_l(\kappa r_\alpha)]$$

$$\times Y_L(\hat{\underline{r}}_\alpha) [P^{ss'}(r_\alpha) - P_R^{ss'}]. \qquad (5.25)$$

Here the D_L without the superscript, denotes the structure constants for a perfect lattice. The summation extends indirect space through a neighbornood σ , and the prime on the summation indicates that $\alpha = 0$ is excluded. Eq.(5.25) offers a convenient way of calculating the structure constants for the disordered lattice. The determination of the phase shifts is straightforward, as in the pure metal band structure problem. The eigenvalues

are then determined by evaluating the determinant (5.18) at a sequence of energies and then locating its zero by interpolation.

The theory outlined above has been applied to α-brass[77] and disordered Cu_3Au.[78] The choice was guided by the availability of experimental data. The former system α-brass does not possess any short range order[71] and the structure constants in this case are related by simple factors to that of the perfect host lattice. The latter Cu_3Au is well known for exhibiting short-range order effects and requires the use of the full form (5.25). We consider these applications in the following.

Application to α-brass:

In this scheme, the potential as well as the structural part depend upon the short-range-order parameters. The absence of short-range order in the case of α-brass, brings about a considerable simplification, because the pair correlation factors $P[A|B(i)]$, $P[B|B(i)]$, etc. depend simply on the concentration of the solute (zinc) and are independent of the neighborhood.

The averaged potentials for Cu and Zn are determined as discussed before. The atomic potentials, employed to calculate the averaged potentials, were derived from a Hartree-Fock-Slater scheme using the Herman-Skillman program. An overlap was carried through 6th neighbors.

It was assumed that there is no change in the lattice parameter upon alloying zinc with copper. The radii of the copper and zinc spheres were both chosen to be equal to the inscribed sphere radius r_{ins}. The constant potential in the interstitial region is chosen to be

$$V_c = 0.5 \left[V_{Cu}(r_{ins}) + V_{Zn}(r_{ins}) \right].$$

The structure constants $D_L^{ss'}$ have a very simple relationship to those for a perfect fcc lattice, because of the short range order. Eq.(5.25) reduces to

$$D_L^{ss'} = m_{s'} D_L$$

where D_L is the structure constant for the perfect f.c.c. lattice and $m_{s'}$ is the atomic concentration of the s'^{th} component.

Calculations were performed for the energies of conduction and d bands at the high symmetry points Γ, X, and L for a range of 0-30% Zn concentration. The results are presented in Table 5.1 and in Table 5.2 we compare the changes in important level separations obtained from the present calculation, with experiment and other theoretical results.

The experimental information is available from the optical studies of α-brass by Biondi and Rayne.[6] Their results are shown in Fig.5.1. They observed that the 2.2 eV absorption peak in pure copper shifts to 2.6 eV

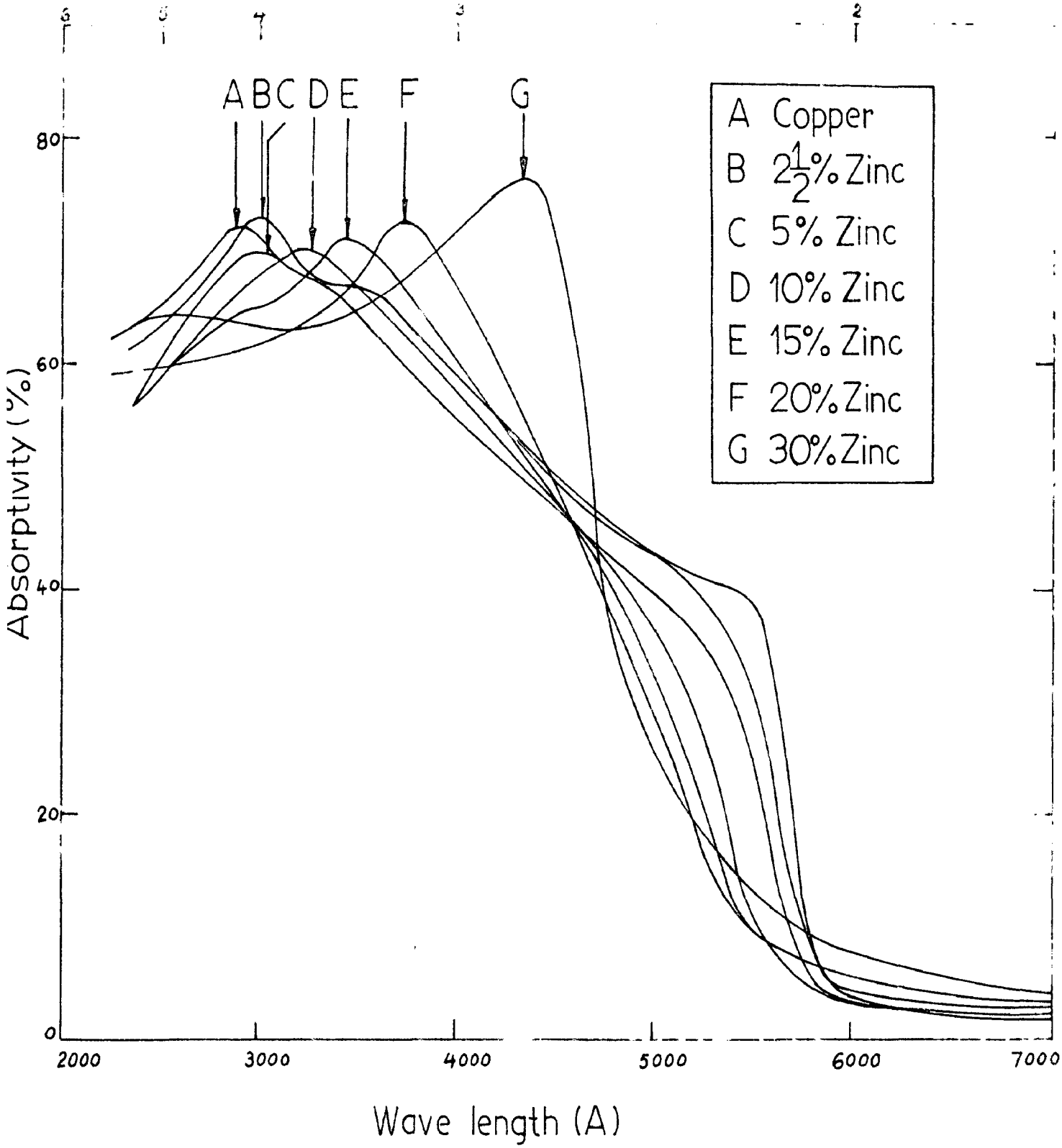

FIG 5.1 Optical absorptivity of ∝-brasses as measured by Biondi and Rayne.

for α-$Cu_{0.70}$ $Zn_{0.30}$. The secondary absorption peak at 4.2 eV in pure Cu shifts to lower energies, with increasing zinc concentration, the reduction being 1.3 eV for 30% Zn.

The other theoretical calculations for α-brass are of Amar, Johnson and Sommers[64] and of Soven.[79] Amar et al. use the virtual crystal approximation for the conduction bands and assume that the d-band are unaltered upon alloying. Soven uses an averaged t-matrix approximation. However, in order to perform numerical calculations, Soven had to separate the conduction and d-band problems. In the present formulation of the disordered alloy problem, both the conduction and d-bands are treated on the same footing, and we find that the downward shift of the X_5 level is in almost exact agreement with that calculated by Soven. Our computed shift for 30% Zn is 0.023 Ry. compared to 0.025 Ry obtained by Soven. We may mention here, that the term d-like states is used here for the d bands originating due to the copper atoms. We do not consider at all the d-bands arising from the Zn atoms. It is well known that in pure Zn and probably in α-brass too, the bands for the d electrons of zinc are highly atomic in character and are not influenced by the environment.

Table 5.2 shows that the predictions of our model are in good agreement with Soven's results but differ considerably from the experimental values. We attribute the discrepancy to the simplified model assumed for an

alloy. It may also be partly be due to the choice of potentials. The almost exact agreement with experiments of AJS is perhaps fortuitous, because for Ag-In alloys those scheme did not give satisfactory results.[67]

It is clear that as the Zn concentration changes, the averaged potentials of the constituents will be modified and also the distribution of the constituents amongst the lattice sites will alter. AJS ignore effects due to change in the arrangement of atoms amongst the lattice sites, and attribute all effects of alloying to changes in potential only. On the other hand, Soven uses potentials which are independent of Zn concentration, thus ignoring certain effects of alloying. In our formulation, both $V_{Cu}(r)$ and $V_{Zn}(r)$ are functions of Zn concentration. The internal arrangement dependence in the problem is introduced via the partial Green's functions of Eq.(5.14), which also depend on the Zn concentration. Thus, from this point of view, our model gives a better picture of the disordered alloy.

However, it must be conceded that the model is still a very simplified approximation to a real disordered alloy. When we employ Bloch-type conditions, we are in effect equating the alloy to a periodic system, implying thereby infinite lifetime of the eigenstates. This is clearly not so. A true eigenfunction of an electron moving in a disordered assembly of atoms will be very complicated and will eventually be diffracted and scattered

into all possible waves. The function assumed by us is an approximate solution, valid only for a limited time. We have assumed them to be valid for ever. Using better theories, like the coherent potential approximation (to be discussed in Chapter 7), to calculate the spectral density of states in α-brass, we find that the widths of the peaks for s-p states are of the order of 1% of a Brillouin Zone dimension. This indicates that the wave functions are very nearly Bloch functions. For d-like states, the widths are slightly larger. The assumptions implicit in defining a Bloch-type condition may not be too bad.

Application to Disordered Cu_3Au

The alloy Cu_3Au is a classical example of one undergoing the order-disorder transformation. For the perfectly ordered state, all Au atoms are at the conners and Cu atoms at the face centers of a cubic lattice. Above the critical temperature of 390°C there is no long range ordering present. But short-range-order exists and both X-ray and electron diffraction methods have been used[72-74] to study the variation of the short-range-order with temperature in this system.

Many physical properties of this alloy have been measured both in the ordered and disordered states. The Hall coefficient was found to be negative for the disordered alloy, but becomes positive for the ordered phase.[80]

However, the variation of the Hall coefficient with the short range-order was small. Airoldi and coworkers have carried out measurements of the magnetic susceptibility as well as thermoelectric power as a function of the short-range-order for Cu_3Au.[81] They conclude that the electronic structure and the Fermi surface (if we may use the term) for Cu_3Au is quite similar to that of pure Cu. The specific heat measurements by Rayne[82] failed to detect a difference in the density of states at the Fermi surface between the ordered and disordered state. Recent and more refined experiments do show a variation of 3.5% with the setting in a order.[83] The soft X-ray emission spectroscopy shows that the spectrum for this alloy is almost identical with the spectrum of pure Cu. Besides, there is no detectable difference between the emission spectra from the alloy in the ordered and disordered conditions.[84] The positron-annihilation experiments by Dakhtyar et al. revealed the maximum conduction-electron momentum to be the same for both the ordered and disordered Cu_3Au.[85] Very recently, both the ordered and disordered Cu_3Au have been studied by optical and photoemission techniques, and the imaginary part of the dielectric constant has been obtained from a Kramers-Kroing analysis of the data. The spectrum of the disordered sample was found to be well represented by a superposition of the spectra of the constituents.[86]

All these properties cannot be interpreted in

terms of the band structure alone. Still, we thought it would be interesting to investigate tne dependence of the band structure of disordered Cu_3Au, on the degree of the short-range order. Fairly detailed calculations of the energy bands have already been carried out for the ordered Cu_3Au by Gray and Brown.[87] They employed the modified plane-wave method in conjunction with the orthogonalized-plane-wave method. The crystal potential was constructed by slightly modifying the atomic potentials of Herman and Skillman.

The method for calculation adopted here for disordered Cu_3Au is very similar to the one discussed before for α-brass. The potentials were determined by considering the overlap from neighboring sites, as indicated in Eqs.(5.19) and (5.20). The occupation probabilities were derived from the available experimental data on short-range-order parameters. The starting atomic potentials and charge densities were obtained from the non-relativistic program of Herman and Skillman. The relativistic wave functions were not employed in view of the fact that the band calculation itself is a non-relativistic one.

The energies were computed for states of different representations at the symmetry points Γ, X, and L for disordered Cu_3Au at temperatures of 405°C, 450°C and 550°C. Cowley's short-range order parameters were used for 550°C while for the other two temperatures, results from the

more accurate measurements of Moss were employed. These parameters are tabulated in Table 5.3. The results of the calculation are presented in Table 5.4. The muffin-tin radius r_{mt} was chosen to be equal for Cu and Au and equal to 2.46095 a.n. In order to see how the alteration of σ affects the results, we performed calculations for $\sigma = 6$, as well as $\sigma = 10$. Except for the Γ_{25}' and Γ_{12} states (which changed by as much as 0.06 Ry), the change was not more than 0.004 Ry. The satisfactory convergence shows that the approximation involved in calculating the partial Greenians is not bad. Although the scheme adopted takes account of short-range-correlations, it is still a simplified treatment of a real disordered alloy. It was therefore felt that a very detailed calculation of the energy bands is not merited at this stage. Even with the limited calculation reported here, it is possible to have some idea of the distortion of the Fermi surface. The results indicate only slight variation in the energy levels with temperature. The fact that the shifts with temperature of some of these levels are not regular is a bit unsatisfactory, and may be ascribed to the different sources of the short-range order parameters employed in the calculation.

If we interpret the peak at 2.4 eV observed by Nilsson and Norris[86] to direct transitions along, we notice that the $X_5 - X_4'$ transition is a suitable one. Our calculation shows this to be significantly constant at

1.5 eV. The calculations also show that although the positions of the s-p bands are appreciably altered, relative to that for pure copper, the d-bands are relatively unchanged. This explains why the soft X-ray emission spectrum for the disordered Cu_3Au is similar that of pure Cu, and conforms to Rookes' interpretation of this effect.[88]

The formalisms and calculations discussed above were virtual crystal models based on a KKR framework. A virtual crystal approximation, based on the APW framework has been proposed by Schoen.[89] His model excludes both long and short-range order. The muffin-tin potential was constructed separately for each component and is similar to that discussed in Ref.67, 77. Schoen starts from APW pseudopotential formalism of Lloyd[25] and uses a random phase approximation to show that the logarithmic derivative of the component spheres on equivalent lattice sites have been replaced by a weighted average or effective logarithmic derivative. The standard APW programs developed for perfect crystals may now be used to determine the energy eigenvalues. Moreover, the symmetry of the alloy superlattice can be exploited to simplify the calculations. The APW VCA was applied to determine the band structure, density of states as a function of vacancy concentration and composition for TiO and hence to study its stability.[90] Applications to most other alloy systems of interest have not been reported.

TABLE 5.1: Energy values (in Ry) for conduction and d-band states in α-CuZn for a range of Zn concentrations

	0%	5%	10%	15%	20%	25%	30%
Γ_1	-1.2970	-1.3334	-1.3356	-1.3379	-1.3417	-1.3448	-1.3487
Γ_{25}'	-0.8531	-0.8557	-0.8555	-0.8552	-0.8545	-0.8540	-0.8535
Γ_{12}	-0.8078	-0.8116	-0.8133	-0.8151	-0.8169	-0.8187	-0.8205
X_4'	-0.5009	-0.5219	-0.5298	-0.5389	-0.5403	-0.5590	-0.5656
X_2	-0.7786	-0.7829	-0.7862	-0.7893	-0.7924	-0.7954	-0.7988
X_3	-0.8514	-0.9486	-0.9431	-0.9317	-0.9414	-0.9263	-0.9218
X_1	-0.1235	-0.1463	-0.1595	-0.1712	-0.1839	-0.1967	-0.2095
X_5	-0.7691	-0.7733	-0.7770	-0.7806	-0.7842	-0.7887	-0.7923
L_1	-0.3506	-0.3604	-0.3823	-0.3944	-0.4067	-0.4195	-0.4319
L_2'	-0.7330	-0.7573	-0.7640	-0.7718	-0.7803	-0.7875	-0.7933
L_3	-0.7773	-0.7663	-0.7792	-0.7720	-0.7782	-0.7824	-0.7870

TABLE 5.2: Comparison of experimental and theoretical results for the level shifts and changes in energy gaps (in Ry) from Cu to α-$Cu_{0.70}Zn_{0.30}$.

	$\Delta X_{4'}$	$\Delta L_{2'}$	ΔL_1	ΔX_5	$\Delta(L_1-L_{2'})$	$\Delta(X_1-X_{4'})$	$\Delta(E_F-L_3)$
Experiment: Biondi and Rayne					0.096		0.026
Theoretical:							
AJS	0.051	0.043	0.139		0.094	0.008	0.035
Soven	0.050	0.045	0.058	0.025	0.013		0.062
Present calculations	0.065	0.060	0.081	0.023	0.021	0.021	0.055

TABLE 5.3: Short-range order parameters p_i for Cu_3Au employed in the present calculation

i	Neighbor lmn	Short-range order parameter 465°C	450°C	550°C
1	110	-0.218	-0.195	0.131
2	200	+0.286	+0.215	+0.105
3	211	-0.012	+0.003	+0.026
4	220	+0.122	+0.077	+0.047
5	310	-0.073	-0.052	-0.032
6	222	+0.069	+0.028	-0.009
7	321	-0.023	-0.010	-0.003
8	400	+0.067	+0.036	+0.019
9	330	-0.028	-0.015	-0.011
	411	+0.004	+0.007	+0.007
10	420	+0.047	+0.015	+0.007

TABLE 5.4: Energy values at the symmetry points Γ, X, and for the disordered Cu_3Au as a function of the temperature. All the energies are in Ry., and relative to the muffin-tin zero $V_0 = -1.1358$. σ denotes the order of the significant neighborhood.

	405°C σ = 6	405°C σ =10	450°C σ = 6	450°C σ = 10	550°C σ = 6	550°C σ = 10
Γ_1	0.0041	0.0042	0.0041	0.0041	0.0041	0.0039
$\Gamma_{25'}$	0.5581	0.6114	0.5572	0.5994	0.6499	0.6076
Γ_{12}	0.6009	0.6410	0.5390	0.6276	0.5717	0.6469
L_{11}(lower)	0.4952	0.4933	0.4950	0.4950	0.4952	0.4828
L_{12}(higher)	0.9938	0.9906	0.9894	0.9883	1.0281	0.9790
$L_{2'}$	0.5539	0.5573	0.5544	0.5544	0.5732	0.5687
L_{31}(lower)	0.6023	0.6016	0.6022	0.6019	0.6005	0.6003
L_{32}(higher)	0.6668	0.6670	0.6673	0.6673	0.6724	0.6724
X_{11}(Lower)	0.5013	0.5017	0.5004	0.5026	0.4981	0.4982
X_{12}(hither)	1.1847	1.1857	1.1861	1.1866	1.2334	1.2341
X_2	0.6548	0.6542	0.6558	0.6558	0.6604	0.6604
X_3	0.5574	0.5570	0.5565	0.5567	0.5499	0.5500
$X_{4'}$	0.7753	0.7693	0.7746	0.7714	0.7930	0.7933
X_5	0.6649	0.6684	0.6650	0.6648	0.6690	0.6690

CHAPTER VI

Spectral Density of States in Disordered Alloys-geometric approximation:

In the preceding chapter, we discussed some simple theories for electron states in disordered alloys, all of them having the common weakness of associating a unique momentum with a given eigenstate, thus assigning to it an infinite lifetime. But $\underline{k}$ will no longer be a good quantum number for electrons in a disordered alloy. In such systems the important and relevant physical quantity is the spectral density of states $\rho(E,\underline{k})$. For the case of a perfect lattice, this has a δ-function peak at the band energies. As a result of disorder, this peak is broadened and its width would indicate the departure from the Bloch-wave character of the alloy wave function.

We will now be concerned with a theory to find the spectral density of states by evaluating the T-matrix for the system of scatterers, and then its application to an actual alloy system-disordered β-brass. We will also point out that for the case of a perfect lattice the formalism reduces exactly to the KKR method of energy-band calculation.

General Formulation:

If G is the Green function of an electron moving under the influence of potentials U_α, we have

$$\left\{ E + \nabla^2 - \sum_\alpha U_\alpha + i\,\varepsilon \right\} G(\underline{r},\underline{r}') = \delta\,(\underline{r} - \underline{r}'). \qquad (6.1)$$

We denote by enclosing in brackets, the average over all possible configurations of the system. Then the spectral density is given by

$$\rho(E,\underline{k}) = - \text{Im} \langle G(\underline{k}) \rangle / \pi \qquad (6.2)$$

where Im denotes the imaginary part of the quantity that follows it, and

$$G(\underline{k}) = \int e^{-i\underline{k}.(\underline{r}-\underline{r}')} G(\underline{r}\underline{r}') d\underline{r} d\underline{r}' \qquad (6.3)$$

and

$$n(E) = \int \rho(\underline{k},E) d\underline{k}. \qquad (6.4)$$

The T-matrix for the system is related to G and the free particle Green's function G_o by

$$G(\underline{r},\underline{r}') = G_o(\underline{r},\underline{r}') + \int G_o(\underline{r},\underline{r}'') \, T(\underline{r}'',\underline{r}''') \, G_o(\underline{r}''',\underline{r}') \, d\underline{r}'' d\underline{r}''' \qquad (6.5)$$

and

$$T(\underline{k}) = \int e^{-i\underline{k}.(\underline{r}-\underline{r}')} T(\underline{r},\underline{r}') \, d\underline{r} \, d\underline{r}' \quad .$$

We have, from Fourier transform of (6.5),

$$G(\underline{k}) = G_o(\underline{k}) + G_o(\underline{k}) \, T(\underline{k}) \, G_o(\underline{k})$$

$$T(\underline{k}) = \{G_o(\underline{k})\}^{-2} \, G(\underline{k}) - \{G_o(\underline{k})\}^{-1} \qquad (6.6)$$

The real and imaginary parts of T(k) are then immediately

$$\begin{aligned} \text{Im } T(\underline{k}) &= (E-k^2)^2 \, \text{Im } G(\underline{k}) \\ \text{Re } T(k) &= (E-k^2)^2 \, \text{Re } G(\underline{k}) - (E-k^2) \end{aligned} \qquad (6.7)$$

One can develop an expansion for G in terms of the t-functions of a single atom. The series looks very much

like that in the potentials U, except that the repetitions of any particular U which appear in the expansion of the t-function of that atom are missing:

$$G = G_o + G_o \sum_\alpha U_\alpha G_o + G_o \sum_\alpha U_\alpha G_o \sum_\beta U G_o + \ldots\ldots\ldots$$

$$G = G_o + G_o \sum_\alpha t_\alpha G_o + G_o \sum_\alpha \sum_{\beta \neq \alpha} (t_\alpha G_o t_\beta) G_o + G_o \sum_\alpha \sum_{\beta \neq \alpha} \sum_{\beta \neq \gamma} t_\alpha G_o t_\beta G_o t_\gamma G_o + \ldots. \quad (6.8)$$

The usual symbolic notation is adopted here, in which integrations are implicit. It may be noted that in the 3rd term, $\alpha = \gamma$ must be included and that t is related to U_1 by

$$t(\underline{r}\,\underline{r}') = U(\underline{r})\delta(\underline{r}-\underline{r}') + \int U(\underline{r}) G_o(\underline{r}-\underline{r}'') t(\underline{r}'', \underline{r}') d\underline{r}''. \quad (6.9)$$

From definitions of T and t (Eqs.6.5, 6.8, 6.9) it follows that

$$T = \sum_\alpha t_\alpha + \sum_\alpha \sum_{\beta \neq \alpha} t_\alpha G_o t_\beta + \sum_\alpha \sum_{\beta \neq \alpha} \sum_{\gamma \neq \beta} t_\alpha G_o t_\beta G_o t_\gamma + \ldots\ldots \quad (6.10)$$

Eq.(6.10) is the starting point of our discussions in this chapter. Let $\underline{R}_\alpha$, $\underline{R}_\beta$....denote the positions of the scattering centres

$$T(\underline{r},\underline{r}') = \sum_\alpha t(\underline{r}-\underline{R}_\alpha, \underline{r}'-\underline{R}_\alpha) + \sum_\alpha \sum_{\beta \neq \alpha} \int\int t(\underline{r}-\underline{R}_\alpha, \underline{r}''-\underline{R}_\alpha) G_o(\underline{r}'', \underline{r}''') \times t(\underline{r}'''-\underline{R}_\beta, \underline{r}'-\underline{R}_\beta) d\underline{r}'' d\underline{r}''' + \ldots\ldots\ldots \quad (6.11)$$

For the case of a perfect lattice, the translational symmetry,

enables us to perform the following manipulations

$$T(\underline{k}) = \sum_{\alpha} \int\int e^{-i\underline{k}(\underline{r}-\underline{r}')} t(\underline{r}-\underline{R}_\alpha, \underline{r}'-\underline{R}_\alpha)\, d\underline{r}\, d\underline{r}'$$

$$+\sum_{\alpha}\sum_{\beta\neq\alpha} \int\int\int\int t(\underline{r}-\underline{R}_\alpha, \underline{r}''-\underline{R}_\alpha) G_o(\underline{r}'', \underline{r}''')$$

$$\times\, t(\underline{r}'''-\underline{R}_\beta, \underline{r}'-\underline{R}_\beta) e^{i\underline{k}(\underline{r}-\underline{r}')} d\underline{r}\, d\underline{r}'\, d\underline{r}''\, d\underline{r}''' + \ldots\ldots$$

$$= \sum_{\alpha}\int\int e^{-i\underline{k}.(\underline{r}-\underline{r}')} t(\underline{r},\underline{r}')\, d\underline{r}\, d\underline{r}' + N\int\int\int\int t(\underline{r}\underline{r}'') G'_k(\underline{r}'',\underline{r}''')\, t(\underline{r}''',\underline{r}')\, e^{-i\underline{k}.(\underline{r}-\underline{r}')} d\underline{r}\, d\underline{r}''\, d\underline{r}'''\, d\underline{r}''' + \ldots.$$

(6.12)

where we have defined the matrix

$$G'_k(\underline{r},\underline{r}') = \frac{1}{N}\sum_{\beta\neq\alpha} G_o(\underline{r} + \underline{R}_\alpha - \underline{r}' - \underline{R}_\beta) e^{i\underline{k}.(\underline{R}_\alpha - \underline{R}_\beta)} \qquad (6.13)$$

The series (6.12) is geometric and can be summed to give

$$T(\underline{k}) = N\int\int e^{-i\underline{k}.(\underline{r}-\underline{r}')} \{t + tG'_k t + tG'_k tG'_k t_t \ldots.\}\, d\underline{r}\, d\underline{r}'$$

$$= N\int\int e^{-ik.(\underline{r}-\underline{r}')} \{t^{-1} - G'_k\}^{-1}\, d\underline{r}\, d\underline{r}' \qquad (6.14)$$

We expect singularities of $T(\underline{k})$ at singularities of the matrix $\{t^{-1} - G'_k\}^{-1}$. These would occur at the zeros of the determinant of this matrix, and this turns out to be Eq.(6.24) first the condition for the KKR method.

We now proceed with application of these ideas to the disordered alloy problem. There are two basic approximations invoked in this analysis.

1) The first approximation is the use of muffin-tin potentials where the potential at each site can be approximated by a spherically symmetric distribution within non-overlapping spheres around each ion, and assumed constant in the interstitial region. This approximation could be improv at the cost of more computational effort, but the muffin-tin approximation has been found to be reasonable in band structures calculations, and the errors due to this should not be too serious.

2) The second simplification introduced here is the geometric approximation discussed by Beeby.[16,91,92] This approximation (which is exact for the perfect lattice) enables us to sum the infinite series expressing the T matrix for the system in terms of the t matrices for the individual scatterers.

We start from Eq.(6.10), and because of the presence of 2 kinds of atoms, the summations have to be done by splitting the T matrix series into 4 parts.

$$T = \sum_{\substack{s=1,2 \\ s'=1,2}} T^{ss'} \qquad (6.15)$$

We have

$$T^{11} = \sum_{\alpha} t_{\alpha}^{1} + \sum_{\alpha}\sum_{\beta\neq\alpha} t_{\alpha}^{1} G_o t_{\beta}^{1} + \sum_{\alpha}\sum_{\beta\neq\alpha}\sum_{\gamma\neq\beta} t_{\alpha}^{1} G_o t_{\beta} G_o t_{\gamma}^{1} + \cdots\cdots\cdots$$

$$T^{12} = \sum_{\alpha}\sum_{\beta\neq\alpha} t_{\alpha}^{1} G_o t_{\beta}^{2} + \sum_{\alpha}\sum_{\beta\neq\alpha}\sum_{\gamma\neq\beta} t_{\alpha}^{1} G_o t_{\beta} G_o t_{\gamma}^{2} + \cdots\cdots \qquad (6.16)$$

$$T^{21} = \sum_{\alpha}\sum_{\beta\neq\alpha} t_{\alpha}^{2} G_o t_{\beta}^{1} + \sum_{\alpha}\sum_{\beta\neq\alpha}\sum_{\gamma\neq\beta} t_{\alpha}^{2} G_o t_{\beta} G_o t_{\gamma}^{1} + \cdots\cdots$$

$$T^{22} = \sum_{\alpha} t_{\alpha}^{2} + \sum_{\alpha}\sum_{\beta\neq\alpha} t_{\alpha}^{2} G_o t_{\beta}^{2} + \sum_{\alpha}\sum_{\beta\neq\alpha}\sum_{\gamma\neq\beta} t_{\alpha}^{2} G_o t_{\beta} G_o t_{\gamma}^{2} + \ldots\ldots$$

In the above expressions, the superscripts 1 and 2 denote the two types of atoms, t_{α}^{s} is the t matrix corresponding to the potential U^{s} at α. $T^{ss'}$ corresponds to that part of the total T function in which the electron scatters, first, off an atom of the s^{th} type and lastly off one of the s'^{th} type. The intermediate scatterers may be of either type and are represented by t's without any superscript in the above series.

In order to obtain a matrix representation, we make an angular momentum expansion of the t-functions. It is convenient to use, as before, real spherical harmonics $Y_L(\hat{\underline{r}})$ of the angles of $\underline{r}$, where L is a compound subscript, denoting both l and m:

$$t(\underline{r},\underline{r}') = \sum_{L} t_{\ell}(r,r')\, Y_L(\hat{\underline{r}})\, Y_L(\hat{\underline{r}}') \qquad (6.17)$$

The Fourier transformation to $T(\underline{k})$ may now be carried out separately for each term of the series in (6.16). The first term of T^{11} or T^{22} gives

$$\int \sum_{\alpha} t_{\alpha}^{s}(\underline{r},\underline{r}') e^{-ik.(\underline{r}-\underline{r}')} d\underline{r}\, d\underline{r}' = (4\pi)^2 N_s \sum_{L} \int j_l(kr)\, j_l(kr')\, t_l^{s}(r,r')\, r^2 dr\, r'^2 dr'\, Y_L(\hat{\underline{k}})\, Y_L(\hat{\underline{k}}). \qquad (6.18)$$

where N_s is the number of potentials of type s. The calculation of a general term in the series involves angular

integrations of the type

$$S_{\alpha\beta}^{ss'} = i^{l-l'}\int Y_L(\underline{r}\,)G_o(\underline{r}-\underline{r}\,'+\underline{R}_\alpha-\underline{R}_\beta)e^{i\underline{k}.(\underline{R}_\alpha-\underline{R}_\beta)}Y_{L'}(\underline{r}')\,d\underline{\Omega}_r d\underline{\Omega}_{r'},$$

besides, the radial integrals involved in t_l and a summation over L. A typical term in the series therefore contains products of the form

$$\Big(\sum_{\beta\neq\alpha} S_{\alpha\beta}^{ss'} \sum_{\gamma\neq\beta} S_{\gamma\beta}^{s's''} \cdots\cdots \sum_{\omega\neq\psi} S_{\psi\omega}^{s'''s''''} \cdots\cdots\Big)_{LL'},$$

where the superscripts on S take the values 1 and 2, depending on the type of atoms at locations specified by the subscripts. The problem is to sum an infinite series with terms of this nature, and then to average such sums over all configurations. Beeby presented a method of tackling this problem by replacing $S_\alpha^{ss'} = \sum_{\beta\neq\alpha} S_{\alpha\beta}^{ss'}$ by some $S^{ss'}$ which does not depend on α. The series then become geometric, and this approximation is therefore called the 'geometric approximation.' Then

$$(S)_{LL'}^{ss'} = \frac{1}{N_S}\sum_{\beta\neq\alpha}(S_{\alpha\beta}^{ss'})_{LL'}$$

$$= \frac{1}{N_S}\sum_{\beta\neq\alpha}\int i^{l-l'}Y_L(\hat{\underline{r}}\,)G_o(\underline{r}-\underline{r}\,'+\underline{R}_\alpha-\underline{R}_\beta)e^{-i\underline{k}.(\underline{R}_\alpha-\underline{R}_\beta)}Y_{L'}(\hat{\underline{r}}\,')\,d\Omega_{\underline{r}}\,d\Omega_{\underline{r}'} \qquad (6.19)$$

The formalism here is identical with that of Beeby. Beeby proceeds further by relating the lattice sums to the Kohn-Rostoker Green's functions.

We can identify

$$\sum_{\beta\neq\alpha} G_o(\underline{r}-\underline{r}'+\underline{R}_\alpha-\underline{R}_\beta)\, e^{i\underline{k}.(\underline{R}_\alpha-\underline{R}_\beta)}$$

as the incomplete Green's function of Chapter 4, with the $\beta=\alpha$ term omitted. This may therefore be expanded as

$$\sum_{\beta\neq\alpha} G_o(\underline{r}-\underline{r}'+\underline{R}_\alpha-\underline{R}_\beta)\, e^{-i\underline{k}.(\underline{R}_\alpha-\underline{R}_\beta)}$$

$$= \sum_{LL'} i^{l-l'} G_{LL'}^{ss'}\, j_l(\varkappa r)\, j_{l'}(\varkappa r')\, Y_L(\hat{\underline{r}})\, Y_{L'}(\hat{\underline{r}}').$$

Therefore,

$$[S^{ss'}]_{LL'} = G_{LL'}^{ss'}\, j_l(\varkappa r)\, j_{l'}(\varkappa r'), \qquad (6.20)$$

where $x = \sqrt{E}$ if $E > 0$ and $i\sqrt{-E}$ if $E < 0$; and $G_{LL'}^{ss'}$ are related to the $B_{LL'}^{ss'}$ discussed in Chapter V. The $G_{LL'}^{ss'}$ are independent of r and r and are collectively denoted by $G^{ss'}$. The radial integrals now involve only Bessel functions and the radial t_l functions. Their most general form is

$$t_l^{\,s}(p,q) = \int j_l(pr)\, t_l^{\,s}(rr')\, j_l(qr')\, r^2\, drr'^2\, dr' \qquad (6.21)$$

with p and q taking the values k or $\varkappa$. We use τ^s to denote $t_l^{\,s}(\varkappa,\varkappa)$. In this notation we have for the series of Eq.(6.16)

$$T^{11} = (4\pi)^2 N_1 \sum_{LL'} Y_L(\hat{\underline{k}})\, Y_{L'}(\hat{\underline{k}}) \Big\{ t_l(k,k)\, \delta_{LL'}$$

$$+ \Big[t^1(k,\varkappa)\Big(G^{11} + \sum_{s=1,2} G^{1s}\tau^s G^{s1} + \sum_{\substack{s=1,2\\ s'=1,2}} G^{1s}\tau^s G^{ss'}\tau^{s'} G^{s'1} + \ldots\Big)$$

106984

$$t(\varkappa,k)\Big]_{LL'} \Big\}\ ,$$

$$T^{12}=(4\pi)^2 N_1 \sum_{LL'} Y_L(\hat{\underline{k}}) \Big[t'(k,\varkappa)\Big(G^{12}+\sum_{s=1,2} G^{1s}\mathcal{T}^{s}G^{s2} + \sum_{\substack{s=1,2\\ s'=1,2}} G^{1s}\mathcal{T}^{s}G^{ss'}\mathcal{T}^{s'}G^{s'2}+\ldots\ldots\Big) t^2(\varkappa,k)\Big]_{LL'} Y_{L'}(\hat{\underline{k}})$$

with similar expressions for T^{21} and T^{22}.

On performing the summations, we get

$$T^{11}= (4\pi)^2 N_1 \sum_{LL'} Y_L(\underline{k})\, Y_{L'}(\underline{k}) \Big[t_1'(k,k)\,\delta_{LL'} + \Big\{ t'(k,\varkappa) M_1^{-1} \big[G^{21}+(1-G^{22}\mathcal{T}^2)(G^{12}\mathcal{T}^2)^{-1}G^{11}\big] \times t'(\varkappa,k)\Big\}_{LL'}\Big]$$

$$T^{12}=(4\pi)^2 N_1 \sum_{LL'} Y_L(\underline{k}) Y_{L'}(\underline{k}) \Big\{ t_l'(k,\varkappa) M_1^{-1} \big[G^{22}+(1-G^{22}\mathcal{T}^2)(G^{12}\mathcal{T}^2)^{-1}G^{12}\big] \times t^2(\varkappa,k)\Big\}_{LL'} \qquad (6.22)$$

and T^{22} and T^{21} may be obtained by interchanging the superscripts 1 and 2 in the above expressions. M_1 and M_2 are defined by the following expressions:

$$\begin{aligned} M_1 &= (1-G^{22}\mathcal{T}^2)(G^{12}\mathcal{T}^2)^{-1}\,(1-G^{11}\mathcal{T}^1) - G^{21}\mathcal{T}^1 \\ M_2 &= (1-G^{11}\mathcal{T}^1)(G^{21}\mathcal{T}^1)^{-1}\,(1-G^{22}\mathcal{T}^2) - G^{12}\mathcal{T}^2. \end{aligned} \qquad (6.23)$$

The above sets of Eqs.(6.21), (6.22) and (6.23) enable us to determine the spectral density of states.

We may mention here that if there was only one kind of atom and the geometric approximation were invoked (which is exact for the case of a perfect lattice), the final expression for $T(\underline{k})$ would be

$$T(\underline{k}) = (4\pi)^2 N \sum_{LL'} Y_L(\underline{k}) Y_{L'}(\underline{k}) \left[t_l(k,k)\,\delta_{LL'} + t_l(k,\varkappa) \left[G'(1 - G'\mathcal{T})^{-1} \right]_{LL'} t_l(\varkappa,k) \right] \qquad (6.24)$$

where G' has been defined before. The zeros of the determinant of the matrix $\left[1 - G'\mathcal{T}\right]_{LL'}$ gives the singularities in the $T(\underline{k})$. We then have

$$\det \left|\left| G'_{LL'} - \mathcal{T}_l^{-1}\,\delta_{LL'} \right|\right| = 0$$

Using the relationship between $\mathcal{T}$ and the phase shifts η_l

$$\mathcal{T}_l^{-1} = -\varkappa \cot \eta_l + i\varkappa$$

The imaginary part of this cancel with the imaginary part of $G_{LL'}$ and we are left with the condition

$$\det \left| B_{LL'} + \varkappa \cot \eta_l\, \delta_{LL'} \right| = 0 \qquad (6.24a)$$

which is identical with the determinantal Eqn. of the KKR method.

From Eqs.(6.22) and (6.23) we see that the peaks in the spectral density curves are given by

$\det |M_1| = 0$ or $\det |M_2| = 0$, both of the which are the same i.e.

$$\begin{vmatrix} 1 - G^{11}\mathcal{T}^1 & G^{12}\mathcal{T}^2 \\ G^{21}\mathcal{T}^1 & 1 - G^{22}\mathcal{T}^2 \end{vmatrix} = 0$$

If we consider an alloy for which the solute atoms are randomly distributed on the lattice sites, we have

$$G^{22} = G^{12} = c\,G$$
$$G^{21} = G^{11} = (1-c)\,G$$

where c is the concentration and G is the Green's function for the corresponding perfect lattice. The above condition then becomes

$$1 - G'\left[(1-c)\mathcal{T}^1 + c\,\mathcal{T}^2\right] = 0$$

Comparing this with the expression Eq.(6.24), we see that for such a system of random substitutional impurities the energy values will be the same as that for a perfect lattice having an averaged t-matrix at each site.[92,79]

In order to calculate the spectral density of states from the above formulae, we need the matrix elements of $G^{ss'}$ and of the t-matrices. It is clear that the calculation of $G^{ss'}$ requires a detailed knowledge of the relative positions of the atoms. In the case of a disordered alloys, the short-range-order parameters may be used to estimate an average distribution pattern of the constituents, thus enabling us to calculate the $G^{ss'}$. A detailed discussion of the use of the short-range order parameters to determine the matrix elements of $G^{ss'}$ has already been given in Chapter V. It is assumed that the short-range-order extends only upto

a certain neighborhood, beyond which the occupation probabilities are those of a randomly occupied lattice. In terms of the Cowley short-range order parameters α_i, this means that $\alpha_i = 0$ for i greater than a certain value σ. The matrix elements $G_{LL'}^{ss'}$ are given by

$$G_{LL'}^{ss'} = 4\pi \sum_{L''} D_{L''}^{ss'} C_{LL'L''} \quad . \tag{6.25}$$

Here $C_{LL'L''}$ are related to the Clebsch-Gordon coefficients and

$$D_L^{ss'} = m_{s'} D_L + i\varkappa(4\pi)^{-1/2} m_{s'} \delta_{Lo} + \varkappa i^{-l} \sum_{\gamma<\sigma}{}' e^{ik.R_\gamma} \left[n_l(\varkappa R_\gamma) - i j_l(\varkappa R_\gamma)\right] Y_L(\hat{R}_\gamma)$$

$$\times \left[P^{ss'}(R_\gamma) - m_{s'}\right]. \tag{6.26}$$

In the above expression, m_s is the atomic concentration of atoms of the s^{th} type and the D_L without superscripts are the familiar structure constants of the ordered lattice, which occur in the KKR method. $P^{ss'}(R_\gamma)$ denotes the probability of finding an atom of the s'^{th} type at a position R_γ with respect to an atom of the s^{th} type. This probability is related to the short range order parameters. The summation is over a neighborhood T in direct space and the prime on the summation indicates that the term with $\gamma = 0$ is to be omitted.

Potentials and t-matrices

The evaluation of the elements $t_l(p,q)$ of Eq.(6.21) is simplified by introducing model potentials in place of

the true potential. In performing calculations on α-brass using the averaged t-matrix approximation, Soven[79] suggested the use of model δ-function potentials in place of the true potentials. The model potentials were chosen to be of the form[24,79]

$$V^s(\underline{x},\underline{x}') = \sum_L Y_L(\hat{\underline{x}}) \frac{\delta(x-r_{mt})}{r_{mt}^2} U_l^s \frac{\delta(x-r_{mt})}{r_{mt}^2} Y_L(\hat{\underline{x}}'). \tag{6.27}$$

where r_{mt} is the radius of the muffin-tin sphere and U_l^s are energy-dependent potential amplitudes. We know from the formalisms of the APW and KKR methods for the perfect lattice and the extension of the KKR Method to disordered alloys, that the potential enters the final formulas only through the logarithmic derivatives of the radial wave function at the muffin-tin sphere. A suitable method for determining $U_l^s(E)$ is then to require it to yield the same logarithmic derivatives as generated by the actual potential. The $U_l^s(E)$ are related to the logarithimic derivative by

$$U_l^s(E) = r_{mt}^2\{\gamma_l^s(E) - \kappa j_l'(\kappa r_{mt})/j_l(\kappa r_{mt})\}, \tag{6.28}$$

where j_l' is the derivative of the Bessel function and $\gamma_l^s(E)$ is the logarithmic derivative of the radial wave function (for angular momentum l and energy E) of the actual potential, The muffin-tin potentials to generate the logarithmic derivative can be constructed by overlapping

the atomic potentials from neighboring sites, taking due account of the probability of occupation of a site by a given type of atom, as discussed already in Chapter V.

For a potential of the form (6.27), the angular momentum components of the t matrix can then be written as

$$t_l(r,r') = t_l \frac{\delta(r-r_{mt})}{r_{mt}^2} \frac{\delta(r'-r_{mt})}{r_{mt}^2} \qquad (6.29)$$

so that

$$t_l = U_l (1-U_l g_l)^{-1} \qquad (6.30)$$

where $g_l = G_l (r_{mt}, r_{mt})$ is the l^{th} component in the angular momentum representation of $G(\underline{r}-\underline{r}')$. The introduction of the δ-function model potentials then leads to the following simple expression for the matrix elements (6.21) of t.

$$t_l(p,q) = t_l \, j_l(pr_{mt}) \, j_l(qr_{mt}). \qquad (6.31)$$

These expressions completely define $T^{ss'}(\underline{k})$ in terms of $G^{ss'}$ and the logarithmic derivatives of the radial functions at the muffin-tin radius. The spectral density of state is then obtained from.

$$\rho(E,\underline{k}) = - \frac{1}{(E-k^2)2\pi\Omega} \operatorname{Im} \sum_{\substack{s=1,2 \\ s'=1,2}} T^{ss'}(\underline{k}) . \qquad (6.32)$$

The use of energy dependent model potentials necessitates

the correction factor

$$\left[1 - \sum_{s=1,2} m_s \frac{dU_1^{(s)}(E)}{dE}\right],$$

with Eq.(6.32).

Applications

The first application of the t-matrix formalism to real alloys was made of Soven, who calculated the spectral density of states for various symmetries in α-brass using an averaged t-matrix approximation.[79] For the case of α-brass experiments did not show the presence of any short-range order. Hence, from the preceding discussion, the averaged t-matrix approximation is applicable. But for the β-brass, for example, where short-range order is significant to a large neighborhood, one should use the more general geometric approximation. We report below in brief the results of such a program.

Neutron diffraction has been used successfully to observe short-range-order diffuse scattering in the alloy.[93] Walker and Keating[94] found that it was not possible to assign unique values to the short-range order parameters in β-brass, because of the long range nature of the short-rang order. They therefore compared the measured scattering with its values calculated from various theoretical approaches and showed that (for 75°C above the critical transition temperature) the short-range order parameters could be given by a Zernike-type expression

$$|\alpha(r)| = 0.540 \frac{e^{-0.400r'}}{r'}$$

where $r' = 2r/a$, and a is the lattice constant. We have used this expression to calculate the short-range-order parameters exmployed in the calculation. Although the disordered β-phase is found for a range of Zn concentrations in the vicinity of the 50-50 stoichiometry, we have chosen the concentrations of Cu and Zn atoms to be equal.

The muffin-tin potentials for Cu and Zn were constructe by overlapping through tenth neighbors. While calculating the $G^{SS'}$, the order of significant neighborhood σ was also set equal to 10. The actual potential for copper and zinc employed in the calculation are shown in Fig.6.1, and some relevant input parameters are given in Table 6.1.

The numerical calculations have been carried out for spectral density of states at the symmetry points Γ, H, P and N of the Brillouin Zone, We have calculated the reduced spectral density

$$\tilde{\rho}(E,\underline{k}) = \sum_{K} \rho(E,\underline{k} + K),$$

where $\underline{K}$ is a reciprocal lattice vector, and $\underline{k}$ is confined to the first Brillouin zone. This reduced spectral density should be convenient for comparison with the energy-versus-momentum curves of an ordered crystal, which are also defined modulo a reciprocal lattice vector. Some plots of $\tilde{\rho}(E,k)$ plotted against E are shown in Figs. 6.2 - 6.3 , and their peak positions are tabulated in Table 6.2. The abscissa is

a dimensionless quantity ϵ in terms of which, the energy is given by $E = (4\pi^2/a^2)\epsilon$. The ordinates give $\tilde{\rho}(E,k)a^3/(4\pi)^2$.

We now make a comparison of the results with the experimental data. Moss[10] has conjectured that nonspherical pieces of the Fermi surface may give rise to a detectable singularity in the intensity of diffusely scattered X-rays, electrons or neutrons. He applied the idea to the neutron-scattering curves for β-brass measured by Walker and Keating,[94] and concluded that along <111>, $k_F = 0.74$ of the Γ- P distance. In order to estimate k_F from our limited calculation we use the Cohen-Heine[95] model, characterising the band structure in terms of the states Γ_1, N_1 and N_1'. An effective mass can then be defined for the $\Gamma_1 - N_1'$ band and the Fermi-energy obtained. The intersection of E_F with $\Gamma_1 - P_4$ band gives $k_F = 0.75$ of the Γ-P distance. The free-electron value for this ratio is 0.82 and the virtual crystal approximation gives the value 0.78. Our calculations thus indicate that the Fermi surface normal to <111> is flatter than that given by the VCA. The calculated flatness compares surprisingly well with Moss's analysis of the neutron scattering data. Of course, Moss's conclusion is subject to a number of uncertainties. The diffuseness in the Fermi surface as a result of the disorder should erode the singularity and render its observation difficult. It has been seen from some calculations that eigenfunction for wave vectors about half way to the zone edge depart seriously from Bloch waves and the Fermi surface would appear to be a concept of limited utility in this

region.[96] Besides, the experimental data used by Moss is of uncertain accuracy in the region of interest. We find that our calculations give a value of 2.2 eV for the $N_1' - N_1$ gap, whereas the value due to Amar, Johnson and Wang for this gap is 1.5 eV. Thus our calculation gives a Fermi surface for which the departure from sphericity is greater than that given by the virtual crystal approximation. In order to carry this comparison further we have calculted the $N_1' - N_1$ gap following the same method, but using atomic potentials for copper and zinc. These were the potentials used by Amar et al.[63] in their VCA calculations for β-brass, with atomic potentials the $N_1' - N_1$ gap was found to be 2.4 eV. Thus the energy gap for the disordered alloy also is sensitive to the choice of potential, but it is clear that the striking differences in the values of the $N_1' - N_1$ gap given by the present method and by the VCA approach originates from the differences in the formalisms.

Table 6.1: Some parameters relevant to the β-brass calculation:

Lattice constant	2.9907Å (5.6514 a.u.)
Atomic concentration of zinc	50%
Atomic concentration of copper	50%
Radii of muffin-tin spheres for Cu and Zn	2.4148 (a.u.)
Radius of inscribed sphere	2.4472 (a.u.)
Order of significant neighborhood	σ, 10
Constant part of muffin-tin potential	-0.9152 Ry.

Table 6.2 Positions of peaks in $\varphi(E,\underline{k})$ versus E curves for states of various symmetries in β-brass. All energies are in Ry and relative to the muffin-tin zero, V_c = -0.9152 Ry.

State	Energy	State	Energy
Γ_1	0.018	P_4	0.158
$\Gamma_{25'}$	0.160	P_3	0.162
Γ_{12}	0.180	P_4	0.896
H_{12}	0.124	P_1	0.985
$H_{25'}$	0.198	N_1	0.120
H_{15}	1.051	N_2	0.141
H_{12}	1.133	N_1	0.165
H_1	1.693	N_4	0.183
E_F(Cohen-Heine method)	0.511	N_3	0.204
		$N_{1'}$	0.404
		N_1	0.571

FIGURE CAPTIONS

Fig.6.1 'Charge' $Z(r) = -rV(r)/2$ for copper and zinc in disordered β-brass at $75^{o}C$ above the transition temperature.

Fig.6.2 Spectral density of states for Γ_{25}' and Γ_{12} (d-like states) in β-brass, plotted as a function of energy.

Fig.6.3 Spectral density of states for N_1' (p-like) state in β-brass, plotted as a function of energy.

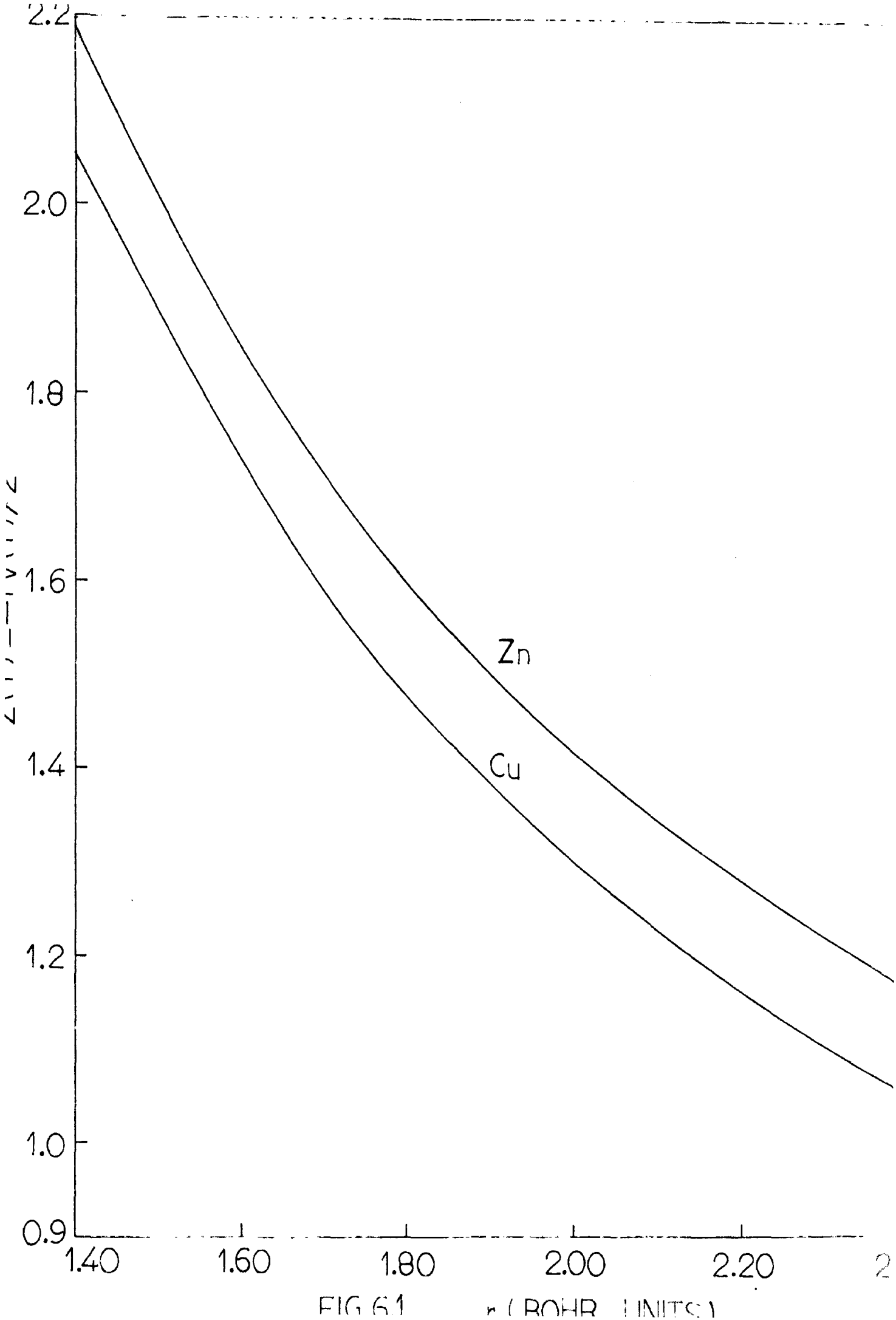

FIG 6.1 r (BOHR UNITS)

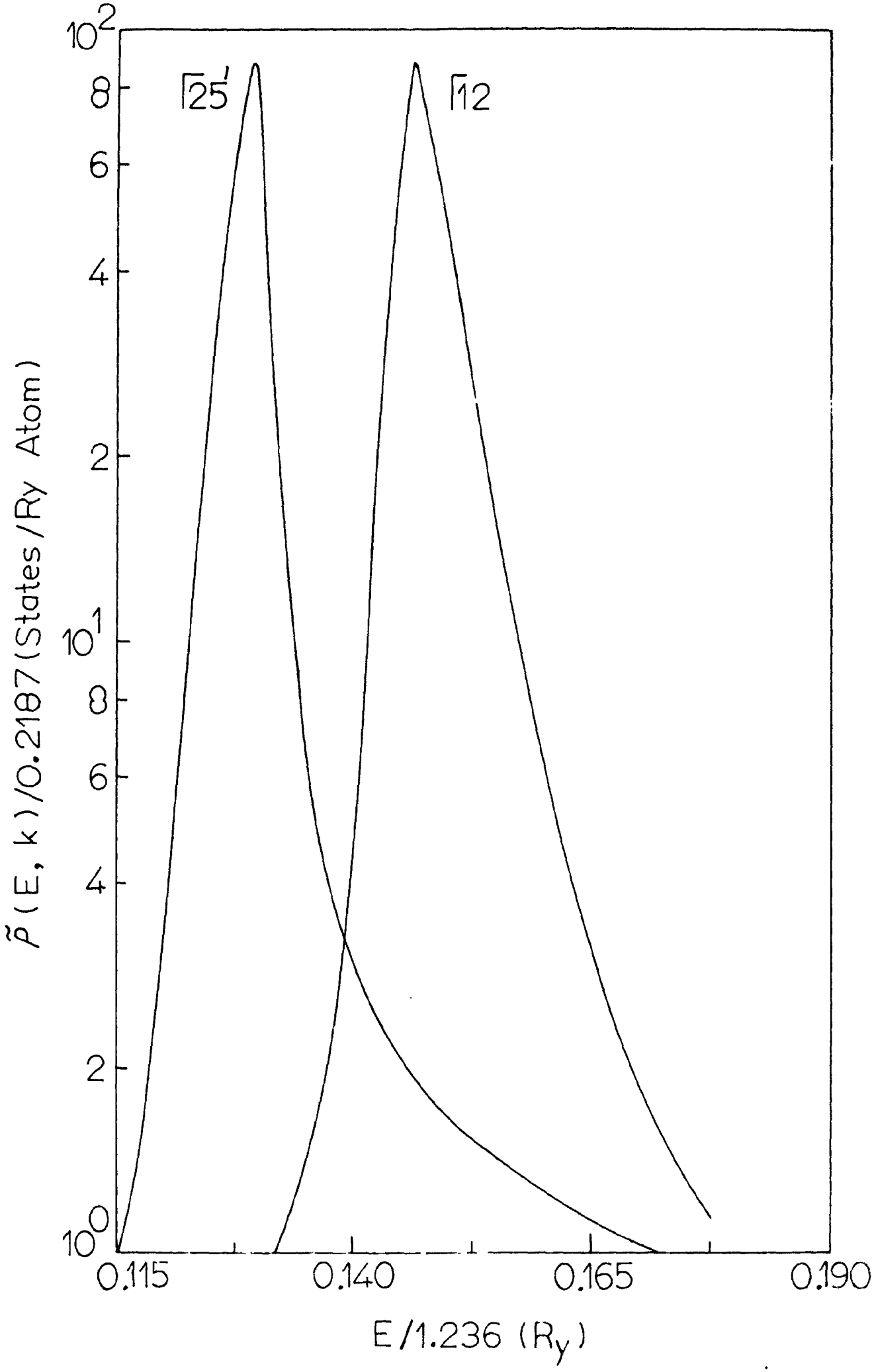
10^2
8
6
4
2
10^1
8
6
4
2
10^0
$\Gamma_{25'}$
Γ_{12}
$\tilde{\rho}(E, k)/0.2187$ (States/Ry Atom)
0.115
0.140
0.165
0.190
$E/1.236$ (R_y)

FIG 6.2

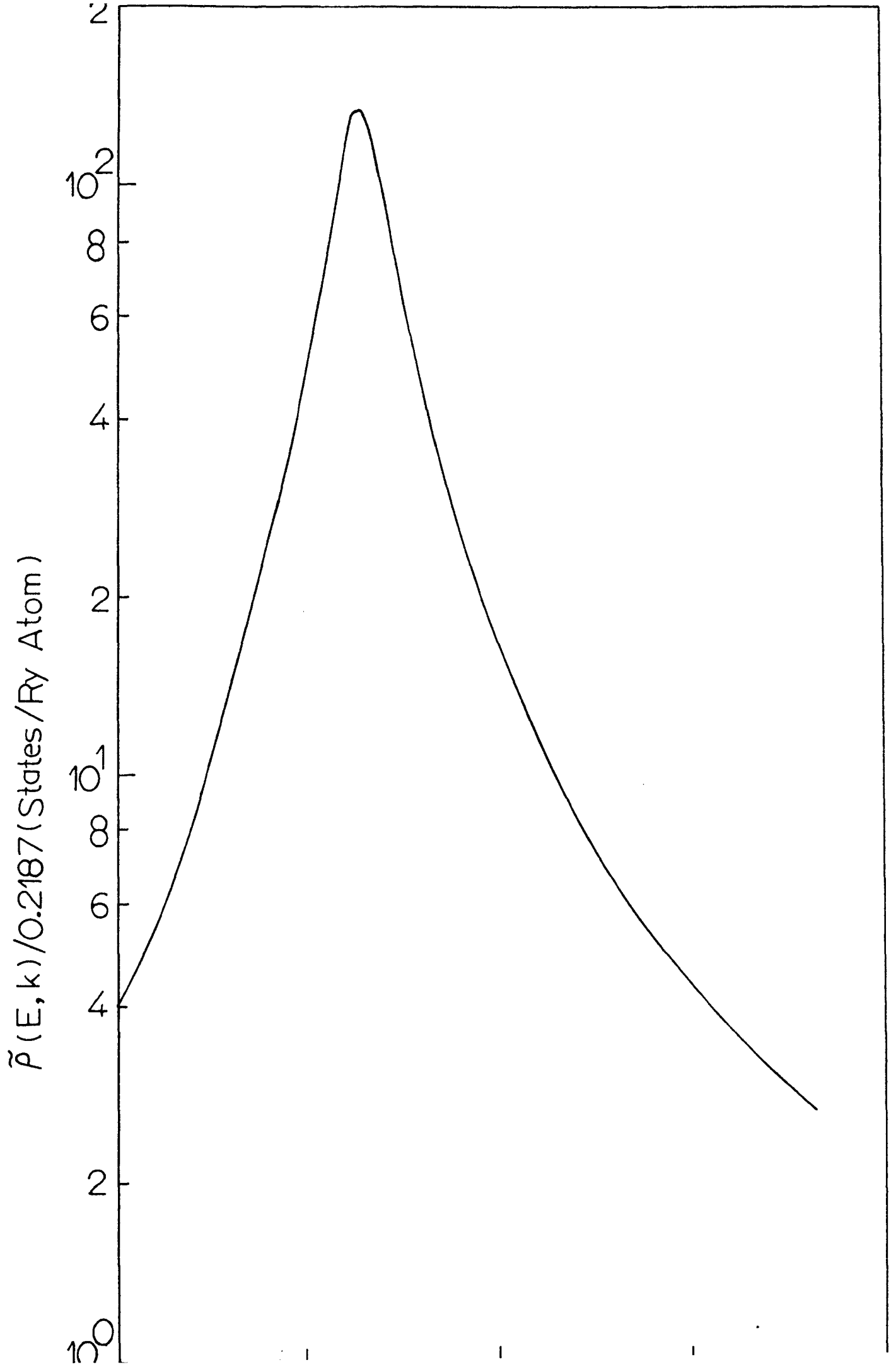
$\tilde{\rho}(E,k)/0.2187$ (States/Ry Atom)
10^2
8
6
4
2
10^1
8
6
4
2
10^0

CHAPTER VII

Coherent Potential Model for Disordered alloys - Application to real Systems:

We have seen in the previous chapter, how the spectral function may be obtained by evaluating the T matrix for a system of random scatterers, under the 'geometric' and 'average t-matrix' approximation. Soven[97] and Velicky et al.[98] developed a more accurate theory by introducing ideas of an effective medium propagator. They view the scatterers as being embedded in an effective medium, whose choice is made self-consistently. This medium is chosen by requiring that a single scatterer embedded in this effective medium should produce no further scattering on the average. This self-consistent Hamiltonian is optimal among all single-site approximations, i.e, those which neglect scattering from clusters of atoms. Similar arguments were used by McMillan and Anderson[99] in their treatment of liquid iron. Onodera and Toyozawa[100] used exactly the same formalism to describe Frenkel excitons in mixed ionic crystals. Closely related to this are the efforts of Hubbard to obtain a self-consistent description of electron correlation in narrow bands. In one of his papers, Hubbard[101] introduces an alloy analogy and by using appropriate decoupling schemes for the Green's functions equations, he arrives at a self-consistent solution of the alloy problem, which is precisely equivalent to the coherent potential approximation.

The first application of the CPA was to a one-dimension array of δ-function potentials, where it was found to give goo agreement with results of machine calculations. A notable feature was that the spurious band gap predicted by the 'averaged t-matrix approximation' was absent.[96] Since then it has been applied to model 3 dimensional alloys, and also to some real alloys. The theory of the CPA as used here ignores the presence of any short-range order. Hence the applications have been made to systems like α-CuZn[102] and Cu-Al[103] for which experiments show that there is no short range order, and not to β-brass for example, which shows short-range correlations upto fairly large distances. When applied to Cu-Al alloys, the results of the CP model agreed well with the data from positron annihilation angular correlation studies.[9] For α-brass too, the results are in better agreement with experiments, than previous calculations[6] with VCA and averaged t-matrix approximations.

Velicky et al's treatment of the Coherent Potential Theory:

The alloy system under consideration may be described as a periodic lattice containing N equivalent sites occupied by two kinds of atoms A and B. The respective concentrations of atoms are c and 1-c, and c can vary from 0 to 1. The physical quantities of interest are ensemble averages. Such an average of an operator O will be denoted by $\langle O \rangle$.

For any configuration, the single-particle Green's function is given as

$$G(z) = (z - H)^{-1} , \qquad (7.1)$$

where H is the one-electron Hamiltonian corresponding to this configuration. All macroscopic quantities of interest are then determined by $\langle G(z)\rangle$ and the averaged $\langle G\rangle$ has the full symmetry of the lattice. The equation determining the effective Hamiltonian H_{eff} is

$$\langle G(z)\rangle = (z - H_{eff})^{-1}. \tag{7.2}$$

If $K = K(z)$ is a starting approximation to H_{eff}, then

$$\langle G\rangle = R + R\,(H_{eff} - K)\,\langle G\rangle \tag{7.3}$$

where $$R = (z - K)^{-1} \tag{7.3a}$$

is the unperturbed Green's function. The T matrix corresponding to a given configuration may be written as

$$G = R + R\,T\,R, \tag{7.4}$$

which gives upon averaging

$$\langle G\rangle = R + R\,\langle T\rangle\,R. \tag{7.5}$$

Comparing Eqs.(7.3) and (7.5), we have

$$H_{eff} = K + \langle T\rangle\,[1+R\langle T\rangle]^{-1}. \tag{7.6}$$

The Eq.(7.6) relates the effective Hamiltonian H_{eff} to the trial function K and the averaged T. The equation can therefore be used in two ways to determine the effective Hamiltonian.

1) Non self-consistent procedure - This consists in determining $\langle T(K)\rangle$ corresponding to a given K and

inserting it into Eq.(7.6).

2) Self-consistent procedure - One chooses the K such that $\langle T(K) \rangle = 0$ and then Eq.(7.6) ensures that

$$H_{eff} = K \quad . \tag{7.7}$$

The next step is to decompose the random-perturbing potential H-K into a sum of contributions of single scatterers associated with each site, i.e.

$$H-K = \sum_n V_n \ , \tag{7.8}$$

where n is a site index.

The Green's function G can be written in terms of K as

$$G = R + R\,(H-K)\,G. \tag{7.9}$$

This, together with Eq.(7.4) gives

$$T = (H-K)\,(1+RT), \tag{7.10}$$

which upon using (7.8) gives

$$T = \sum_n V_n\,(1 + RT) \tag{7.11}$$

which expresses the T matrix as a sum of contributions arising from the individual scatterers. We define a quantity Q_n by

$$T \equiv \sum_n Q_n \ . \tag{7.12}$$

The T matrix associated with site n is

$$T_n = (1-V_nR)^{-1}\,V_n. \tag{7.13}$$

Substitution into (7.11) gives

$$Q_n = T_n \left(1 + R \sum_{m \neq n} Q_m\right) \quad . \tag{7.13}$$

Averaging Eqs.(7.12) and (7.13), we have

$$\langle T \rangle = \sum_n \langle Q_n \rangle \tag{7.14}$$

$$\langle Q_n \rangle = \langle T_n \left(1 + R \sum_{m \neq n} Q_m\right) \rangle \tag{7.15}$$

Eq.(7.15) may be rewritten as

$$\langle Q_n \rangle = \langle T_n \rangle \left(\langle 1 + R \sum_{m \neq n} Q_m \rangle\right)$$

$$+ \langle T_n R \sum_{m \neq n} (Q_m - \langle Q_m \rangle) \rangle \tag{7.16}$$

In this equation, the first term described the effect of the averaged effective wave seen by the n^{th} atom, and the second term corresponds to fluctuations about the effective wave. The basic approximation is to neglect the 2nd term. Eq.(7.16) then reduces to

$$\langle Q_n \rangle = \langle T_n \rangle \left(1 + R \sum_{m \neq n} \langle Q_m \rangle\right)$$

or

$$\langle Q_n \rangle = \left(1 + \langle T_n \rangle R\right)^{-1} \langle T_n \rangle \left(1 + R\langle T \rangle\right) \tag{7.17}$$

Substituting this into Eq.(7.6), we have for the effective Hamiltonian

$$H_{eff} = K + \sum_n \langle T_n \rangle \left(1 + R\langle T_n \rangle\right)^{-1} \tag{7.18}$$

which relates it to the average scattering arising from the n^{th} scatterer.

The self consistent procedure mentioned after Eq.(7.6) then simplifies to

$$\langle T_n(K) \rangle = 0 \text{ for all } n. \qquad (7.19)$$

Because of the periodicity of the averaged quantities, it is sufficient to consider only one, say the zeroth site. This is identical with the condition imposed by Soven[96] to determine H_{eff}.

The validity of the neglect of the 2nd term in Eq.(7.16), i.e. the assumption that

$$\langle T_n R \sum_{m \neq n} (Q_m - \langle Q_n \rangle) \rangle = 0 \qquad (7.20)$$

implies neglect of all statistical correlations between n and all other sites m. These correlations arise from the presence of short-range-order and multiple scattering.

Application to a Model Hamiltonian:

We choose a single-band model, closely related to the tight-binding approximation. A single orbital $|n\rangle$ is associated with each site n. Hence the name 'single-band model.' The one-electron Hamiltonian for this system is

$$H = \sum_n |n\rangle \epsilon_n \langle n| + \sum_{n \neq m} |n\rangle t_{mn} \langle m| \qquad (7.21)$$

$$= D + W$$

The Hamiltonian H is thus split up into a diagonal part D and an off-diagonal part W with respect to the Wannier representation. The matrix elements of H depend in general on the configuration of A and B atoms in the crystal. The model is physically realizable when the orbitals are sufficiently localized and the atomic potentials are not too different. We then find that the diagonal elements D are random but the off-diagonal W is translationally invariant.

The operator W is diagonal in the Bloch representation

$$\langle k|W|k'\rangle = \delta_{kk'} \sum_n t_{on}\, e^{i\underline{k}\cdot\underline{a}_n} = \delta_{kk'}\omega s(\underline{k}) \qquad (7.22)$$

where $$|k\rangle = N^{-1/2} \sum_n e^{i\underline{k}\cdot\underline{a}_n} |n\rangle$$

relates the Bloch and Wannier bases and ω is one-half the bandwidth. The quantity $s(k)$ describes the k dependence of the band energy, and is dimensionless. For example, in the case of a simple cubic lattice, with nearest neighbor tight-binding bands, we have

$$-1 < S(\underline{k}) < +1 \quad .$$

We choose the same units for the atomic energy levels ϵ^A and ϵ^B and choose the energy zero such that

$$\epsilon^A = \frac{1}{2}\omega\delta$$
$$\epsilon^B = -\frac{1}{2}\omega\delta$$

and hence $\delta = (\epsilon^A - \epsilon^B)/\omega$.

For a given operator W, the ensemble of Hamiltonians is completely specified in terms of two dimensionaless parameters c and δ, characterising the concentration, and separation between atomic levels. Here c ranges from 0 to 1, and δ can assume any value. But it is clear from symmetry arguments that only the range $0 < c < 1/2$ and $\delta > 0$ need be considered.

We want to apply the coherent potential criterion (7.19) to the model Hamiltonian (7.21). Since $H_{eff}(z)$ has the full symmetry of the crystal, both $H_{eff}(z)$ and $\langle G(z)\rangle = (z - H_{eff})^{-1}$ are diagonal in the k representation.

$$\langle k|H_{eff}(z)|k'\rangle = [s(k) + \Sigma(k,z)]\ \delta_{kk'} . \quad (7.23)$$

$\Sigma(k,z)$ is the self energy with respect to the perfect crystal having Hamiltonian $\mathcal{H}$. Another important quantity is

$$G(\underline{k},z) \equiv \langle\langle k|G(z)|k\rangle\rangle = [z-s(k)-\Sigma(\underline{k},z)]^{-1} \quad (7.24)$$

which is related to the spectral density $\rho(k,E)$ by

$$\rho(\underline{k},E) = -\pi^{-1}\ \mathrm{Im}\ G(\underline{k},E + io) \quad (7.25)$$

and the average density of states is

$$n(E) = -(\pi N)^{-1}\ \mathrm{Im\ Tr}\ \langle G(E + io)\rangle . \quad (7.26)$$

It is useful to introduce an anxiliary function F(z) defined by

$$F(z) = \int_{-\infty}^{\infty} \frac{dE}{z-E}\ n(E) \quad (7.27)$$

All the quantities defined in Eqs. (7.24 - 7.27) when superscripted with a o, denote the corresponding quantity for the perfect crystal.

We choose the unperturbed Hamiltonian K to be of the form

$$K = W + \sum_n |n\rangle\, u(z) \langle n| = W + u(z)\, I \qquad (7.28)$$

u(z) is independent of k and hence the entire k dependence is contained in W and hence s(k). For the K defined in Eq.(7.28), the unperturbed Green's function is, from Eq.(7.3a),

$$R(z) = (z - K)^{-1}$$

$$= [z - u(z) - W]^{-1} = G^{\circ}\,[z - u(z)]. \qquad (7.29)$$

Considering the Eqs.(7.21) and (7.28) for H and K, we use

$$H - K = \sum_n |n\rangle\, [\epsilon_n - u(z)] \langle n|, \qquad (7.30)$$

so that using Eq.(7.8) we have

$$V_n = |n\rangle\, [\epsilon_n - u(z)]\, \langle n| \qquad (7.31)$$

which can be written as

$$V_n = |n\rangle\, v_n \langle n| \qquad (7.32)$$

T_n can be obtained by substitution into Eq.(7.12a),

and is

$$T_n(z) = |n\rangle v_n \left[1-v_n F^{(o)}(z-u(z))\right]^{-1} \langle n|$$

$$= |n\rangle v_n \left[1-v_n \bar{F}(z)\right]^{-1} \langle n| \qquad (7.33)$$

where $\bar{F}(z) = F^{(o)}(z - u(z))$. (7.34)

The coherent potential condition, then is to set the configurational average of Eq.(7.33) to zero. We see that

$$\langle T_n(z)\rangle = |n\rangle \left[\frac{c[\epsilon^A-u]}{1-(\epsilon^A-u)\bar{F}} + \frac{(1-c)[\epsilon^B-u]}{1-(\epsilon^B-u)\bar{F}} \right] \langle n|$$

$$= |n\rangle \{c\,\mathcal{T}^A + (1-c)\,\mathcal{T}^B\} \langle n|$$

$$= |n\rangle \mathcal{T} \langle n|$$

The equation for the self energy $\Sigma(z)$ is then obtained by setting $\mathcal{T}(z) = 0$, that is

$$\frac{c(\epsilon^A - u)}{1-(\epsilon^A-u)\bar{F}} + \frac{(1-c)(\epsilon^B-u)}{1-(\epsilon^B-u)\bar{F}} = 0 \qquad (7.36)$$

and then we have

$$u(z) = \epsilon - (\epsilon^A - u)\bar{F}(\epsilon^B - u)$$

and from the CP criterion we have the self-energy $\Sigma(z)$

$$\Sigma(z) = u(z) = \epsilon - [\epsilon^A - \Sigma(z)]\bar{F}(z)[\epsilon^B - \Sigma(z)] \qquad (7.37)$$

with $\epsilon = c\,\epsilon^A + (1-c)\,\epsilon^B$, which is exactly the form obtained by Soven.[96] Alternatively Eq.(7.37) may be written in a form obtained by Onodera and Toyozawa[100] viz.

$$\Sigma(z) = \epsilon + \frac{c(1-c)\delta^2 F^o\,[z - \Sigma(z)]}{1+[\Sigma(z)+\epsilon]\,F^o\,[z - \Sigma\,(z)\,]} \qquad (7.38)$$

We have seen that $\Sigma(z)$ is completely determined by c, δ and the host density of states $n^o(E)$. For $n^o(E)$ we use the form used before by Hubbard

$$\begin{aligned} n^o(E) &= (2/\pi\omega^2)\,(\omega^2 - E^2)^{1/2} && |E| \leqslant \omega \\ &= 0 && |E| > \omega\ . \end{aligned} \qquad (7.39)$$

The function $F^o(z)$ defined in (7.27) corresponding to this form of the density of states is

$$F^o(z) = (2/\omega^2)\,[z - (z^2 - \omega^2)^{1/2}] \qquad (7.40)$$

Using (7.37), (7.38) and (7.40) we find that

$$\Sigma(z) = z - [F(z)]^{-1} - \tfrac{1}{4}\,F(z) \qquad (7.41)$$

and $F(z)$ satisfies the cubic eauation

$$\tfrac{1}{16}\,F^3 - \tfrac{1}{2}\,zF^2 + [z^2 - \tfrac{1}{4}\,(\delta^2-1)]F-(z+\epsilon) = 0 \qquad (7.42)$$

These Eqs.(7.41) and (7.42) may be solved to yield either 3 real roots or one real root and a complex pair. In the latter case the one in the lower half-plane is physical, since it results in a non-negative density of states.

The theory and the model outlined above have been discussed in great detail in the original papers of Velicky et al. and Soven. We will here touch on two main points - 1) the comparison of results with those predicted by other approximation schemes and 2) the change in the density of states, as predicted by the coherent-potential model, when the parameters c and δ are varied. These two features are illustrated in the two figures (7.1) and (7.2).

In the first case, the results of the CPA are compared with those obtained by the virtual crystal model and the averaged t matrix approximation. Fig.(7.1) shows that in the virtual crystal case, the band is always symmetrical and even for large δ there is no splitting into two subbards. The averaged t-matrix approximation on the other hand, shows that the band always splits. This spurious band gap was also observed by Soven in his calculations on one-dimensions model alloy. The results of the CPA appear to be most satisfactory. Ofcourse, in the case of large δ, the split band limit, the results of the CPA are not expected to be correct.

The other figure (7.2) shows the density of states calculated with the model $n^{o}(E)$ for a range of c, δ values, as obtained by the CPA. The general features of the results are as follows. For small concentration (and δ not too large), the density of states is slightly modified

from the host density of states. When δ is small, this results from a resonance in the band. When δ is greater than the half width ω, localized states will start forming and as c increases, these broaden into an impurity band and when δ is large enough, there will be essentially two bands, one for each atom type. We have shown[104] that the same features can be predicted qualitatively from arguments from a density matrix approach, in a much simpler way.

Applications to real alloy Systems:

It is not quite easy to apply the ideas of the coherent potential to a realistic system, because the self-consistent equation for the coherent-potential cannot be solved for an arbitrary system. The only efforts so far have been by Kirkpatrick et al.[105] and by us.[102,103]

Kirkpatrick et al. have essentially generalized the arguments above to asymmetric density of states and to systems having orbital degeneracy in order to be able to calculate the density of states in paramagnetic NiCu alloys.

The object of the calculation is to obtain the density of states for NiCu using only the host density of states as input. The function $F^{o}(z)$ corresponding to Eq.(7.27) is thus obtained by approximating $n^{o}(E)$, to the accuracy desired by a straight line interpolation connecting the points $n^{o}(E_i)$. The band edges being taken at E_o and E_n,

the resulting function $F^{(o)}$ may be written as

$$F^{(o)}(z) = \sum_{i=o}^{n} a_i (z-E_i) \ln(z-E_i), \qquad (7.43)$$

where a_i may be determined by performing the integrations in (7.27). This is the form of $F^{o}(z)$ used to solve Eq.(7.37) by an iterative procedure. To take account of sharp structures and overall asymmetries, such as encountered in Ni and Cu, Kirkpatrick et al. introduce a 'steeple' model for the density of states. This consists of a sharp peak, one tenth as wide as the whole band, located at the top of the band, and a low wide shoulder region.

The potentials placed on the Ni and Cu sites are atomic Hartree-Fock potentials for neutral configurations. Kirkpatrick et al. argue that the s-bands in NiCu will be unaffected by alloying and concentrate attention on the tight-binding like-d bands and represent the model Hamiltonian in terms of the interpolation schemes of Hodges and Mueller.[106] The alloy Hamiltonian expressed in a basis of tight-binding Bloch functions and OPW's will be separated into a random part D and a configuration-independen part W:

$$H = W + D = \begin{vmatrix} W_{ss} & W_{sd} & \\ & W_{EE} & W_{ET} \\ W_{ds} & W_{TE} & W_{TT} \end{vmatrix} + \begin{vmatrix} 0 & 0 & \\ & \mathcal{D}_{EE} & 0 \\ 0 & 0 & \mathcal{D}_{TT} \end{vmatrix}$$

The various blocks in (7.44) are labelled by the indices s for the plane-wave like states, d for the tight-binding d-states and E, T denote d states constructed from orbitals of e_g or t_{2g} symmetry. The CPA self-consistency equation is applied to this Hamiltonian to yield two equations for Σ_E and Σ_T.

$$\Sigma_E = \langle \epsilon_E \rangle - (\epsilon_E^{Cu} - \Sigma_E) F_E(\epsilon_E^{Ni} - \Sigma_E) \qquad (7.45)$$

$$\Sigma_T = \langle \epsilon_T \rangle - (\epsilon_T^{Cu} - \Sigma_T) F_T(\epsilon_T^{Ni} - \Sigma_T) \qquad (7.46)$$

Using the above scheme, Kirkpatrick et al. calculated the density of states for a range of Cu concentrations ranging from 0 to 60% at intervals of 10%. It is seen that the strong peaks characteristic of pure Ni and Cu persist in all cases studied, but the effects of alloying are strong. At low concentrations, the peaks loose intensity and broaden, at the same time, the many wiggles due to fine features of the density of states are quickly damped out. After about a concentration of 30%, the band shape changes only slightly. The peaks continue to reduce in height and the second peak becomes stronger. These features are in distinct contrast from the predictions of the virtual crystal approximation which predicts a uniform shift without any change in structure. Even if scattering corrections are included the resulting change affects all parts of the band equally.

The density of states predicted by the CPA is in good agreement with the photoemission data of Deib and Spicer, 10

But one must bear in mind that interpretation of photo-emission data is not unambiguous.

Quite another approach, which is perhaps as approximate but of more general applicability was suggested by us and applied to real systems such as Cu-Al and α-CuZn alloys. The idea is essentially to make use of model potentials of the type used by Soven[96] in his application of the averaged t matrix approximation to α-brass. The motivation is that in the calculation of electron states in solids, the effect of the potential enters the final equations, only through the logarithmic derivative of the corresponding radial function at the muffin-tin radius. We can thus replace the actual potential by a model potential which yields logarithmic derivatives identical with those generated by the real potentials. The model potential is chosen to be energy- and angular momentum dependent δ-function potential.

We rewrite here the formulas for the CP theory, as introduced originally by Soven and show how the introduction of model potentials of the type specified above results in simple expressions for the density of states. The essence of the CP theory is to place at each site an effective potential V_o, which will simulate the electronic properties of the actual alloy. The Green's function for this lattice is

$$G = G_o + G_o V_o G \qquad (7.47)$$

where G_o is the free-electron Green's function. The actual alloy consists of perturbing potentials V_1-V_o and V_2-V_o and the t matrix describing the scattering of an electron in this medium is

$$t_i = (V_i - V_o) + (V_i - V_o)\, G t_i \qquad (7.48)$$

The coherent-potential criterion then says that the average of the constituent t-matrices must be zero, i.e.

$$c t_1 + (1-c)\, t_2 = 0 \qquad (7.49)$$

Substituting from (7.48) into (7.49), we have

$$cV_1 + (1-c)V_2 - V_o = (V_1-V_o)G(V_2-V_o), \qquad (7.50)$$

Eq.(7.50) must be solved self-consistently because G is itself dependent on V_o. At this stage, we introduce the model potentials described above and replace the muffin-tin potentials at each site by potentials of the form:

$$V_s(\underline{x},\underline{x}') = \sum_L Y_L(\hat{\underline{x}})\ \frac{\delta(x-R)}{R^2}\ V_s^l\ \frac{\delta(x'-R)}{R^2}\ Y_L(\hat{\underline{x}}'), \qquad (7.51)$$

where the potential amplitudes V_s^l are related to the logarithmic derivative of the actual wave function. Inserting Eq.(7.51) into (7.50), we have

$$cV_1^l + (1-c)V_2^l - V_o^l = (V_1^l - V_o^l)\left[g_l/(1-V_o^l g_l)\right](V_2^l - V_o^l), \qquad (7.52)$$

where $g_l = G_l(R,R)$ and $G_l(x,x')$ is the l^{th} component of the angular momentum expansion of $G_o(\underline{x}-\underline{x}')$. We than have for V_o^l, the following expression

$$V_o^l = \frac{g_l V_1^l V_2^l - (C_1 V_1^l + C_2 V_2^l)}{g_l [C_2 V_1^l + C_1 V_2^l] - 1} \quad . \tag{7.53}$$

For a potential of the form (7.51), the T matrix is of the form

$$T(\underline{x},\underline{x}') = \sum_L Y_L(x) \frac{\delta(x-R)}{R^2} t^l \frac{\delta(x'-R)}{R^2} Y_L(x') . \tag{7.54}$$

Thus the elements of the angular momentum expansion of the t matrix corresponding to V_o are

$$t_o^l = V_o^l / (1-V_o^l g_l) \quad . \tag{7.55}$$

The calculation of the spectral density of states is now straightforward. One places the t matrix corresponding to (7.55) at each site and works out the spectral function by using the usual formula

$$\rho(E,\underline{k}) = - \frac{1}{(E-k^2)^2 \pi \Omega} \operatorname{Im} T(\underline{k}) \tag{7.56}$$

and

$$T(\underline{k}) = 4\pi^2 N \sum_{LL'} Y_L(\hat{k}) Y_{L'}(\hat{k}) \left\{ t_l(k,k) \delta_{LL'} + [t(k,\kappa) [G'(1-G' t(\kappa,\kappa)]^{-1} t(\kappa,k)]_{LL'} \right\} \tag{7.57}$$

where N is the number of sites and Ω the volume of the assembly and

$$t(p,q) = t^{1}\, j_1(pR)\, j_1(qR) \qquad (7.58)$$

with p and q, being k or κ. The matrix elements of G' are given in terms of the familiar structure constants of the Kohn-Rostoker method, by

$$G'_{LL'} = D_{LL'} + i\kappa\, \delta_{LL'} \qquad (7.59)$$

Application to α-brass:

The method outlined above has been applied to determine the spectral density of states for various representations at the symmetry points Γ, X, and L and along the Δ axis for α-$Cu_{0.70}\, Zn_{0.30}$. Fig.(7.3) shows plots of the reduced spectral density $\bar{\rho}(E,\underline{k})$ against energy for the $\Delta_{2'}$ representation. We notice that the curve for $k_x = 0.50$ is broader than those for $k_x = 0.75$ or 0.25, an observation which is in general agreement with Soven's conclusions on a hypothetical alloy. A plot of $\bar{\rho}(E,\underline{k})$ against $\underline{k}$ is shown in Fig.(7.4), again for the $\Delta_{2'}$ representation. We find that for both the curves, peaked at $k_x = 0.33$ and $k_x = 0.55$, the halfwidth is the same about 3% of the Brillouin Zone dimension, compared to the value of 5% for this ratio, obtained by Soven from

an averaged t matrix calculation. But there is no experimental method of directly probing $\rho(E,\underline{k})$ and so we will limit comparison with experiments to the shifts in the peak positions relative to pure copper (as given by a similar potential) and predictions of other models. We refer again to the optical absorption measurements of Biondi and Rayne. If the secondary absorption peak which shifts to lower energies by 1.3 eV is attributed to the $L_2' - L_1$ transition, then the coherent potential result is still in disagreement with experiments. Our calculated value for the reduction in this gap is 0.167 Ry. compared to the experimental value of 0.096 Ry. But one must bear in mind that even for pure metals indirect transitions may be important. A more meaningful comparison of the various approximations could be made if additional experimental information, for example from positron annihilation experiments were available.

Application to Cu-Al alloy:

As another example, we have applied the above theory to a Cu-Al alloy. Positron annihilation experiments[9] have been made for this and the measurements indicate that the Fermi surface in the $Cu_{0.904}\ Al_{0.096}$ alloy has a neck radius which is twice that of pure copper. We calculated the spectral function for a $Cu_{0.90}Al_{0.10}$ alloy as a function of E, for the symmetry points Γ, X and L. One such plot is shown in Fig.(7.5) and the positions of

the peaks in the spectral density are tabulated in Table (7.2). In order to make a comparison of the results of the coherent potential theory with experiments, we made a crude estimate of the neck radius from our calculations. It was found to be 0.30d, where d is the Γ -L distance, whereas for copper the value is 0.18d. This shows reasonably good agreement with experiments. Comparing the L_2'-L_1 gap for pure copper and for $Cu_{0.90}Al_{0.10}$ we find a reduction by 2.48 eV. This could be compared with optical absorption measurements, but to our knowledge no such measurements are available for this alloy.

TABLE 7.1: Peak positions (in energy measured in Ry. with respect to the muffin-tin zero, $V_c = -0.9121$ Ry.) in the reduced spectral density of states in α-$Cu_{0.70}Zn_{0.30}$ for various representations at the symmetry points Γ, X, and L, and along the Δ axis.

Representation	Energy	Representation	Energy
$\Gamma_{25'}$	0.157	$\Delta_2(0.25,0.0)$	0.195
Γ_{12}	0.188	$\Delta_2(0.50,0.0)$	0.198
X_1	0.085	$\Delta_2(0.75,0.0)$	0.212
X_2	0.212	$\Delta_{2'}(0.25,0,0)$	0.144
X_3	0.110	$\Delta_{2'}(0.50,0,0)$	0.127
$X_{4'}$	0.635	$\Delta_{2'}(0.75,0,0)$	0.110
X_5	0.229	$\Delta_5(0.25,0,0)$	0.173
L_1(lower)	0.249	$\Delta_5(0.50,0,0)$	0.224
L_1(higher)	0.680	$\Delta_5(0.75,0,0)$	0.237
$L_{2'}$	0.465		
L_3(lower)	0.260		
L_3(higher)	0.339		

TABLE 7.2: Peak positions in reduced spectral density of states in $Cu_{0.90}Al_{0.10}$ for various representations at the symmetry points.

Representation	Energy (ryd)	Representation	Energy (ryd)
Γ_{25}'	0.116	X_4'	0.668
Γ_{12}	0.157	X_5	0.203
X_1	0.093	L_1	0.720
X_2	0.195	L_2'	0.466
X_3	0.051	L_3	0.347
		L_3	0.448

FIGURE CAPTIONS

Fig.7.1 Comparison of the density of states as calculated in (a) virtual crystal approximation, (b) coherent potential approximation and (c) averaged t-matrix approximation. In each case c = 0.5 and δ = 0.4, 1.0 and 2.0.

Fig.7.2 Density of states in the coherent-potential approximation, for a variety of concentrations for constant δ = 0.25, 0.50 and 0.75.

Fig.7.3 The reduced spectral density of states $\tilde{\rho}(E,k)$ plotted against E (expressed in terms of $\epsilon = Ea^2/4\pi^2$) for $\Delta_{2'}$ representation in α-$Cu_{0.70}Zn_{0.30}$ The numbers next to the curves denote the value of k_x in units of $2\pi/a$.

Fig.7.4 The reduced spectral density of states $\tilde{\rho}(E,\underline{k})$ plotted against k_x (in units of $2\pi/a$) for $\Delta_{2'}$ representation in α-$Cu_{0.70}$ $Zn_{0.30}$. The numbers next to the curves denote the value of the parameter $\epsilon = Ea^2/4\pi^2$ where a is the lattice parameter.

Fig.7.5 Reduced spectral density of states for $\Gamma_{25'}$ and Γ_{12} representations for $Cu_{0.90}Al_{0.10}$ plotted as a function of energy.

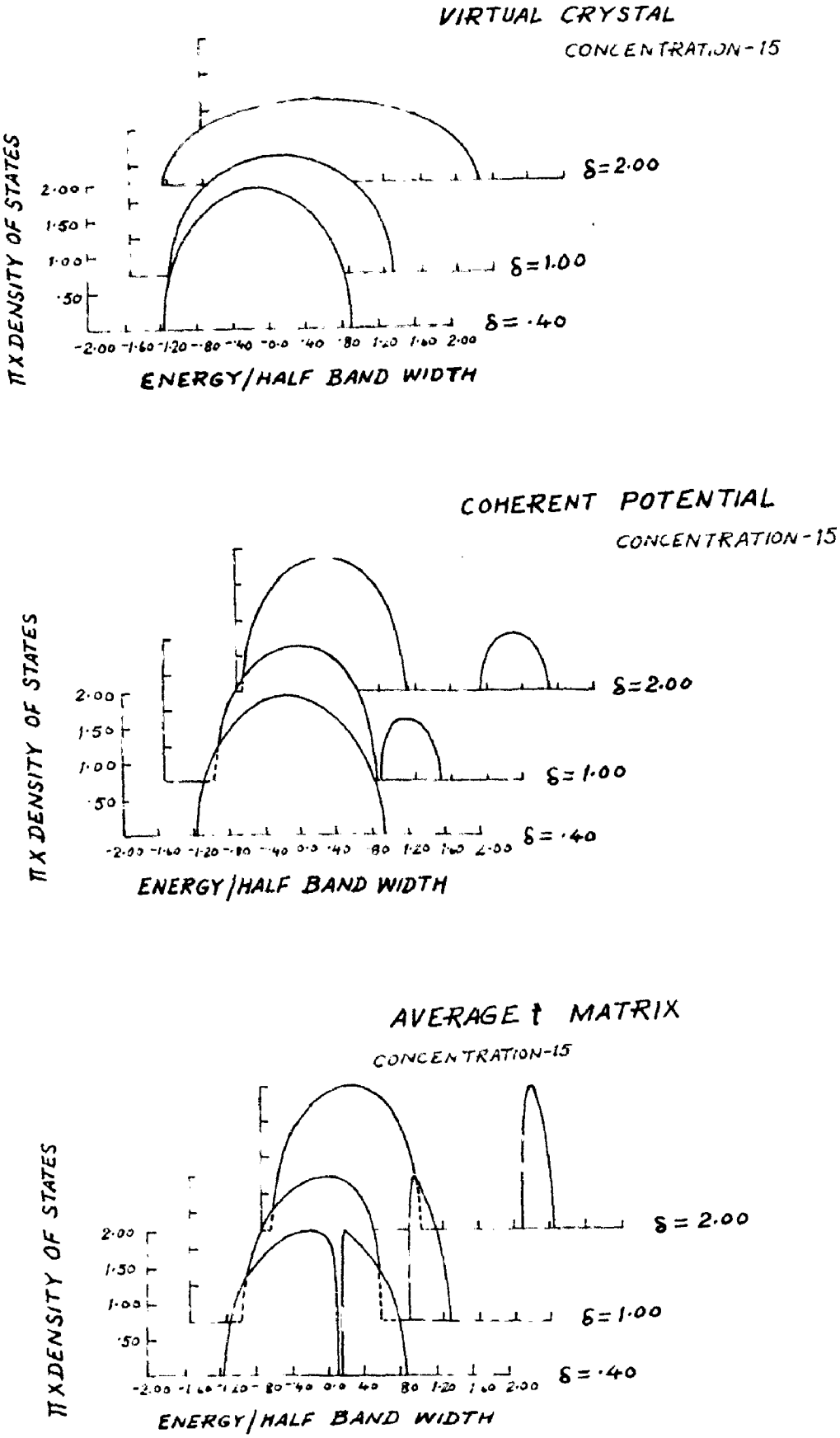
VIRTUAL CRYSTAL
CONCENTRATION-15
π X DENSITY OF STATES
2·00
1·50
1·00
·50
δ=2·00
δ=1·00
δ=·40
-2·00 -1·60 -1·20 -·80 -·40 -0·0 ·40 ·80 1·20 1·60 2·00
ENERGY/HALF BAND WIDTH
COHERENT POTENTIAL
CONCENTRATION-15
π X DENSITY OF STATES
2·00
1·50
1·00
·50
δ=2·00
δ=1·00
δ=·40
ENERGY/HALF BAND WIDTH
AVERAGE t MATRIX
CONCENTRATION-15
π X DENSITY OF STATES
2·00
1·50
1·00
·50
δ=2·00
δ=1·00
δ=·40
-2·00 -1·60 -1·20 -·80 -·40 0·0 ·40 ·80 1·20 1·60 2·00
ENERGY/HALF BAND WIDTH

FIG. 7.1

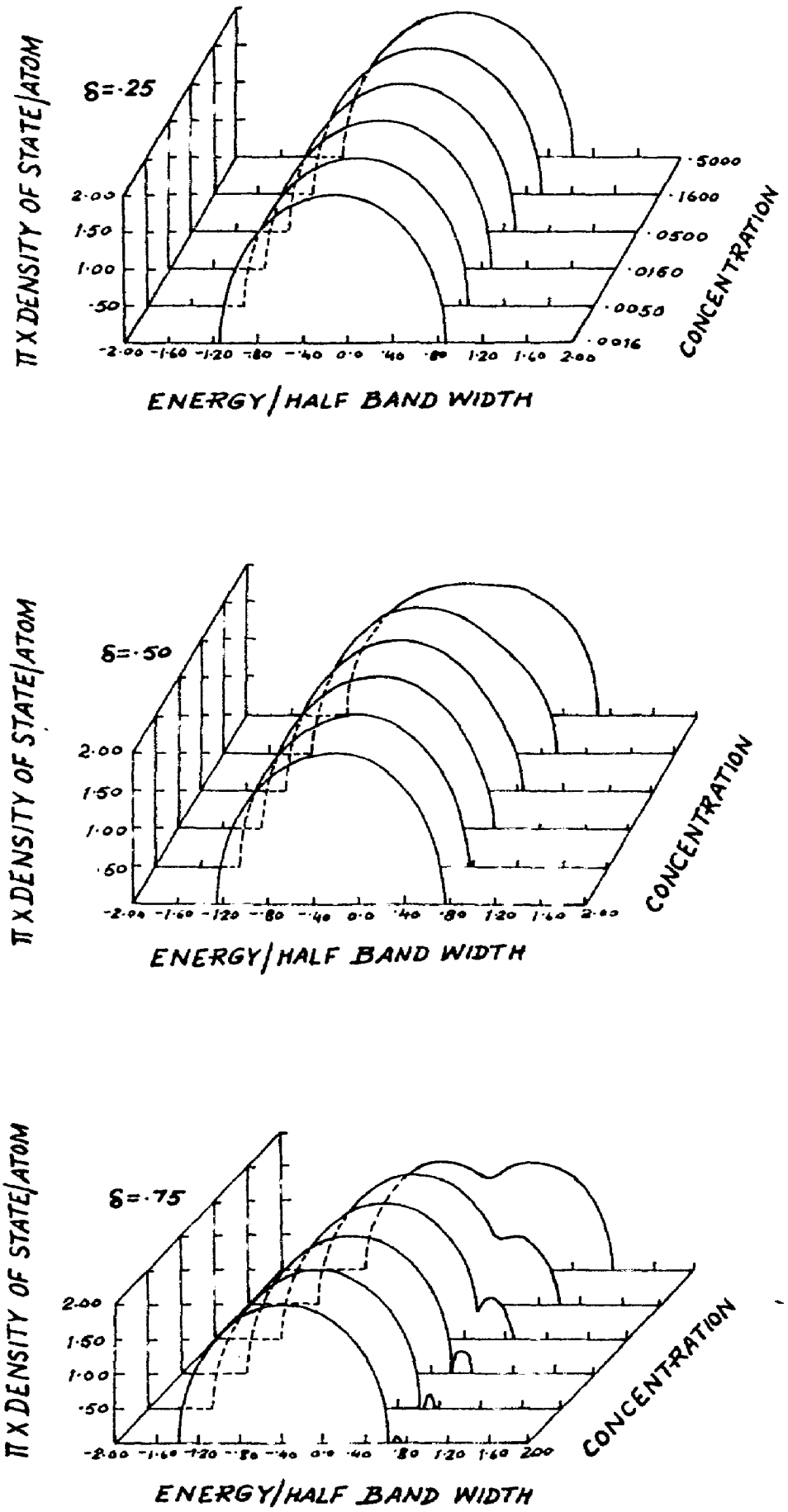
δ=·25
δ=·50
δ=·75
π X DENSITY OF STATE/ATOM
ENERGY/HALF BAND WIDTH
CONCENTRATION
·5000
·1600
·0500
·0160
·0050
·0016
2·00
1·50
1·00
·50
-2·00 -1·60 -1·20 -·80 -·40 0·0 ·40 ·80 1·20 1·40 2·00

FIG. 7.2

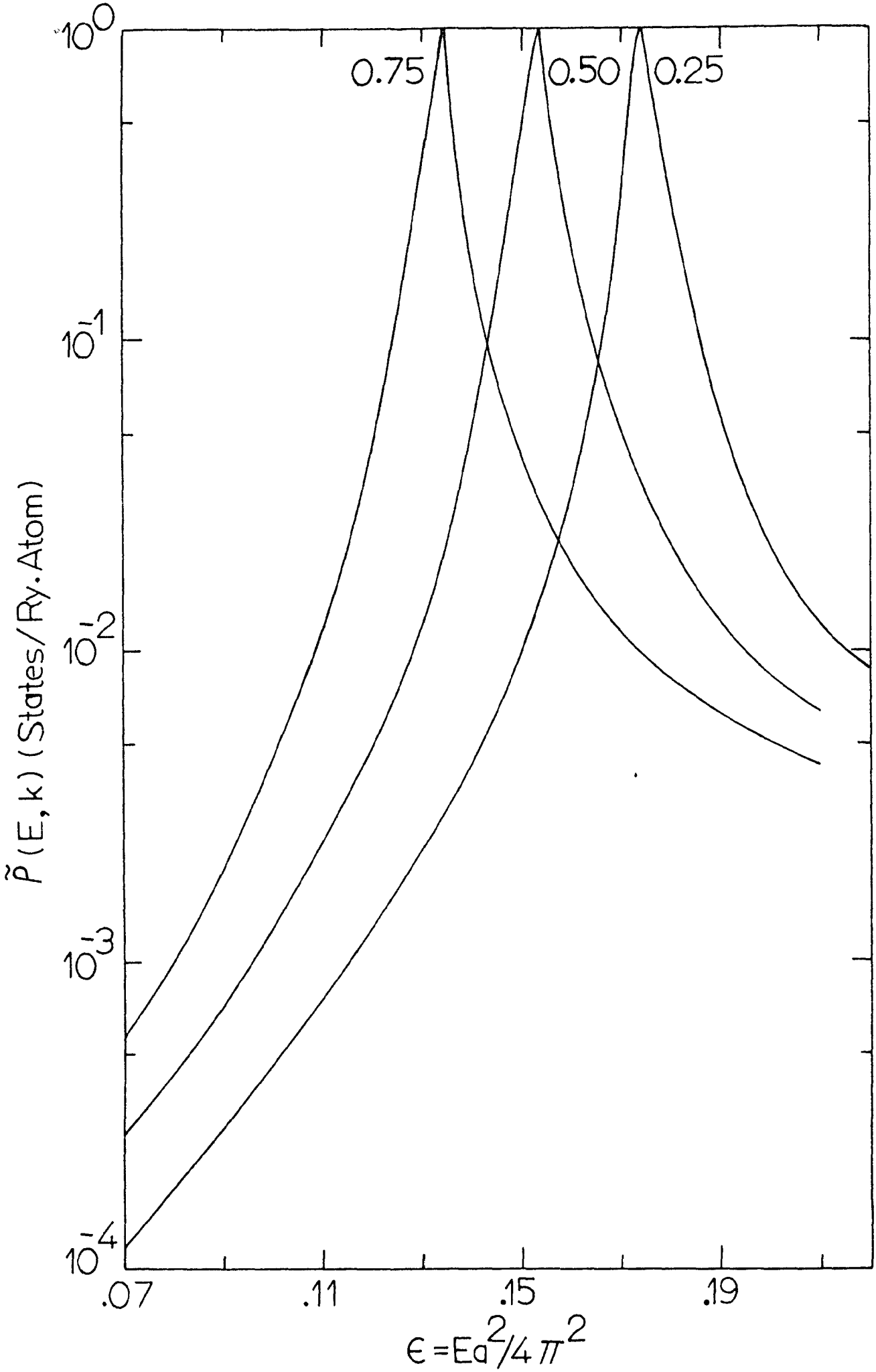

FIG 73 $\tilde{P}(E,k)$ against E for α-$Cu_{0.70}$ $Zn_{0.30}$

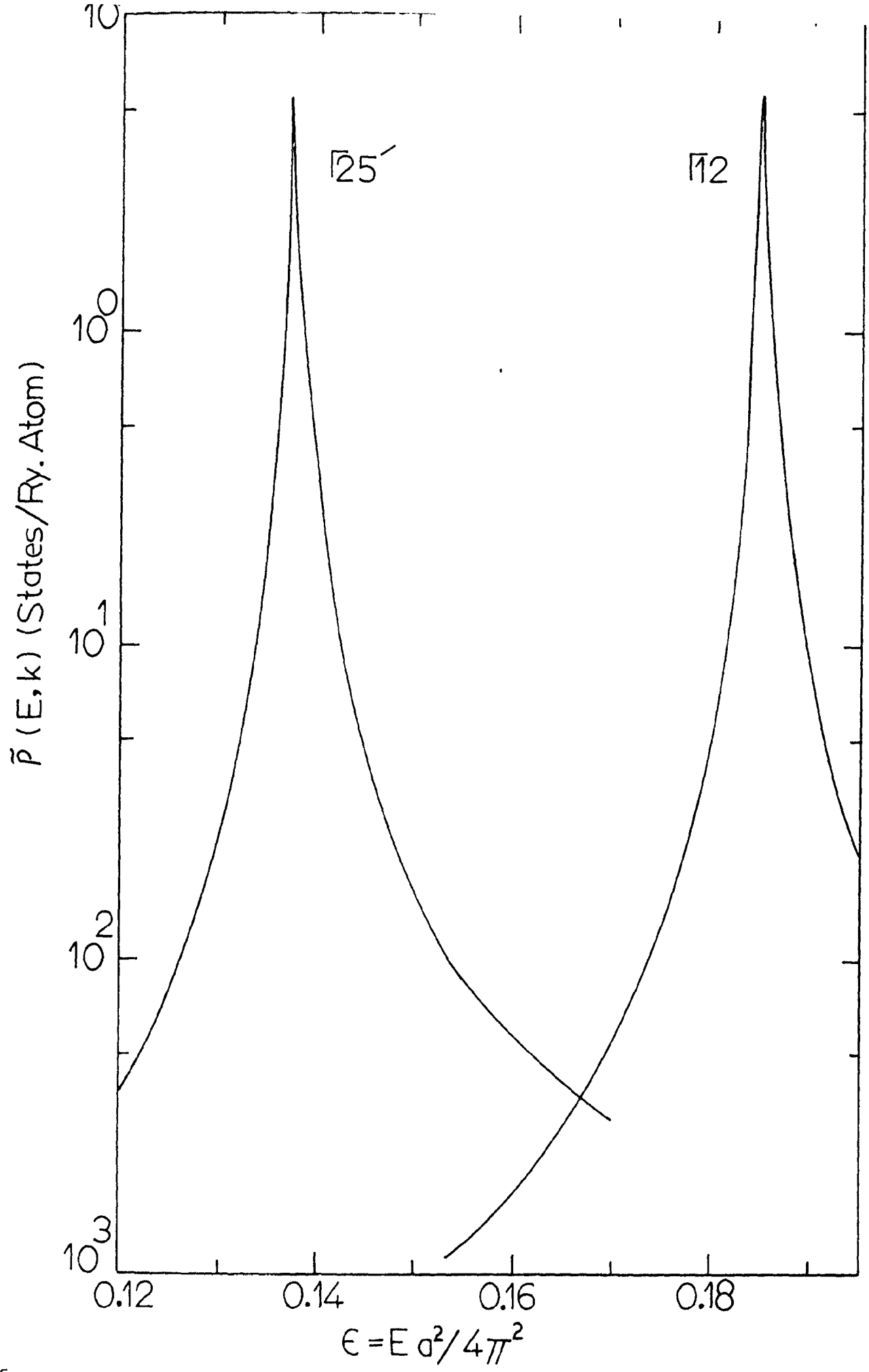

IG.7.5 REDUCED SPECTRAL DENSITY OF STATES FOR Γ_{25}' AND Γ_{12} REPRESENTATIONS FOR $Cu_{0.90}Al_{0.10}$ PLOTTED AS A FUNCTION ENERGY IS THE LATTICE PARAMETER.

EPILOGUE

The theories of electron states in disordered alloys are still far from satisfactory. The Coherent potential approximation seems to be the best amongst those discussed here. Numerical results given by the coherent potential calculations for three-dimensional models of random alloys, have proved superior to other approximate solutions. However, in spite of its general plausibility and success, the coherent potential model has one serious shortcoming. It takes no account of the correlation between the positions of the scatterers. Gyorffy[108] has attempted a generalization of the coherent-potential approximation to a system with short-range order to find the ensemble averaged Green's function $\langle G \rangle$. The correlations between the position of the scatterers were explicitly taken into account. A quasi-crystalline approximation is used to obtain $\langle G \rangle$ in terms of the scattering potential and the correlation functions. He considers partial average of the operators Q_n (Chapter VII) and uses a decoupling scheme similar to that discussed in Appendix 3 except that Gyorffy deals with partial averages for scattering operators, whereas the previous discussion (Ref. 77) was in terms of partially averaged wave functions. No applications to real systems has been made yet, but it is hoped that use of model potentials of the form discussed in Chapter VI and of incomplete Green's functions in Chapter V will result in enough

simplifications to make calculations for an alloy like β-brass, feasible.

In order to make a meaningful evaluation of the various approximations, it is essential to have a systematic experimental study of some alloy systems. We saw, for example, that for α-brass positron annihilation angular correlation studies had not been done, whereas on the other hand, for Cu-Al alloys no optical absorptivity data were available. We hope that a coordinated experimental program, where some or all the techniques discussed in the Introduction are used to study the same alloy systems, will be very useful in deepening our understanding of electrons in disordered alloys.

On the theoretical side, there is another direction in which progress should be made. A good understanding of the theory of electron states in pure metals led to the development, by Hubbard[109] and others,[110] of approximate schemes, which could be used to calculate rapidly the band structure and hence other related properties. An example of such an application is the study by Pettifor[111] of the stability of various possible structures. A development along similar lines for alloys would be very useful. The theories discussed in the thesis are apparently well suited to be reduced to such rapid computational schemes.

An investigation of the transport properties of disordered alloys would also be very illuminating. Velicky's attempt[112] at evaluating the average of $\langle GG \rangle$ using the ideas

of the coherent potential approximation showed that the terms thrown away in making a single site approximation may be important when considering two-particle Green's functions.

A host of other physical properties like phonon frequencies, specific heat, optical properties, remain yet to be explored. Understanding these physical properties in terms of the behavior of the electronic states are challenging problems in solid state theory today.

APPENDIX 1

Calculation of the Structure Constants:

We have seen that the structure of the lattice enters through the coefficients D_{LM} in the angular momentum expansion of $G(\underline{r},\underline{r}')$. This Green's function may be written as

$$G(\underline{R}) = -\frac{1}{4\pi} \sum_{\alpha} \frac{\exp[i\kappa|\underline{R}-\underline{r}_\alpha|]}{|\underline{R}-\underline{r}_\alpha|} \exp(i\underline{k}.\underline{r}_\alpha) \qquad (A1.1)$$

where $\underline{R} = \underline{r} - \underline{r}'$, $\kappa = \sqrt{E}$ and the sum is over all lattice sites. In order to perform this summation to an adequate convergence (an accuracy of six significant figures), it is necessary to make an Ewald transformation and express the series (A1.1) in terms of a summation in direct space, as well as reciprocal space.

We use the relation

$$\frac{\exp[i\kappa|\underline{R}-\underline{r}_\alpha|]}{|\underline{R}-\underline{r}_\alpha|} = \frac{2}{\sqrt{\pi}} \int_0^\infty \exp[-(\underline{R}-\underline{r}_\alpha)^2\xi^2 + \kappa^2/4\xi^2]d\xi \qquad (A1.2)$$

In the above integration, the contour for $\xi > \frac{1}{2}\eta^{1/2}$ is chosen to run along the real axis, η being arbitrary. The integral can be broken into two parts $(0,\frac{1}{2}\eta^{1/2})$ and $(\frac{1}{2}\eta^{1/2}, +\infty)$ and $G(R)$ may be written as

$$G(\underline{R}) = G_1(\underline{R}) + G_2(\underline{R}) \qquad (A1.3)$$

We can now express $G_1(\underline{R})$ as a series in reciprocal space by making use of the following identity, which is valid at each point along the contour $(0,\frac{1}{2}\eta^{1/2})$:

$$\sum_\alpha \exp\left[-(\underline{R}-\underline{r}_\alpha)^2\xi^2 + i\underline{k}.(\underline{r}_\alpha-\underline{R})\right] = \left(\frac{\pi^{3/2}}{\mathcal{T}\xi^3}\right)\sum_n \exp\left[-(\underline{K}_n+\underline{k})^2/4\xi^2+i\underline{K}_n.\underline{R}\right]$$

(A1.4)

where $\underline{K}_n$ denotes reciprocal lattice vectors, and $\mathcal{T}$ is the volume of the unit cell. We then obtain for $G_1(\underline{R})$ and $G_2(\underline{R})$, the following expressions,

$$G_1(\underline{R}) = -\frac{1}{\mathcal{T}}\sum_n \exp\left[i(\underline{K}_n+\underline{k}).\underline{R}\right]\exp\left[\{-(\underline{K}_n+\underline{k})^2+E\}/\eta\right]$$

$$G_2(\underline{R}) = -\frac{1}{2}\pi^{-3/2}\int_{\frac{1}{2}\eta^{1/2}}^{\infty}\sum_\alpha \exp\left[i\underline{k}.\underline{r}_\alpha-(\underline{r}_\alpha-\underline{R})^2\xi^2+E/4\xi^2\right]d\xi$$

where we have written E for κ^2.

We can obtain expressions for the structure constants D_{LM} by expanding $G_1(\underline{R})$ and $G_2(\underline{R})$ termwise in spherical harmonics with respect to $\underline{R}$, to arrive at

$$D_{LM} = D_{LM}^{(1)} + D_{LM}^{(2)} + D_{LM}^{(3)}\ \delta_{LO}$$

Since the structure constants are independent of $\underline{R}$, we may take the limit $R \to 0$ obtaining

$$D_{LM}^{(1)} = -(4\pi/\mathcal{T})\kappa^{-L}\exp(E/\eta)\sum_n \frac{|\underline{K}_n+\underline{k}|^L \exp\left[-(\underline{K}_n+\underline{k})^2/\eta\right]}{(\underline{K}_n+\underline{k})^2-E}\, Y_{LM}(\hat{\underline{K}_n+\underline{k}})$$

$$D_{LM}^{(2)} = \pi^{-1/2}(-2)^{L+1}i^L\kappa^{-L}\sum_\alpha r_\alpha^L \exp(i\underline{k}.\underline{r}_\alpha)Y_{LM}(\hat{\underline{r}_\alpha})$$

$$\times\int_{\frac{1}{2}\eta^{1/2}}^{\infty}\xi^{2L}\exp\left[-\xi^2 r_\alpha^2 + E/4\xi^2\right]d\xi$$

$$D_{00}^{(3)} = -\frac{\eta^{1/2}}{2\pi}\sum_{\alpha=0}^{\infty}\frac{(E/\eta)^\alpha}{\alpha!(2\alpha-1)}$$

The prime in the summation in the expression for $D_{LM}^{(2)}$ indicates that the term with $\underline{r}_\alpha = 0$ is to be excluded.

These are the basic expressions employed in the calculation of the structure constants. In practice, the number of independent constants required is reduced by using symmetry considerations. We choose the $Y_{LM}(\hat{\underline{R}})$ of the angular coordinates of $\underline{R}$ to transform according to the irreducible representations of the group of the wave vector $\underline{k}$. Then only those D_{LM} are non-zero which correspond to the symmetric representation.

APPENDIX 2

Numerical Solution of the Schrödinger Equation:

We have seen during the discussion, that the effect of the potential, enters the final formulation, only through the phase shifts at the radius of the muffin-tin spheres. This calculation was done numerically using the Numerov method for integrating the Schrödinger equation. The method and its advantages are discussed below briefly.

The equation to be solved is

$$\left[-\frac{1}{r^2}\frac{d}{dr}\left(r^2\frac{d}{dr}\right)+\frac{l(l+1)}{r^2}+V(r)-E\right]R_l(r)=0. \qquad (A2.1)$$

It is convenient to work in terms of another function $P_l(r) = rR_l(r)$, and then the above equation reduces to the form

$$\left[-\frac{d^2}{dr^2}+\frac{l(l+1)}{r^2}+V(r)-E\right]P_l(r)=0. \qquad (A2.2)$$

The advantage of this form is that the first derivative is absent, and one can use the Numerov method for numerical integration. In the case of the atomic problem discussed by Hartree, the equation has to be solved to give E and $P_l(r)$ subject to the conditions

1) $P_{nl} = 0$ at $r=0$ and $r \to \infty$
2) In the range $0<r<\infty$, the function $P_{nl}(r)$ must have n-l-1 nodes.

The method for doing this had been given by Hartree,

where one starts with the solutions at the origin and integrates outwards, thus generating a trial radial wave function with a given energy. The outward integration is stopped at a point which lies outside the last peak of the trial radial wave function. If the number of nodes of this function is n-l-1, an inward integration is started.

If the trial energy were equal to the true energy eigenvalues, the logarithmic derivative at the matching radius of the trial wavefunction, generated by the inward integration would be identical with the corresponding quantity generated by the outward integration. If this is not so, the energy is changed till the required degree of match is achieved. A program to perform this has been given by Herman and Skillman.

The problem in our case is simpler. The equation has to be solved for a given energy and subject to the condition $P_l(r) = 0$ at the origin. The iteration in energy part of the Herman Skillman program is therefore not required. We now give a short discussion of the basic iteration procedure in the Numerov method.

The radial Schrodinger equation (A.2.2) can be written as

$$\frac{d^2P(r)}{dr^2} = g(r)\ P(r) \qquad (A2.3)$$

(we drop the subscript l), where

$$g(r) = \left[V(r) - E + \frac{l(l+1)}{r^2} \right]. \qquad (A2.4)$$

We perform the integration on a mesh, which is closely subdivided in the region of small r and gradually with larger steps for large values of r. The subscripts to the symbols of the functions, denote values of the function at the corresponding mesh point.

We can write the expansion for the function P_n about a point $r = r_n$ in a Taylor's series as

$$P_{n+1} = P_n + hP_n' + \frac{h^2}{2!} P_n'' + \frac{h^3}{3!} P_n''' + \qquad (A2.5)$$

where h is the spacing in the mesh and the primes denote differentiation with respect to r. $(h = r_{n+1} - r_n)$.

Differentiating the above equation twice, we have

$$P_{n+1}'' = P_n'' + hP_n''' + \frac{h^2}{2!} P_n^{(iv)} + \frac{h^3}{3!} P_n^{(v)} + \qquad (A2.6)$$

Let $y_n \equiv P_n - \frac{h^2}{12} P_n''$ be a new variable, then

$$y_{n+1} = P_{n+1} - \frac{h^2}{12} P_{n+1}''$$

$$= P_n + hP_n' + \frac{5h^2}{12} P_n'' + \frac{h^3}{12} P_n''' - \frac{h^5}{180} P_n^{(v)} - \frac{h^6}{480} P_n^{(vi)} +$$

We note that the coefficient of $P_n^{(iv)}$ is identically zero. Now y_{n-1} can be obtained from the above expression simply by replacing h by -h.

$$y_{n-1} = P_n - hP_n' + \frac{5h^2}{12} P_n'' - \frac{h^3}{12} P_n''' + \frac{h^5}{180} P_n^{(v)} - \frac{h^6}{480} P_n^{(vi)} +$$

The second difference in y at r_n is therefore

$$\delta^2 y_n = y_{n+1} + y_{n-1} - 2y_n$$
$$= h^2 P_n'' - \frac{h^6}{240} P_n^{(vi)} .$$

If we neglect the second term on the right hand side, we have the simple relationship

$$\delta^2 y_n = h^2 P_n'' = h^2 g_n P_n \qquad (A2.7)$$

Thus, if we know the solutions for P_n, y_n at two points n-1 and n, we can find the solution at y_{n+1}, and hence the integration can be carried forward. The truncation error is determined by the term $\frac{h^6}{240} P^{(vi)}$ so that by keeping h small this error can be readily controlled.

The starting values required to use Eq.(A2.7) to continue the outward integration are obtained by expanding $P_l(r)$ in terms of a power series of the form

$$P_l(r) = r^{l+1} \left[1 + A_1 r + A_2 r^2 + A_3 r^3 + A_4 r^4 \right], \qquad (A2.8)$$

Substituting into Eq.(A2.2) and solving the results for the coefficients A_1 to A_4. Once these coefficients are known, Eq.(A2.8) gives the starting values at the first few points of the integration mesh.

APPENDIX 3

Proof of Bloch type conditions for averaged wave function

Ziman has shown that the 'configurationally averaged' wave function satisfies a Bloch-type condition for a one-component disordered system, where all scatterers are identical. The concept of configuration averaging is, however, quite general and not limited to the case of identical scatterers.

We denote by s the scattering properties of the scattering centre. In the present application s is merely an identifying index. A particular configuration of the scatterers is therefore defined if we know their position vectors $\underline{x}_1, \underline{x}_2, \ldots\ldots \underline{x}_N$, and scattering parameters (identifying indices) $s_1, s_2 \ldots\ldots s_N$. In the case of a binary alloy, $s_1 \ldots\ldots s_N$ can have either of two values corresponding to the two components. The probability that the set of N scatterers will be located at $\underline{x}_1, \underline{x}_2 \ldots \underline{x}_N$ is denoted by $n(\underline{x}_1, \underline{x}_2 \ldots \underline{x}_N | s_1 s_2 \ldots s_N)\, d\underline{x}_1 d\underline{x}_2 \ldots d\underline{x}_N$.

If one scatterer is held fixed and all the other scatterers averaged over, the configurational average will be given by

$$\langle \psi(\rho|\underline{x}_1) \rangle = \int\ldots\int \psi_1(\rho)\, n(\underline{x}_1 s_1 | \underline{x}_2 x_3 \ldots \underline{x}_N;\ s_2 s_3 \ldots s_N)\, d\underline{x}_2 \ldots d\underline{x}_N$$

where $n(\underline{x}_1 s_1 | \underline{x}_2, \underline{x}_3 \ldots \underline{x}_N;\ s_2 s_3 \ldots s_N)$ is the probability of finding sphereres of type s_2 at $\underline{x}_2$, s_3 at $\underline{x}_3$ etc., given

that there is a sphere of type s_1 at $\underline{x}_1$. If two spheres are held fixed, we have:

$$n(\underline{x}_1 s_1 | \underline{x}_2 \ldots \underline{x}_N; s_2 \ldots s_N) = n(\underline{x}_1 s_1, \underline{x}_2 s_2 | \underline{x}_3 \ldots \underline{x}_N; s_3 \ldots s_N) \; P^{s_1 s_2}(\underline{x}_2 - \underline{x}_1), \quad \text{(A3.2)}$$

where $P^{s_1 s_2}(\underline{x}_2 - \underline{x}_1)$ denotes the probability of finding a sphere of type s_2 at $\underline{x}_2$, given that the sphere at $\underline{x}_1$ is of type s_1.

We now take the configurational average of Eq.(5.6)

$$\psi_j(\underline{\rho}) = \sum_{j'} \int G_o(\underline{\rho} - \underline{\rho}' + \underline{x}_j - \underline{x}_{j'}) U_{j'}(\underline{\rho}') \psi_{j'}(\underline{\rho}') \, d\underline{\rho}'.$$

Let the $j=1$ site be an A atom. Then the contribution of the A sites to $\langle \psi_1(\rho | \underline{x}_1) \rangle_A$ is:

$$\int \int G_o^{AA}(\underline{\rho} - \underline{\rho}' + \underline{x}_1 - \underline{x}_2) \, P^{AA}(\underline{x}_2 - \underline{x}_1) \, U_A(\underline{\rho}') \psi_2^A(\underline{\rho}') \, d\underline{\rho}'$$

$$n(\underline{x}_1 A, \underline{x}_2 A | \underline{x}_3 \ldots \underline{x}_N; s_3 \ldots s_N) \, d\underline{x}_3 \ldots d\underline{x}_N$$

Similarly the contribution from B sites is:

$$\int \int G_o^{AB}(\underline{\rho} - \underline{\rho}' + \underline{x}_1 - \underline{x}_2) \, P^{AB}(\underline{x}_2 - \underline{x}_1) U_B(\underline{\rho}') \psi_2^B(\underline{\rho}') d\underline{\rho}'$$

$$n(\underline{x}_1 A, \underline{x}_2 B | \underline{x}_3 \ldots \underline{x}_N; s_3 \ldots s_N) d\underline{x}_3 \ldots d\underline{x}_N$$

We define

$$\langle \psi_2(\rho' | \underline{x}_2, \underline{x}_1) \rangle_{s_2, s_1} = \int \int \psi_2^{s_2}(\rho) n(\underline{x}_1 s_1, \underline{x}_2 s_2 | \underline{x}_3 \ldots \underline{x}_N; s_3 \ldots s_N) \; d\underline{x}_3 \ldots d\underline{x}_N \quad \text{(A3.3)}$$

and make the approximation

$$\langle \psi_2(\underline{\rho}'|\underline{x}_2,\underline{x}_1)\rangle_{s_2 s_1} = \langle \psi_2(\underline{\rho}'|\underline{x}_2)\rangle_{s_2} \qquad (A3.4)$$

We then arrive at

$$\langle \psi_1(\underline{\rho}|\underline{x}_1)\rangle_A = \int G_o^{AA}(\underline{\rho}-\underline{\rho}')U_A(\rho')\langle \psi_1(\rho'|\underline{x}_1)\rangle_A \, d\underline{\rho}'$$

$$+ \int\int G_o^{AA}(\underline{\rho}-\underline{\rho}'+\underline{x}_1-\underline{x}_2)U_A(\underline{\rho}')P^{AA}(\underline{x}_2-\underline{x}_1)\langle \psi_2(\underline{\rho}'|\underline{x}_2)\rangle_A d\underline{\rho}' d\underline{x}_2$$

$$+ \int\int G_o^{AB}(\underline{\rho}-\underline{\rho}'+\underline{x}_1-\underline{x}_2)\, U_B(\underline{\rho}')\, P^{AB}(\underline{x}_2-\underline{x}_1)\langle \psi_2(\underline{\rho}'|\underline{x}_2)\rangle_B d\underline{\rho}' d\underline{x}_2 .$$

A similar expression is obtained if the j = 1 site is chosen to be a B atom. Both these expressions may be written in the abstract form:

$$\langle \psi_1(\underline{\rho})\rangle_A = \int \Gamma(\underline{x}_2-\underline{x}_1)\, \langle \psi_2(\underline{\rho})\rangle_A \, d\underline{x}_2$$

$$\langle \psi_1(\underline{\rho})\rangle_B = \int \Gamma'(\underline{x}_2-\underline{x}_1)\, \langle \psi_2(\underline{\rho})\rangle_B \, d\underline{x}_2$$

These equations are translationally invariant in the space of $\underline{x}_1, \underline{x}_2$ and, therefore, have solutions

$$\langle \psi_1(\underline{\rho})\rangle_A = \exp[i\underline{k}.(\underline{x}_1-\underline{x}_2)]\, \langle \psi_2(\rho)\rangle_A$$

$$\langle \psi_1(\underline{\rho})\rangle_B = \exp[i\underline{k}.(\underline{x}_1-\underline{x}_2)]\, \langle \psi_2(\rho)\rangle_B .$$

Equation (A3.4) is an 'insensitivity' relation implying that the wave function within a particular sphere is, on the average,

insensitive to the exact whereabouts and arrangement of neighboring spheres, but depends only on the position and kind of the sphere. This is almost the same approximation as made by Ziman for liquid metals. It does not appear to be a bad approximation for the case of alloys, as it is eviden that very distant spheres do not affect the wave function within the sphere under consideration, and the effect of near neighbours is more or less taken into account by the averaging process.

REFERENCES

1. For a general review of the various methods of energy band calculations, see for instance, 'Methods in Computational Physics, Vol.8' Editors B. Adler, S. Fernbach and M. Rotenberg, Academic Press (1968).
2. The Fermi Surface, Editors W.A. Harrison and M.B. Webb, John Wiley, (1960).
3. T.G. Berlincourt, R.R. Hake and A.C. Thorsen, Phys. Rev. 127, 710 (1962).
4. Optical Properties and Electronic Structure of Metals and alloys, Editor F. Abeles, North Holland Publishing Company-Amsterdam (1966).
5. Soft X-ray Band Spectra and the Electronic Structure of Metals and Materials, edited by D.J. Fabian, Academic Press Inc. New York, (1968).
6. M.A. Biondi and J.A. Rayne, Phys. Rev. 115, 1522 (1964), M.A. Biondi and J.A. Rayne, Phys. Rev. 121, 456 (1961). B.W. Veal and J.A. Rayne, Phys. Rev. 128 , 551 (1962); ibid 130, 2156 (1963); 132, 1617 (1963).
7. E.A. Stern, J.C. McGroddy and W.E. Harte, Phys. Rev. 135, A1306 (1964).
8. I.Ya Dekhtyar, D.A. Zevina and V.S. Mikhalenkov, Soviet Physics Doklady, 9, 492 (1964).
9. K. Fujiwara and O. Sueoka, J. Phys. Soc. Japan 21, 1947 (1967); K. Fujiwara, O. Sueoka and T. Imura, J. Phys. Soc. Japan 24, 467 (1968).
10. S.C. Moss, Phys. Rev. Letters 22, 1108 (1969).

11. R.J. Higgins and H.D. Kaehn, Phys. Rev. 182, 649(1969).

12. J. Bardeen, B.R. Cooper and J.R. Schreiffer, Phys. Rev. 108, 1175 (1957).

13. M.H. Cohen, H. Fritzche, and S.R. Ovshinsky Phys. Rev. Letters 22, 1065 (1969).

14. T. Liu and H. Amar, Rev. Mod. Phys. 40, 782 (1968).

15. J. Korringa, Physica 13, 392 (1947); W. Kohn and N. Rostoke Phys. Rev. 94, 1111(1954).

16. J.L. Beeby, Proc. Roy. Soc. A279 , 82 (1964).

17. J.M. Ziman, Proc. Phys. Soc. 86, 337 (1965).

18. J.M. Ziman, Principles of Theory of Solids, Cambridge University Press (1964).

19. H. Jones, Brillouin Zones and Electronic States in Crystals North Holland Publishing Company, Amsterdam (1962).

20. J. Callaway, Energy Band Theory,Academic Press (1964).

21. W.A. Harrison, Pseudopotentials in the Theory of Metals, W.A. Benjamin (1966).

22. B. Segall, Phys. Rev. 125, 109 (1962).

23. G.A. Burdick, Phys. Rev. 129 , 138 (1963).

24. J.C. Slater, Phys. Rev. 145, 599 (1966).

25. P.Lloyd, Proc. Phys. Soc. 86, 825 (1965).

26. K.H. Johnson, Phys. Rev. 150 , 429 (1966).

27. P. Soven, Phys. Rev. 137, A1706 (1965).

28. T.L. Loucks, Phys. Rev. 139, A1333 (1965).

29. Y. Onodera, M. Okazaki and T. Inui, J. Phys. Soc. Japan, 21, 816 (1966).

30. R. Gaspar and K. M.Ivanecsko, Acta Phys. Hungarica, 6,105, (1956).

31. F. Herman and S.Skillman, Atomic Structure Calculations, (Prentice Hall, Inc. Englewood Cliffs, N.J. 1963).

32. V. Heine, Proc. Roy. Soc. 240A, 340 (1957).

33. L.M. Falicov, Phil. Trans. Roy. Soc. 255, 55 (1962).

34. G.D. Gaspari and T.P. Das, Phys. Rev. 167, 660 (1968).

35. J.C. Slater, Phys. Rev. 81, 385 (1951).

36. J.E. Robinson, F. Bassani, R.S. Knox and J.R. Schrieffer, Phys. Rev. Letters 9, 215 (1962).

37. F. Herman, J. Callaway and F.S. Acton, Phys. Rev. 95, 371 (1954).

38. W. Kohn and L.J. Sham, Phys. Rev. 140, A1133 (1965).

39. E.C. Snow and J.T. Waber, Phys. Rev. 157, 570 (1967).

40. B.I. Lundqvist, Phys. Stat. Solidi, 32, 273 (1969).

41. D.Liberman, J.T. Waber and D.T. Cromer, Phys. Rev. 137, A27 (1964).

42. L.F. Mattheiss, Phys. Rev. 134, A970 (1964).

43. P.O. Lowdin, Adv. Phys. 5, 1 (1956).

44. W.E. Rudge, Phys. Rev. 181, 1024 (1969).

45. M. Chodorow, thesis, Massachusetts Institute of Technology 1939 (Unpublished).

46. S. Wakoh, J. Phys. Soc. Japan 20, 1894 (1965).

47. R.A. Ballinger and C.A.W.Marshall, Proc. Phys. Soc. (Londo 91, 203 (1967).

48. L.F. Mattheiss, Phys. Rev. 134, A970 (1964).

49. E.C. Snow, Phys. Rev. 171, 785 (1968).

50. H.L. Davis, J.S. Faulkner and H.W. Joy, Phys. Rev. 167, 601(1968).

51, A.S. Joseph and A.C. Thursen, Phys. Rev. 138 , A1159 (1965)

52. H.V. Bohm and V.J. Easterling, Phys. Rev. 128, 1026 (1962).

53. J.P. Jan and I.M. Templeton, Phys.Rev. 167 ,556(1967).

54. H.Ehrenreich and H.R. Phillipp, Phys. Rev. 128 , 1622 (1962).

55. C.N. Berglund and W.E. Spicer, Phys. Rev.136 A1044 (1964).

56. D.R. Hartree, Calculation of Atomic Structures, John Wiley and Sons, N.Y. (1957).

57. B.Noumerov; Publ. Observ. Astrophys. Cent. Russie 11, (Moscu, 1923) Monthly Not. Roy. Astron. Soc. 84, 592 (1924).

58. G.W. Pratt Jr., Phys. Rev. 88, 1217 (1952).

59. T.R.McCalla, Introduction to Numerical Methods and FORTRAN Programming 'John Wiley, New York (1967)

60. M.M. Pant and S.K. Joshi, Phys. Rev. 184, 639 (1969).

61. L. Nordheim, Ann. Physik 9, 607 (1931).

62. R.H. Parmenter, Phys. Rev. 97, 587 (1955).

63. H. Amar, K.H. Johnson and K.P. Wang, Phys. Rev. 148, 672 (1966).

64. H. Amar, K.H. Johnson and C.B. Sommers, Phys. Rev. 153, 655 (1967).

65. K.H. Johnson and H. Amar, Phys. Rev. 139, A760 (1965).

66. M.M. Pant and S.K. Joshi, Phys. Letters 28A, 556 (1969).

67. M.M. Pant and S.K. Joshi, Phys. Rev. 184, 635 (1969).

68. P. Phariseau and J.M. Ziman, Phil. Mag. 8, 1487 (1963).

69. J.M. Ziman, Proc. Phys. Soc. 88, 387 (1966).

70. L.L. Foldy, Phys. Rev. 67, 107 (1945).

71. D.T. Keating, Acta Met. 2, 885 (1954).

72. J.M. Cowley, J. Appl. Phys. 21, 24 (1950).

73. L.M. Van Torne, Phys. Stat. Solidi 19, K87 (1967).

74. S.C. Moss, J. Appl. Phys. 35, 3547 (1964).

75. M.J. Klein, Am. J. Phys. 19, 153 (1951).

76. F.S. Ham and B. Segall, Phys. Rev. 124, 1786 (1961).

77. M.M. Pant and S.K. Joshi, Phys. Rev. 186, 675 (1969).

78. M.M. Pant and S.K. Joshi, Phys. Rev. B1 , 506 (1969).

79. P. Soven, Phys. Rev. 151, 539 (1966).

80. A.R. Von Neida and R.B. Gorden, Phil. Mag. 7,1129 (1962).

81. G. Airoldi and M. Drossi, Phil. Mag. 19, 349 (1969); G. Airoldi, M. Asdente and E. Rimini, Phys. Matiere Condensee 2, 180 (1964).

82. J.A. Rayne, Phys. Rev. 108, 649 (1957).

83. D.L. Martin, Can. J. Phys. 46, 923 (1968).

84. J.A. Catterall and J. Trotler, Proc. Phys. Soc. 79 , 691 (1963).

85. I. Ya Dekhtyar, S.G. Litovchenko and V.S. Mikhalenkov, Dokl. Acad. Nauk SSSR 147, 1332 (1962) [English transl: Soviet Phys. Doklady 7, 1135 (1968)].

86. P.O. Nilsson and C. Norris, Phys. Letters 29A, 22 (1969); P.O. Nilsson, A. Persson and S. Hagstron, Solid State Commun. 6, 297 (1968).

87. D. Gray and E. Brown, Phys. Rev. 160, 567 (1967).

88. G.A. Rooke in Ref.5 p.185.

89. J.M. Schoen, Phys. Rev. 184, 858 (1969).

90. J.M. Schoen and S.P. Denker, Phys. Rev. 184, 864(1969).

91. J.L. Beeby, Proc. Roy. Soc. A302 , 113 (1967).

92. J.L. Beeby, Phys. Rev. 175 , A130 (1964).

93. J.Als Nielson and O.W. Dietrich, Phys. Rev. 153, 706(1967

94. C.B. Walker and D.T. Keating, Phys. Rev. 130 , 1726(1963)

95. M.I. Cohen and V. Heine, Adv. Phys. 7, 395 (1961).

96. P. Soven, Phys. Rev. 156, 809 (1967).

97. P.Soven, Phys. Rev. 178, 1136 (1969).

98. B. Velicky, S. Kirkpatrick, and H. Ehrenreich, Phys. Rev. 175, 747 (1968).

99. P.W. Anderson and W.L. McMillan in Proceedings of the International School of Physics'Enrico Fermi' Course 37, edited by W. Marshall (Academic Press, Inc. New York, 1967).

100. Y. Onodera and Y. Toyozawa, J. Phys. Soc. Japan 24, 341 (1968).

101. J. Hubbard, Proc. Roy. Soc. A281, 401 (1964).

102. M.M. Pant and S.K. Joshi, Phys. Rev. (Aug.1970).

103. M.M. Pant and S.K. Joshi, Phys.Letters 31A, 238 (1970).

104. M.M. Pant, Solid State Communications (to be published).

105. S.Kirkpatrick, B. Velicky and H.Ehrenreich, Phys. Rev. B1 3250 (1970).

106. L. Hodges and H.Ehrenreich and N.D. Lang, Phys. Rev. 152, 505 (1966); F.M. Mueller, Phys. Rev. 153, 659(1967)

107. D.H. Leib and W.E. Spicer, Phys. Rev. Letters 20, 1441 (1968).

108 B.L. Gyorffy, Phys. Rev. B1, 3290 (1970).

109. J. Hubbard, Proc. Phys. Soc. 92, 921 (1967).

110. V. Heine, Phys. Rev. 153, 673 (1967); R.A. Deegan, Phys. Rev. 186 , 619 (1969).

111. D.G. Pettifor, J. Phys. C 2 , 1051 (1969).

112. B. Velicky, Phys. Rev. 184, 614 (1969).

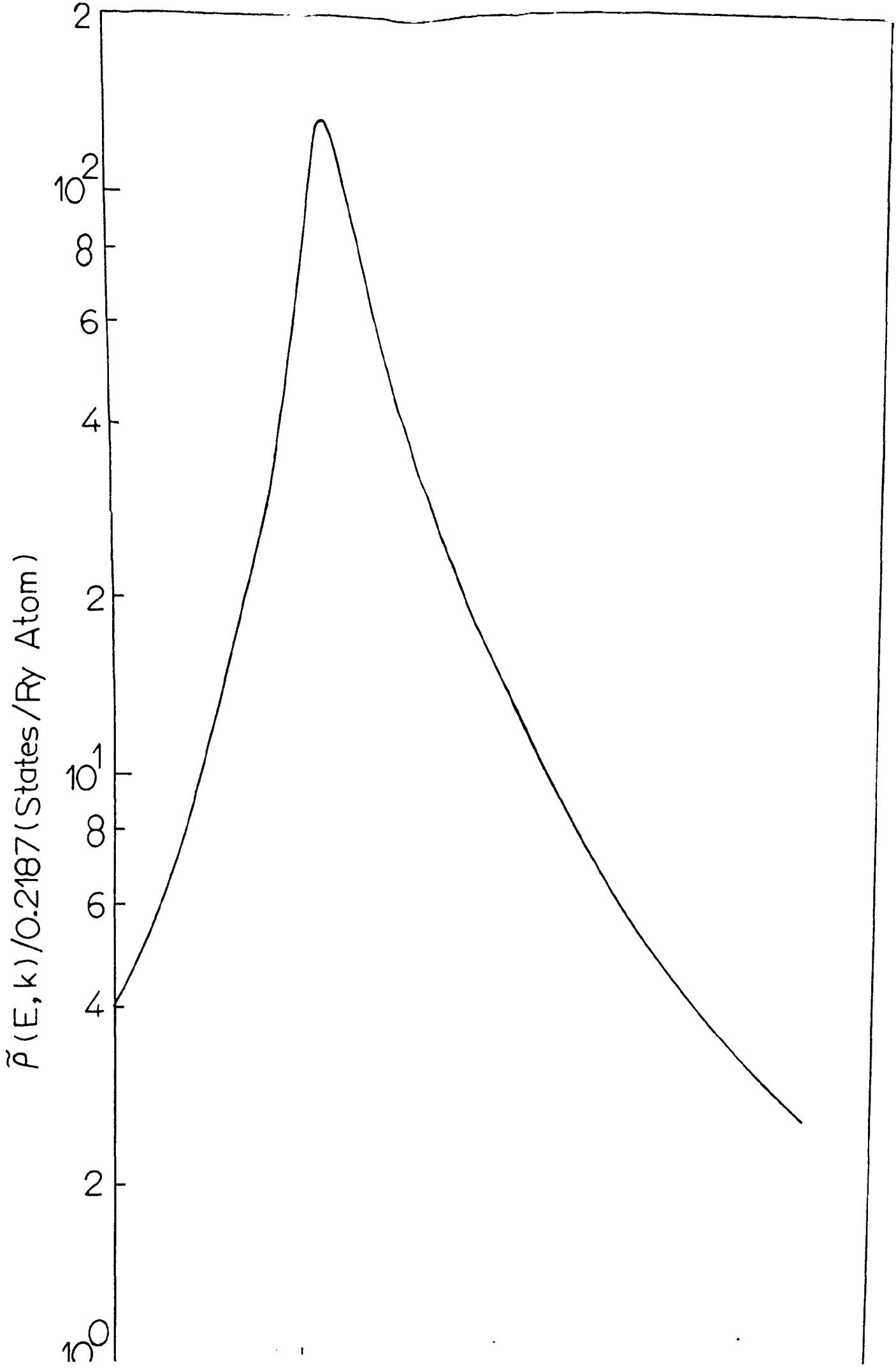
2
10^2
8
6
4
2
10^1
8
6
4
2
10^0
$\tilde{\rho}(E,k)/0.2187$ (States/Ry Atom)

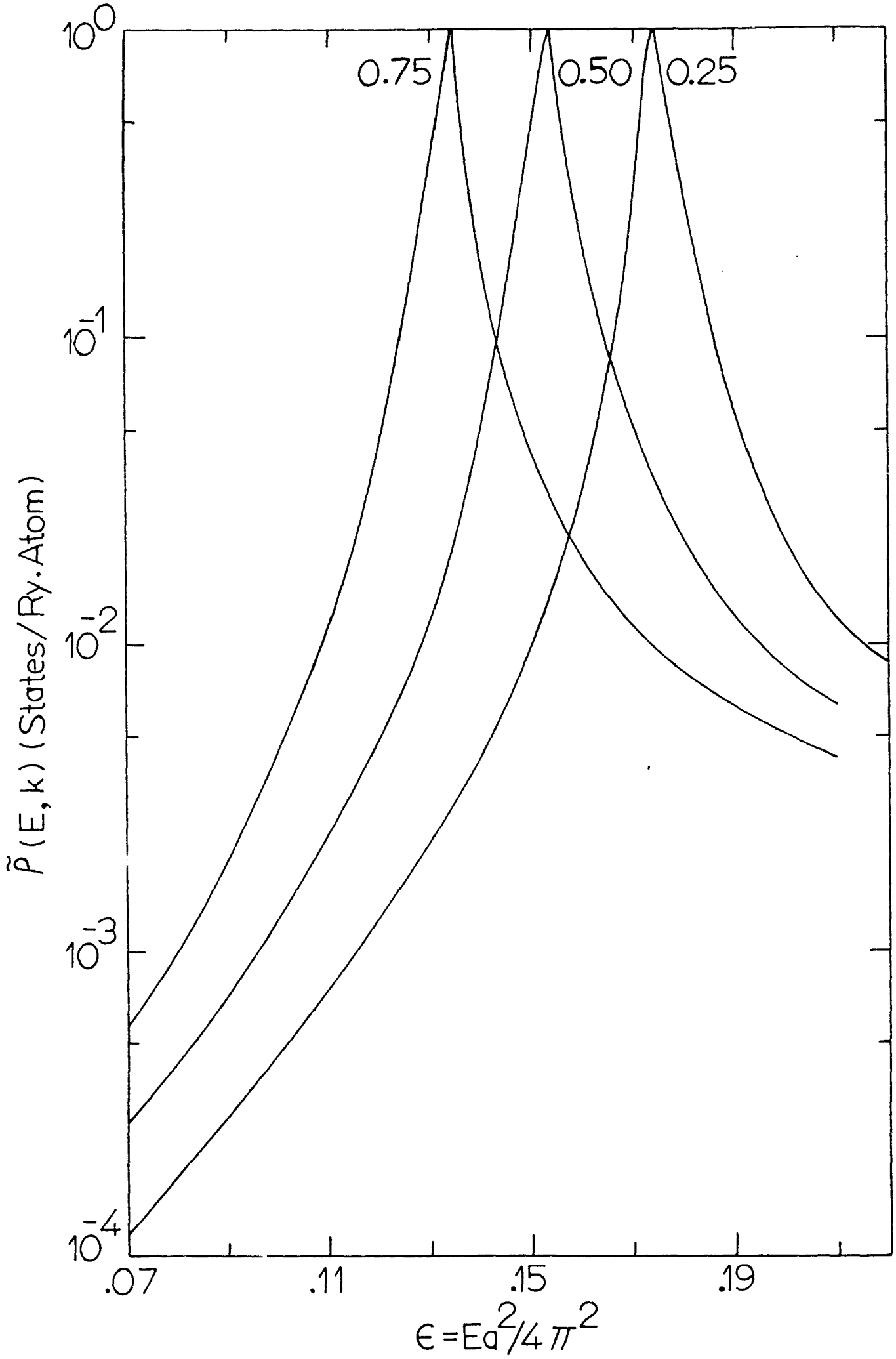

FIG. 7.3 $\tilde{P}(E,k)$ against E for α-$Cu_{0.70}$ $Zn_{0.30}$

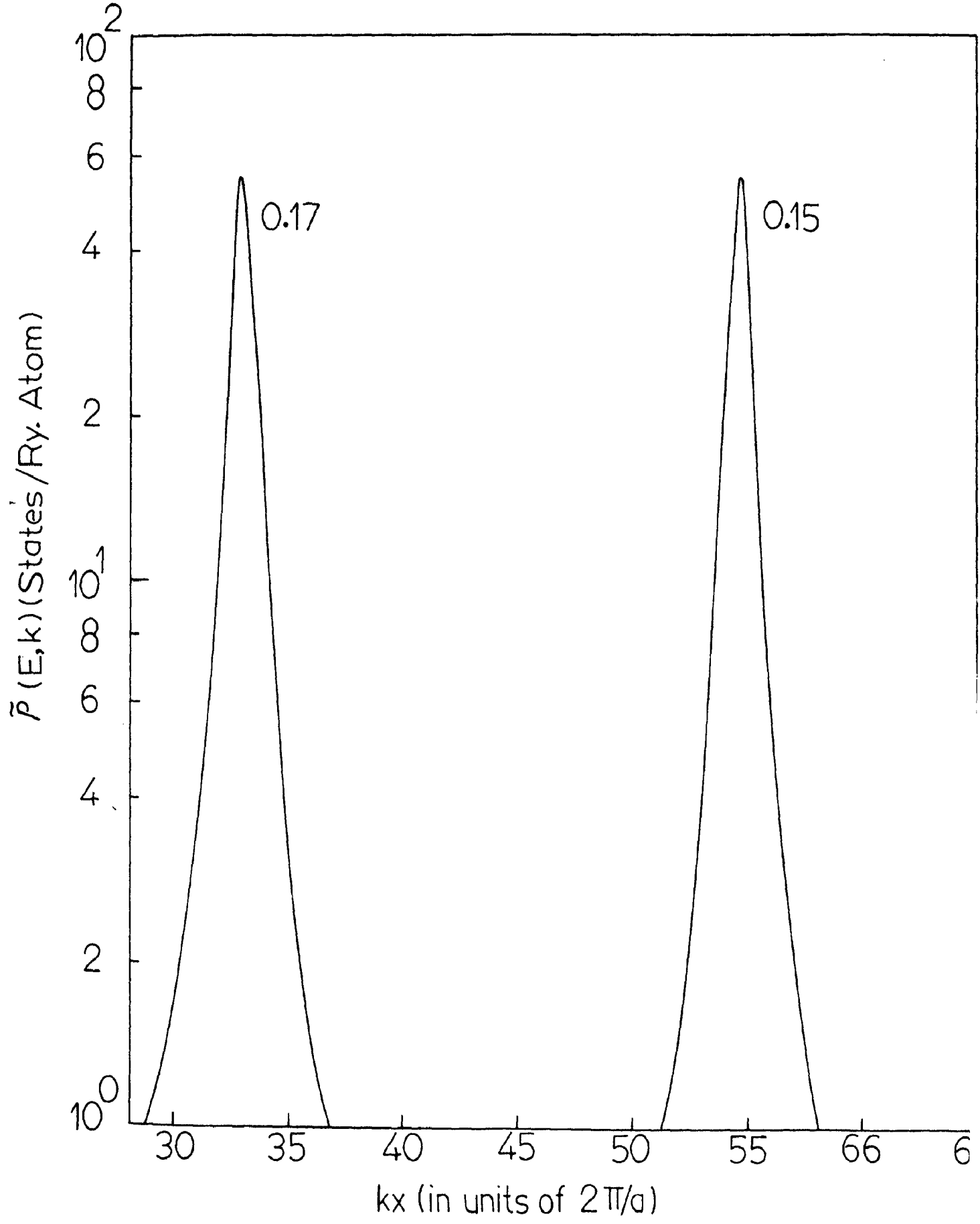
10^2
8
6
4
2
10^1
8
6
4
2
10^0
$\tilde{P}$ (E,k) (States/Ry. Atom)
0.17
0.15
30
35
40
45
50
55
66
6
kx (in units of 2π/a)

FIG. 7.4